

LA-7779-M

Manual
(ISPO-53)

1

**The High-Level Neutron Coincidence
Counter (HLNCC):
Users' Manual**

For Reference

Not to be taken from this room



USA
IAEA

PROGRAM FOR
TECHNICAL ASSISTANCE
TO IAEA SAFEGUARDS

Department of Energy
Safeguards & Security



LOS ALAMOS SCIENTIFIC LABORATORY

Post Office Box 1663 Los Alamos, New Mexico 87545

University of California

This report was not edited by the Technical Information staff.

Work supported by the US Department of Energy,
Office of Safeguards and Security, and by the
Program for Technical Assistance to IAEA Safeguards.

This report was prepared as an account of work sponsored by an Agency of the United States Government. Neither the United States nor the United States Department of Energy, nor any of their employees, nor any of their contractors, sub-contractors, or their employees, makes any warranty, express or implied, or assumes any legal liability or responsibility for the accuracy, completeness, or usefulness of any information, apparatus, product, or process disclosed, or represents that its use would not infringe privately owned rights. Further, neither the subject matter nor the content of this report reflects any policy, expressed or implied, by the United States Government.

LA-7779-M
Manual
(ISPO-53)

Special Distribution
Issued: June 1979

The High-Level Neutron Coincidence Counter (HLNCC): Users' Manual

Merlyn Stewart Krick
Howard O. Menlove

LOS ALAMOS NATL LAB. LIB.
3 9338 00193 7258



PREFACE

This publication is a systems, operations, and applications manual for the High-Level Neutron Coincidence Counter (HLNCC) and is intended as a detailed instruction manual for the user and assayer. A technical manual¹ is available for the designer and technician and a pictorial operating manual¹⁴ is available for safeguards inspectors. In addition a short paper summarizing the features and applications of the HLNCC has been published.¹⁹ For general discussions on thermal-neutron coincidence counting the reader is referred to the publications by Böhnelt,⁴ Ensslin et al.,¹¹ Sher,²⁹ Strain³¹ and the references therein.

The principle of operation of thermal-neutron coincidence counters and shift-register coincidence counter electronics is presented briefly in chapter 1. A description of the mechanical and electrical components and the general measurement characteristics of the system is given in chapter 2. Detailed operating procedures for setting up and testing the system are the subject of chapter 3; short-form operating procedures are listed in section 3.5; the instrument should not be operated until section 3.1 titled Warnings (page 35) is consulted. Chapter 4 discusses items of general interest for neutron coincidence measurements, such as statistical errors, deadtime corrections, and calibration procedures; this section also describes some specific measurements, such as the assay of plutonium in fuel rods.

Two versions of the HLNCC and associated shift-register electronics packages have been produced at LASL.^{12,21,22,33} After the development of the low-deadtime coincidence circuitry, the neutron detector was redesigned for higher counting efficiency; it now has more polyethylene than the earlier model and uses 18 ³He proportional counters instead of the original 24. The new shift-register electronics package contains a microcomputer and is interfaced to a Hewlett-Packard HP-97 programmable, printing calculator and to RS-232-C communications devices. This manual discusses only the new versions of these instruments.

Other LASL contributors to the development of the HLNCC include: Paul Collinsworth, who performed much of the breadboarding and testing of the electronics; Norbert Ensslin, who analyzed deadtime and multiplication effects; Mike Evans, who did the neutronic design calculations; John Foley, who instructed the International Atomic Energy Agency (IAEA) on the use of the earlier version of the HLNCC, wrote operating manuals for the instrument and studied the use of the HLNCC for uranium assay; Charles Hatcher, who promoted the HLNCC; Evita Medina Ortega, who performed assays and measured system parameters; Joseph Sapir, who did neutron multiplication calculations; Clint Shonrock, who did the mechanical design; Carmen Spirio, who managed the commercial development of the instrument; and Jim Swansen, who designed the HLNCC electronics.

CONTENTS

FIGURESviii
TABLES	xi
ABSTRACT	1
1. PRINCIPLE OF OPERATION	1
1.1 Introduction	1
1.2 Coincidence Counting	3
1.3 Summary	7
2. SYSTEM DESCRIPTION	7
2.1 Neutron Detector	7
2.2 Electronics	9
2.2.1 Introduction	9
2.2.2 System Configuration	9
2.2.3 Portable Electronics Package	11
2.2.3.1 Shift-Register Coincidence Logic	11
2.2.3.2 System Configuration	12
2.2.3.3 Panel Control and Test Functions	14
2.3 ²⁵² Cf Source	24
2.4 Measurement Characteristics	24
2.4.1 Absolute Detector Efficiency	24
2.4.2 Coincidence-Counting Efficiency	25
2.4.3 Counting Rates and Sensitivity for Plutonium Measurements	26
2.4.4 Detector Die-Away Time	28
2.4.5 Deadtime	29
2.4.6 Radial and Axial Detector Response	30
2.4.7 Accidental Counting Rates	30
2.4.8 Bias	32
2.5 HLNCC Specification Summary	34

3. OPERATING PROCEDURES	35
3.1 Warnings	35
3.2 Assembly	35
3.3 Power	38
3.4 Instrument Setup and Testing: Primary Procedures	39
3.5 Short-Form Setup Procedures	45
3.6 Instrument Setup and Testing: Secondary Procedures	48
3.6.1 Predelay Setting	48
3.6.2 Amplifier Test Outputs	50
3.6.3 Discriminator Output	50
3.6.4 High Voltage Test Point	50
3.6.5 Discriminator Test Point	50
3.7 Field Diagnostics	51
4. APPLICATIONS	57
4.1 Introduction	57
4.2 Counting Statistics Calculations	58
4.3 Coincidence-Gate-Length Selection	60
4.4 Deadtime Correction	62
4.5 ²⁴⁰ Pu-Effective	63
4.6 Matrix Effects	65
4.7 Multiplication Effects	67
4.7.1 Introduction	67
4.7.2 Multiplication in Plutonium Metal Samples	67
4.7.3 Multiplication in Samples with (α ,n) Backgrounds	69
4.8 Criticality	74
4.9 Total Plutonium	75
4.10 Calibration Procedures	77
4.11 HP-97 Programming	78
4.12 Examples	83
4.12.1 Plutonium in Fast Critical Assembly (FCA) Drawers	83
4.12.1.1 General Considerations	83
4.12.1.2 FCA Matrix Effects	86
4.12.1.3 Multiplication Effects	88
4.12.2 Plutonium in Cans or Bottles	88
4.12.3 Plutonium in Fuel Rods or Assemblies	89
APPENDIX: Two-Parameter Calibration Procedure	91
REFERENCES	97

FIGURES

- 1.1 a) Simplified relative neutron detection probability distribution.
b) Coincidence gate timing diagram.
- 1.2 Conceptual block diagram of shift-register coincidence counter logic.
- 1.3 Example of shift-register coincidence counting in the R+A gate (see text).
- 2.1 Schematic diagram of the HLNCC detector body showing the ^3He counter and cadmium liner locations.
- 2.2 HLNCC detector with one section of tubes partially removed.
- 2.3 HLNCC electronics package and HP-97 calculator.
- 2.4 High-voltage distribution and preamplifier box.
- 2.5 HLNCC system block diagram.
- 2.6 Detector-preamplifier configuration.
- 2.7 Block diagram of the HLNCC shift-register coincidence logic.
- 2.8 Simplified block diagram of the HLNCC electronics package.
- 2.9 Front panel of the electronics package.
- 2.10 Example of RS-232-C output to a Texas Instruments model 743 printing terminal.
- 2.11 Rear panel of the electronics package.
- 2.12 Diagram showing effect of finite gate width on coincidence counting efficiency.
- 2.13 Coincidence counting efficiency vs integral multiplicity for the HLNCC; the predelay is $4.5\ \mu\text{s}$ and the gate width is $32\ \mu\text{s}$.
- 2.14 Sensitivity of the HLNCC for the assay of ^{240}Pu -effective vs the background totals counting rate; sensitivity is defined as the mass of ^{240}Pu which is determined with a standard deviation of 25% in a 1000 s measurement.
- 2.15 Normalized real coincidence rate vs the gate width t_g for the HLNCC with end plugs. The points are measured values; the curve is a least-squares fit with $\tau = 33\ \mu\text{s}$.
- 2.16 Normalized logarithm of real coincidence rate vs the predelay t_d for the HLNCC with end plugs. The points are measured values; the line is a least-squares fit with $\tau = 33\ \mu\text{s}$.
- 2.17 Normalized logarithm of observed real coincidence counts per fission vs the totals rate \dot{T} . The points are measured values; the line is a least-squares fit to the form $\exp(-\delta\dot{T})$ with $\delta = 2.4\ \mu\text{s}$.

- 2.18 Axial totals and coincidence rates for the HLNCC with and without end plugs normalized to unity at the center of the detector. (From ref. 34.)
- 2.19 Radial coincidence rates with end plugs at the axial center of the HLNCC normalized to unity on the axis. (From ref. 24.)
- 2.20 Measured bias vs predelay for a totals rate of 50 kHz.
- 3.1 a) HLNCC detector body
b) top and bottom end plugs
c) preamplifier package
d) ^{252}Cf calibration source and positioning rod
e) HV cables
f) preamplifier cable
g) sample rotator
h) lab jack
- 3.2 Assembled operating system.
- 3.3 a) Top view of electronics package with the top cover removed showing the location of the predelay switches, the circuit board clamp and the nylon pin.
b) Electronics package with circuit boards rotated to their upright position.
c) Predelay switches on shift register circuit board.
- 3.4 Oscilloscope display of an amplifier test point signal with the ^{252}Cf calibration source in the detector. Vertical scale = 2 V/div; horizontal scale = 1 μs /div.
- 3.5 Oscilloscope display of the discriminator output test point signal with the ^{252}Cf source in the detector. Vertical scale = 2 V/div; horizontal scale = 0.2 μs /div.
- 4.1 Relative assay error vs coincidence gate length for a 600 g PuO_2 sample in the HLNCC. The error is normalized to 1.000 at the 42 μs minimum. The circles indicate the errors at 8, 16, 32, 64, and 128 μs .
- 4.2 Optimum gate length vs real/accidental coincidence ratio for the HLNCC.
- 4.3 Diagram of neutron multiplication experiment with two groups of fast critical assembly fuel plates.
- 4.4 Relative coincidence counts per second vs the separation between two groups of ZPPR fuel plates. The upper and lower curves show the data before and after correction for multiplication, respectively. (From ref. 35.)

- 4.5 Relative coincidence counts per gram of effective ^{240}Pu vs the PuO_2 sample mass. The upper and lower curves show the data before and after correction for multiplication, respectively. (From ref. 35).
- 4.6 ZPPR drawer containing two rows of plutonium plates interspersed with plates of depleted uranium, sodium, aluminum, carbon, and iron to mock up structure and coolant materials in a fast critical assembly. (From ref. 28.)
- 4.7 Measurement setup for a ZPPR drawer, showing the HLNCC for neutron coincidence counting and the IAEA intrinsic germanium detector with its collimator for measurement of plutonium gamma-ray line ratios. (From ref. 28.)
- 4.8 Axial coincidence efficiency for the two-position count to obtain a uniform sum over an extended region (40 cm). (From ref. 24.)
- 4.9 Mixed-oxide BWR fuel-rod assembly mockup for measurement with the HLNCC. (From ref. 25.)
- 4.10 Coincidence response measured with the HLNCC vs number of fuel rods in a $\text{PuO}_2\text{-UO}_2$ fuel assembly mockup. (From ref. 25.)
- A.1 Calibration curve and data points from PuO_2 standards.

TABLES

- 1.1 Spontaneous-Fission Data for the Plutonium Isotopes
- 2.1 Format for RS-232-C Data Transmission
- 2.2 Pin Assignments for Preamplifier Cable Connectors
- 2.3 Pin Assignments for RS-232-C Connector
- 2.4 Neutron Emission Probabilities for the Spontaneous Fission of ^{252}Cf , ^{238}Pu , ^{240}Pu , and ^{242}Pu
- 2.5 HLNCC Counting Rates for ^{240}Pu
- 2.6 Data From a Series of Measurements With a $^{241}\text{Am-Li}$ Source.
- 3.1 Parts List for HLNCC Operating System
- 3.2 HP-97 Program to Print HLNCC Data
- 3.3 HP-97 Program to Study the Stability of the HLNCC
- 3.4 Sample Output from HP-97 Stability Test Program
- 4.1 HLNCC Data Acquired with Combined ^{252}Cf and $^{241}\text{Am-Li}$ Sources
- 4.2 Neutron Emission Rates of Even-Mass Plutonium Isotopes Relative to ^{240}Pu
- 4.3 Relative Responses of a Shift-Register Coincidence Counter to the Even-Mass Plutonium Isotopes
- 4.4 Matrix Material Effects on HLNCC Assays
- 4.5 Correction of Matrix Material Effects on the Passive Neutron Assay of Plutonium in One-gallon Scrap Recovery Cans
- 4.6 (α, n) Neutron Production Rates from Various Light Elements
- 4.7 (α, n) Neutron Yields from the Oxides and Fluorides of Plutonium
- 4.8 HP-97 Basic Utility Routine for the HLNCC
- 4.9 Sample HP-97 Output from Basic Utility Routine
- 4.10 HP-97 Program to Calculate ^{240}Pu -Effective Mass from HLNCC Data and a Calibration Curve
- 4.11 HP-97 Register Usage for ^{240}Pu -Effective-Mass Program
- 4.12 Sample HP-97 Output from ^{240}Pu -Effective-Mass Program
- 4.13 Matrix Materials Effects on the Assay of Fast Critical Assembly Fuel Drawers with the HLNCC
- A.1 Data on PuO_2 Standards for Construction of Calibration Curve
- A.2 Convergence Data from Iterative, Least-Squares Fitting Procedure

THE HIGH-LEVEL NEUTRON COINCIDENCE COUNTER (HLNCC): USERS' MANUAL

by

Merlyn Stewart Krick and Howard O. Menlove

ABSTRACT

This manual describes the portable High-Level Neutron Coincidence Counter (HLNCC) developed at the Los Alamos Scientific Laboratory (LASL) for the assay of plutonium, particularly by inspectors of the International Atomic Energy Agency (IAEA). The counter is designed for the measurement of the effective ^{240}Pu mass in plutonium samples which may have a high plutonium content. The following topics are discussed: principle of operation, description of the system, operating procedures, and applications.

1. PRINCIPLE OF OPERATION

1.1 Introduction

The neutron coincidence counter assays plutonium-bearing material by detecting spontaneous fission neutrons from the plutonium in the presence of a random neutron background originating principally from (α, n) reactions in the material. The coincidence logic of the system separates the time-correlated spontaneous fission neutrons from these random neutrons. The counter is termed a high-level coincidence counter because it is designed to handle the high counting rates associated with large masses of plutonium (several kg).

When a plutonium isotope undergoes spontaneous fission, two or more neutrons may be emitted almost simultaneously. E.g., the probability $P(\nu)$ for ν neutrons to be emitted by the spontaneous fission of ^{240}Pu is shown below.⁷

<u>v</u>	<u>P(v) (%)</u>
0	4.9
1	21.4
2	32.1
3	28.2
4	11.2
5	2.1
6	0.1

For the major plutonium isotopes Table 1.1 shows the spontaneous-fission half-lives, the number of spontaneous fissions per gram per second, the average number of neutrons emitted per spontaneous fission, and the number of neutrons from spontaneous fission emitted per gram per second. Because the odd-mass plutonium nuclei (^{239}Pu and ^{241}Pu) have very low spontaneous-fission rates, the coincidence counter measures the even-mass (^{238}Pu , ^{240}Pu , and ^{242}Pu) plutonium content of a sample. The effective ^{240}Pu content of a sample is the mass of ^{240}Pu which would give the same response to the measurement system as the actual ^{238}Pu , ^{240}Pu , and ^{242}Pu content of the sample; effective ^{240}Pu content is discussed in section 4.5. The production of neutrons from (α ,n) reactions in plutonium-bearing materials is discussed in section 4.7.3.

The coincidence counter basically consists of a sample-counting cavity surrounded by ^3He -proportional-counter, thermal-neutron detectors embedded in cadmium-lined polyethylene slabs. Neutrons are absorbed by the polyethylene or cadmium of the counter, leak out the sides or ends of the counter, or are thermalized by the polyethylene and are captured by the ^3He proportional counters. The ^3He counter produces a detector pulse via the $^3\text{He}(n,p)^3\text{H}$ reaction. (For more information on ^3He proportional counters as neutron detectors, see references 26 and 27.) The fraction of neutrons emitted in the counter which produces detectable pulses from the ^3He proportional counters is the absolute detector efficiency ϵ and is approximately 12% for this counter.

The HLNCC is an example of a thermal-neutron counter because most of the neutrons are thermalized in the polyethylene before being captured in the ^3He tubes. The die-away time τ of the counter is the average lifetime of a neutron in the counter and is approximately 33 μs for the HLNCC. The probability for

TABLE 1.1

SPONTANEOUS-FISSION DATA FOR THE PLUTONIUM ISOTOPES^a

	<u>²³⁸Pu</u>	<u>²³⁹Pu</u>	<u>²⁴⁰Pu</u>	<u>²⁴¹Pu</u>	<u>²⁴²Pu</u>
Spontaneous fission half life (y)	4.9x10 ¹⁰	5.5x10 ¹⁵	1.17x10 ¹¹	5.0x10 ¹⁵	6.8x10 ¹⁰
Spontaneous fissions per gram per second	1100	0.010	471	0.011	800
Average number of prompt neutrons per fission ($\bar{\nu}_p$)	2.26	2.2	2.17	2.2	2.16
Number of sponta- neous fission neutrons per gram per second	2490	0.022	1020	0.024	1730

^a Data from reference 2.

a neutron to survive to time t following its emission is $\sim \exp(-t/\tau)$. The die-away time may also be defined as the time required for 63.2% ($1-e^{-1}$) of the neutrons to be captured or lost.

1.2 Coincidence Counting

Neutrons originating from (α, n) reactions in the sample, from room background, or from different fissions are uncorrelated in time (i.e., random), whereas neutrons emitted by a fissioning nucleus are time correlated. This correlation is exploited by the coincidence circuitry of the counter to distinguish between the spontaneous fission neutrons and the random background neutrons.

Figure 1.1a is a simplified diagram showing the relative probability for detecting a neutron at time t following the detection of another neutron for a fissioning source (or a fissioning-plus-random neutron source). Neutrons from a particular fission are detected at different times due to the detector die-away time. The probability for detecting another neutron from the same

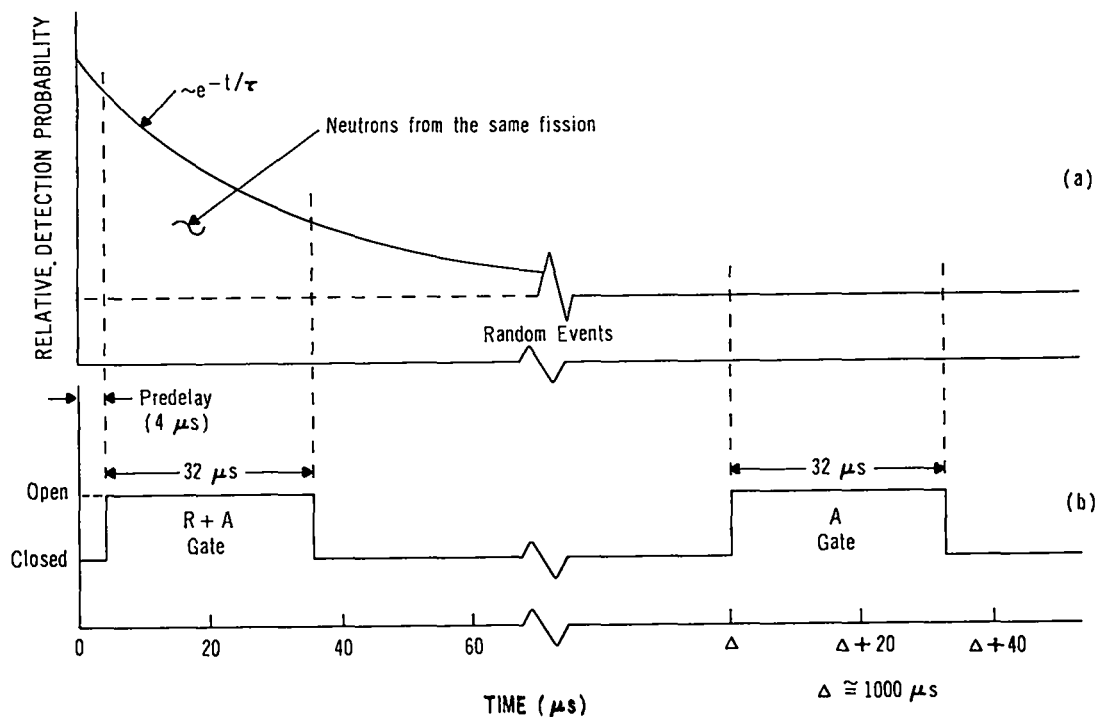


Fig. 1.1.

- a) Simplified relative neutron detection probability distribution.
 b) Coincidence gate timing diagram.

fission decreases approximately exponentially with time, whereas the probability for detecting a random neutron is constant with time (neglecting detector and amplifier recovery time). Note that random neutrons are present even for a purely fissioning source, because spontaneous fissions occur at random and neutrons detected from one fission can overlap those detected from another.

To distinguish correlated neutron events from random events (including neutrons from different fissions), two equal time periods are sampled by the coincidence circuit for each neutron detected (refer to Fig. 1.1b). The circuit has a predelay (about $4 \mu s$) after a neutron has been detected to allow the amplifiers to recover and prepare for detecting subsequent neutrons. The first time gate is then opened for typically $32 \mu s$ to detect the other neutron (or neutrons) associated with the fission event that gave rise to the first neutron. The neutrons detected during the first gate can be due to either time-correlated spontaneous fission events or random neutron events. As a result, the counts accumulated during this gate are called the R+A counts (Real fission counts + Accidental counts).

Following a long delay to ensure that any time correlation is removed, a second time gate is opened for the same duration as the first. The long delay should be at least several times as long as the detector die-away time and is

$\sim 1000 \mu\text{s}$ in the HLNCC. This second gate counts only random events and is called the accidental (A) gate. Since the two gates are the same length, the net difference in counts received during the two gates is the net real (R) coincidence count and is related to the spontaneous fission rate in the sample.

A conceptual block diagram of the shift-register coincidence counter logic is shown in Fig. 1.2. The circuitry is based on a concept of Böhnel⁴ as developed by Stephens, Swansen and East³² and improved by Swansen³³ for the present instrument.

The predelay, real-plus-accidental gate, long delay and accidental gate are all shift registers operating with a 2 MHz clock. E.g., a $32 \mu\text{s}$ gate uses 64 shift-register stages with $0.5 \mu\text{s}/\text{stage}$. Pulses from the ^3He counters, synchronized with the 2 MHz clock, travel through the four shift register sections from predelay to accidental gate. The predelay must be at least as long as the recovery time of the detector and amplifier stages; otherwise, the system deadtime affects the R+A gate more than the A gate and introduces a bias on the net real count R.

The number of pulses in the R+A and A gates at any time is determined by a pair of up-down counters. A pulse entering the R+A shift-register gate increments the counter; a pulse leaving the shift register decrements the counter. Thus the number of pulses in the R+A gate is just the count in the up-down counter. The accidental gate operates identically. The contents of the up-down counters are added to the R+A and A accumulator registers for each input pulse as indicated by the strobe arrows in Fig. 1.2. Because a neutron pulse which enters the predelay shift register is produced at a later time than those neutron pulses already in the gate shift register, the R+A and A accumulators actually tally events which precede the neutron pulses which strobe the accumulators; this is functionally equivalent to the conceptual timing diagram in Fig. 1.1.

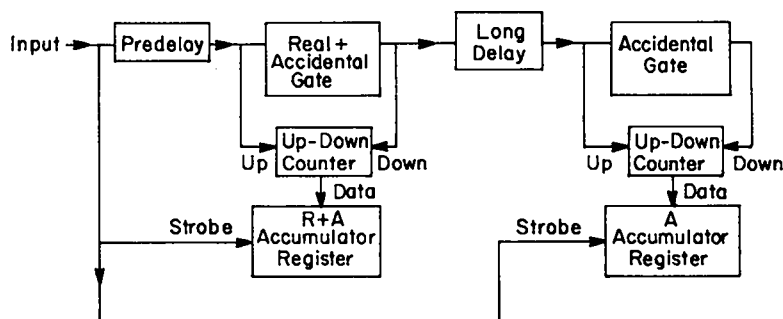


Fig. 1.2

Conceptual block diagram of shift-register coincidence counter logic.

The principal advantage of the shift-register coincidence circuitry is that each input pulse generates its own R+A and A sampling gates; it is not necessary for one gate to close before the next can open. This results in a very low system deadtime and allows operation of the HLNCC to counting rates of several hundred kHz.

The operation of the R+A coincidence gate is illustrated by an example in Fig. 1.3. The first nine pulses to enter the shift registers are displayed and numbered at the top of the diagram. The R+A coincidence gates generated by the first five pulses are shown below the pulse distribution. An arrow shows the coincidence gate associated with each pulse. Each gate opens after a predelay of $4.5 \mu\text{s}$ and remains open for $32 \mu\text{s}$. Coincident pulses are shown by solid circles within the gates. At the right of the figure the coincidence counts per gate and the accumulated R+A coincidence counts are listed. Note that the first five pulses produce twelve coincidence events; it is common for the coincidence rate to exceed the total count rate.

In practice, a variation of the conceptual block diagram shown in Fig. 1.2 is preferable for fabrication; the block diagram for the circuit used with the HLNCC is shown and discussed in section 2.2.3.1.

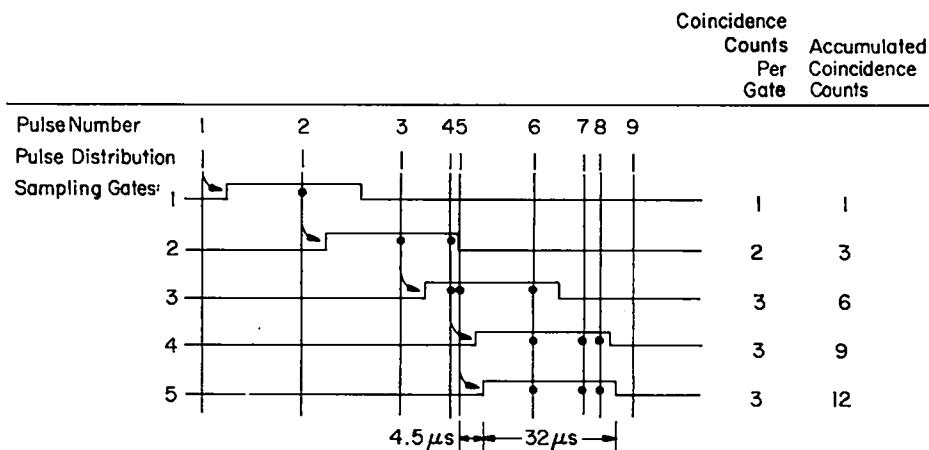


Fig. 1.3.

Example of shift-register coincidence counting in the R+A gate (see text).

1.3 Summary

This chapter has shown that the spontaneous fission of the even-mass plutonium isotopes produces correlated detector events in a thermal-neutron coincidence counter and that these events can be distinguished from random background events at high counting rates and with low deadtime by the use of shift-register coincidence counting electronics.

Ideally the net real coincidence count rate would be directly proportional to the plutonium mass of the sample and independent of geometry and chemical composition. This is only approximately the case. The interpretation of coincidence counter data is discussed in chapter 4.

2. SYSTEM DESCRIPTION

2.1 Neutron Detector

The HLNOC was designed for field assay by International Atomic Energy Agency (IAEA) inspectors, so restrictions were placed on its weight and size to facilitate transportation and handling. To give flexibility in the physical configuration to accommodate a wide variety of sample containers, the counter is fabricated as six separate slabs that form an hexagonal well* as shown in Figs. 2.1 and 2.2. The width of the well (18 cm minimum) accepts most PuO_2 sample cans, fast critical assembly fuel drawers, and some fuel rod assemblies; the slabs can be further separated to accept larger containers or, alternatively, two slabs can be used in a sandwich configuration to measure small samples or fuel rods. Three 2.5-cm-diam by 50-cm-long ^3He tubes (pressurized to 4 atm) are embedded in each section of the hexagon.

The HLNOC detector has three 0.4-mm-thick cadmium liners. The outside liner shields the detector from low-energy room background neutrons; the liner on the inside of the well prevents low-energy neutrons from returning to the sample after scattering in the detector and then causing neutron multiplication; the middle cadmium liner lowers the detector die-away time and reduces the sensitivity to hydrogenous materials in the sample or container.

* - During the original design of the counter, a square configuration consisting of four rectangular slabs was considered. Acceptable values for ϵ and τ were obtained, but only with excessive weight relative to the hexagonal counter.¹²

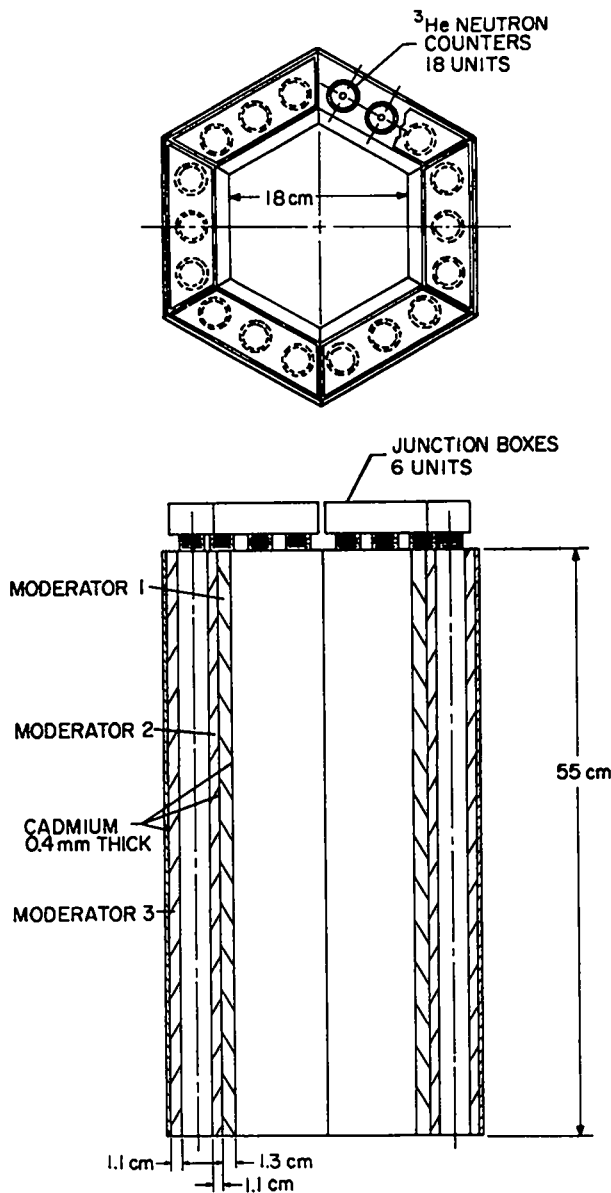


Fig. 2.1.
Schematic diagram of the HLNCC detector body showing the ^3He counter and cadmium liner locations.

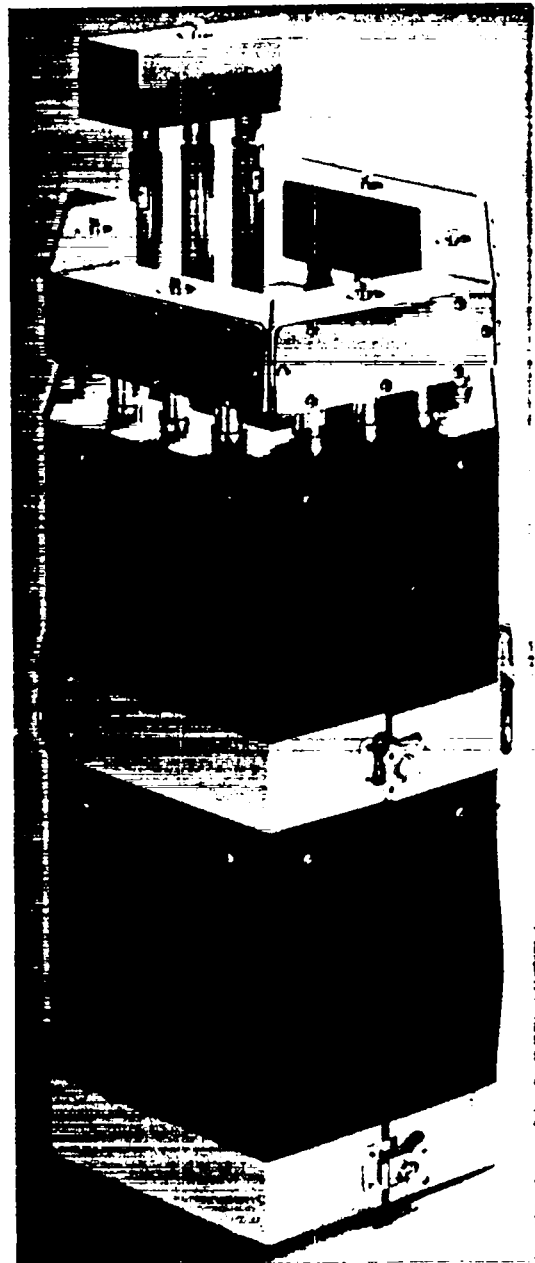


Fig. 2.2.
HLNCC detector with one section of tubes partially removed.

The HLNCC is frequently used to assay PuO_2 in cans. Because the fill height of the PuO_2 in the cans varies with the mass and density in the can, it is desirable to have the detector's counting efficiency insensitive to these height variations. The dependence of the efficiency on axial position can be greatly reduced by placing plugs at both ends of the well to reflect into the detector neutrons that would otherwise escape through the ends. The

effect of the end plugs is greater for the HLNCC than for most neutron well counters because the HLNCC is under-moderated and hence the polyethylene in the plugs has a large effect. The HLNCC units have 7.6-cm-thick end plugs with cadmium liners; these plugs are used for applications in which a flat central response is desired. The effect of the end plugs on the detector characteristics is discussed in section 2.4.6.

Design calculations for well counters show that in the low-efficiency range (<10%) the efficiency is directly proportional to the weight and die-away time (or the CH_2 thickness).¹³ The present detector weighs approximately 35 kg, including 7 kg for the end plugs. This particular efficiency and weight was chosen to give a total neutron counting rate of roughly 80,000 counts/s for a 2-kg PuO_2 sample (20% ^{240}Pu). The detector measures approximately 65 cm high by 35 cm wide.

2.2 Electronics

2.2.1 Introduction. The portable electronics package supporting the neutron detector is shown with its associated Hewlett-Packard HP-97 programmable calculator in Fig. 2.3. Except for the detector preamplifiers, all of the electronic subsystems required for the operation of the counter are contained in the portable electronics package. The preamplifiers are contained in a high-voltage distribution and preamplifier box, which mounts to the side of the detector (see Fig. 2.4). The system will operate with or without the HP-97 calculator. The electronics package contains high- and low-voltage power supplies, six channels of amplification and discrimination, shift-register coincidence circuitry, and control, display and readout circuitry.

The package is operable either from a 100/115/230-Vac, 50/60-Hz supply or from a dc supply with a 10- to 30-V output; power consumption is approximately 24W. The instrument case is 9 cm high, 29 cm wide, and 43 cm deep. The instrument and calculator are packed in an instrumentation suitcase for transportation.

2.2.2 System Configuration. A system block diagram is shown in Fig. 2.5. The hexagonal neutron detector contains three ^3He proportional counters per segment for a total of 18 ^3He counters. The three counters in each segment are connected in parallel; six channels of preamplification, amplification, and discrimination are used. Multiple analog channels are required to reduce the system deadtime; this is an important consideration in high-count-rate

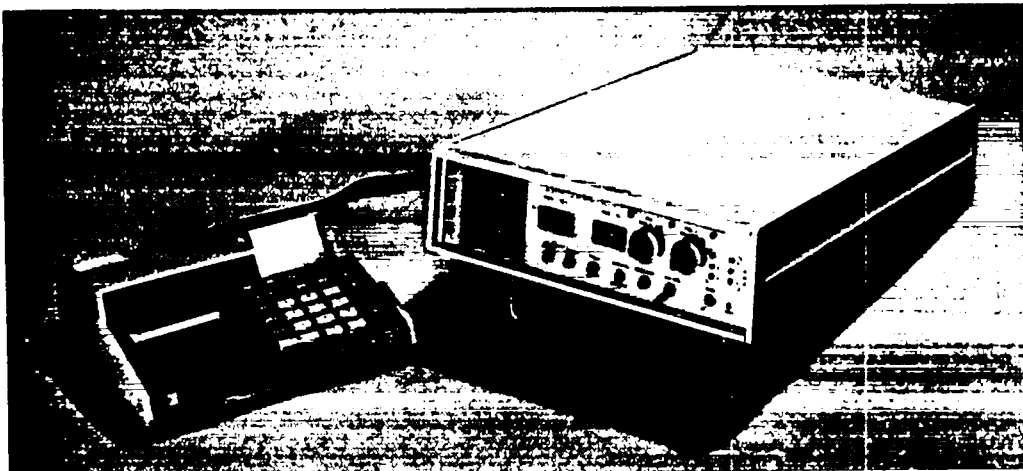


Fig. 2.3.
HLNCC electronics package and HP-97 calculator.

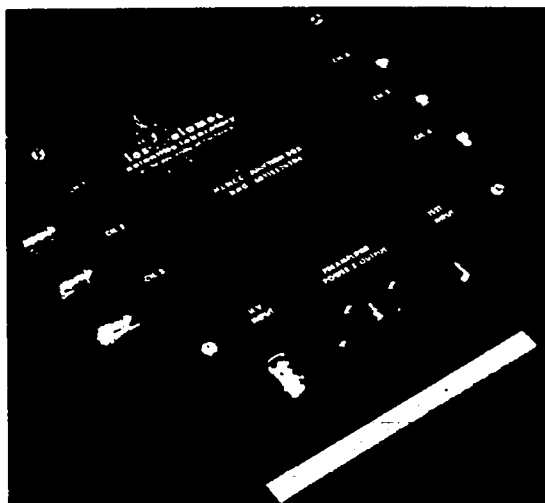


Fig. 2.4.
High-voltage distribution and pre-amplifier box.

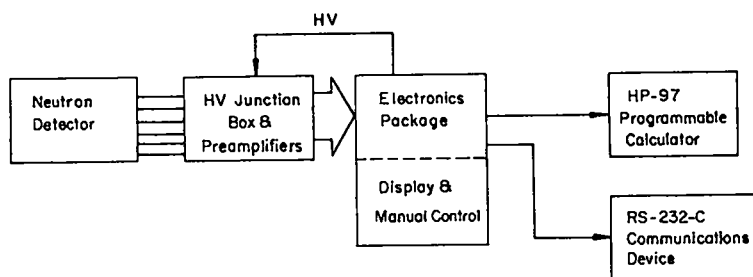


Fig. 2.5.
HLNCC system block diagram.

applications. A single high-voltage power supply is used for all ^3He tubes. A schematic diagram of the detector-preamplifier configuration is shown in Fig. 2.6.

The high voltage is distributed to three ^3He tubes in each of six distribution boxes located at the top of the neutron detector. Six high voltage coaxial cables (RG-59/U with SHV connectors) connect the distribution boxes to the preamplifier junction box. These cables are as short as practicable to reduce the system noise.

Two cables connect the electronics package to the preamplifier box. One is the high-voltage cable (RG-59/U with SHV connectors) and one is a bundled cable which contains six twisted pairs of wire carrying the preamplifier signals and two twisted pairs which supply the preamplifier power. The data acquired by the instrument are displayed on the front panel of the electronics package. Optionally an HP-97 programmable calculator and/or an (RS-232-C)-compatible communication device may also be used for data output.

2.2.3 Portable Electronics Package.

2.2.3.1 Shift-Register Coincidence Logic. A block diagram of the shift-register (SR) coincidence logic is shown in Fig. 2.7. The circuit differs from the conceptual block diagram of Fig. 1.2 in one important aspect: instead of having two gates separated by a long delay with a single strobe applied simultaneously to each, one gate is used with two strobes separated by a long delay. The two arrangements are functionally equivalent; however, the single gate version is considerably less complex to construct.

The standardized logic input pulses are first synchronized with the 2 MHz SR clock and then sent through the predelay SR and gate SR. The predelay SR has a selectable length from 1.0 to 32.5 μs in 0.5 μs steps. The gate SR has a selectable length of 8, 16, 32, 64, or 128 μs . A preset timer allows measurements to be made from 1 to 9×10^9 s. The timer in conjunction with the stop, start, and reset controls opens an AND gate to allow the collection of data. Each pulse passing through the AND gate is counted in the totals scaler.

The up-down counter continuously monitors the contents of the gate and presents the data simultaneously to the real-plus-accidental (R+A) and accidental (A) accumulators. Each pulse passing through the AND gate immediately strobes the R+A accumulator and then, following a 1024 μs delay, strobes the A accumulator. Each strobe adds the contents of the up-down counter to the R+A or A accumulator.

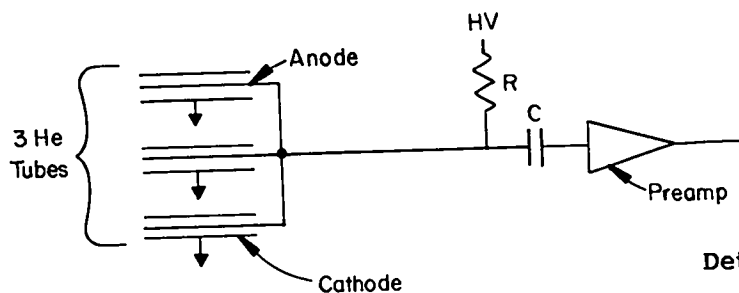


Fig. 2.6.
Detector-preamplifier configuration.

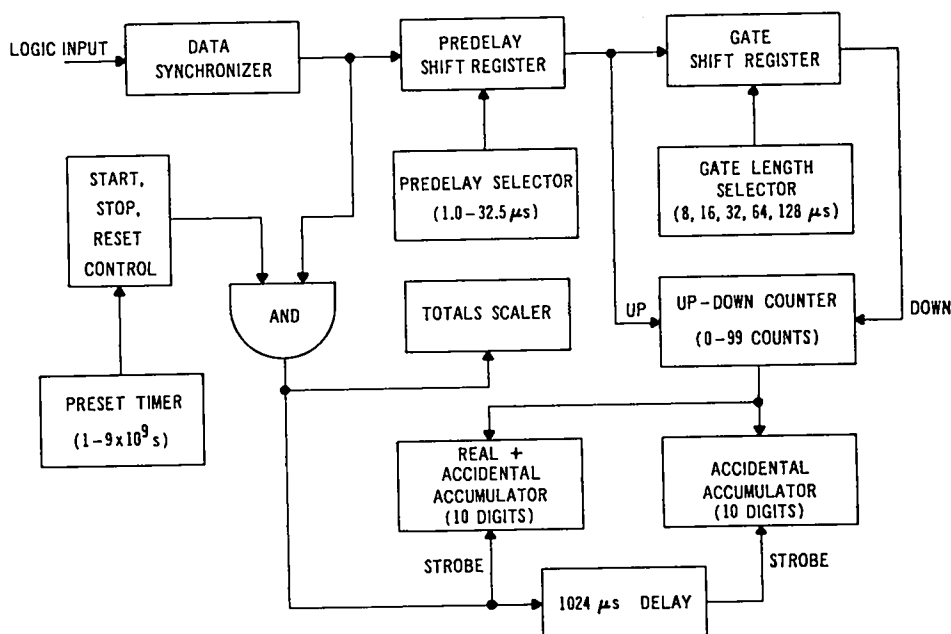


Fig. 2.7.
Block diagram of the HLNCC shift-register coincidence logic.

2.2.3.2 System Configuration. A simplified block diagram of the electronics package is shown in Fig. 2.8. The block labeled "SR coincidence logic" is described in the previous section. The six preamplifier input signals are processed by six linear, pulse-shaping amplifiers (with 0.5 μs time constants) and six discriminators. The amplified signals can be monitored at six amplifier test points on the front panel of the instrument. The discrimination level can be set by a helipot on the front panel and verified from a test point on the front panel. The six discriminator outputs are ORed to form a single standard logic signal for the SR coincidence logic; this signal is also available on the front and rear panels. A rear-panel switch allows either internal or external signals to be used as inputs to the SR logic; the external signal, if used, is supplied via a rear-panel coaxial

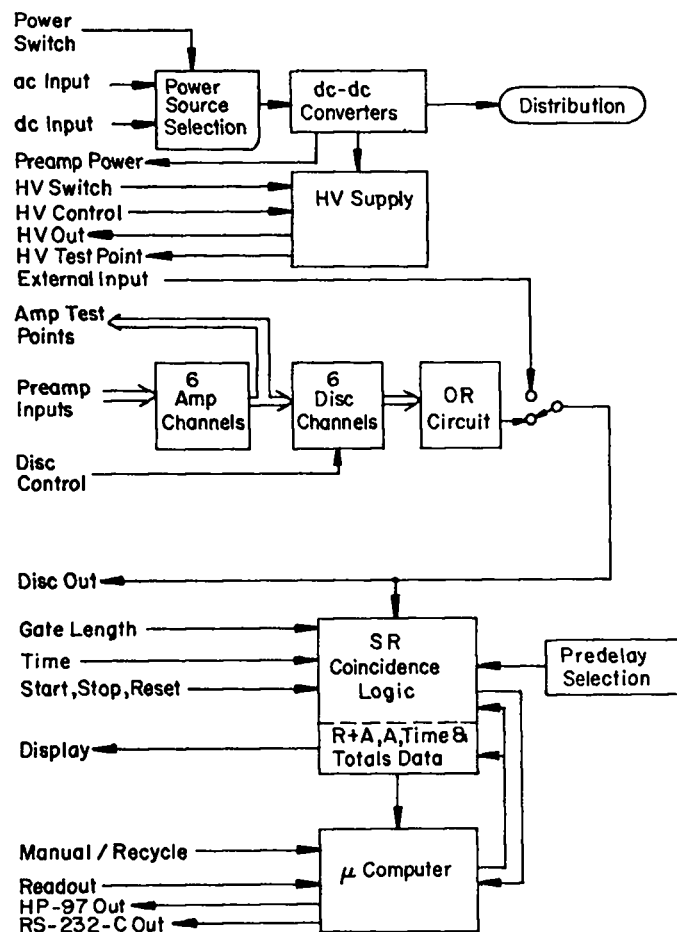


Fig. 2.8.

Simplified block diagram of the HLNCC electronics package.

connector. The measurement time and gate length are selected by front-panel switches. The predelay, which is infrequently changed, is set by internal switches.

The data from the SR logic circuit (measurement time, total counts, real-plus-accidental coincidence counts, and accidental coincidence counts) are displayed simultaneously on the front panel. A microcomputer in the system is used in part to read the data from the display circuitry and transmit the results to an HP-97 calculator and an (RS-232-C)-compatible communications terminal or data link, such as to a computer. The microcomputer also controls the SR logic circuit when the instrument is in the recycle mode. In the manual or the recycle mode, the instrument can be controlled by the start, stop, and reset pushbuttons.

The instrument derives all dc power supply voltages from dc-dc converters operating off of a single dc supply voltage, which is obtained either from a 100/115/230 Vac, 50/60 Hz line or a battery. The high voltage is set by a

front-panel helipot and monitored from a front-panel test point. A separate locking toggle switch is provided to turn the high voltage off and on. Pre-amplifier power is supplied through a rear panel connector, which also contains the preamplifier signal connections.

2.2.3.3 Panel Control and Test Functions

2.2.3.3.1 Front Panel (refer to Fig. 2.9).

a. Display.

A four-line, seven-segment, light-emitting-diode (LED) display continuously shows the counting time in seconds, the total counts, the real-plus-accidental (R+A) coincidence counts, and the accidental (A) coincidence counts. Nine digits are displayed for the total counts, R+A, and A; six digits are displayed for the counting time. Leading zeros are suppressed, except for the least significant two decades. (Note: The total count, R+A, and A internal registers are ten digits long. The most significant digit (MSD) is rarely used and is not displayed; however, the MSD is read out to the HP-97 and RS-232-C interfaces. Also, although the counting time is only displayed to six digits (11 days maximum), the time can be set to 9×10^9 s (300 years, if desired; however, only six digits are read out to the HP-97 and RS-232-C interfaces).

b. Gate width switch [GATE (μ s)].

The width of the R+A and A SR gates is set by a thumbwheel switch. Switch settings are labeled 8, 16, 32, 64 and 128 and correspond to the gate widths in μ s.

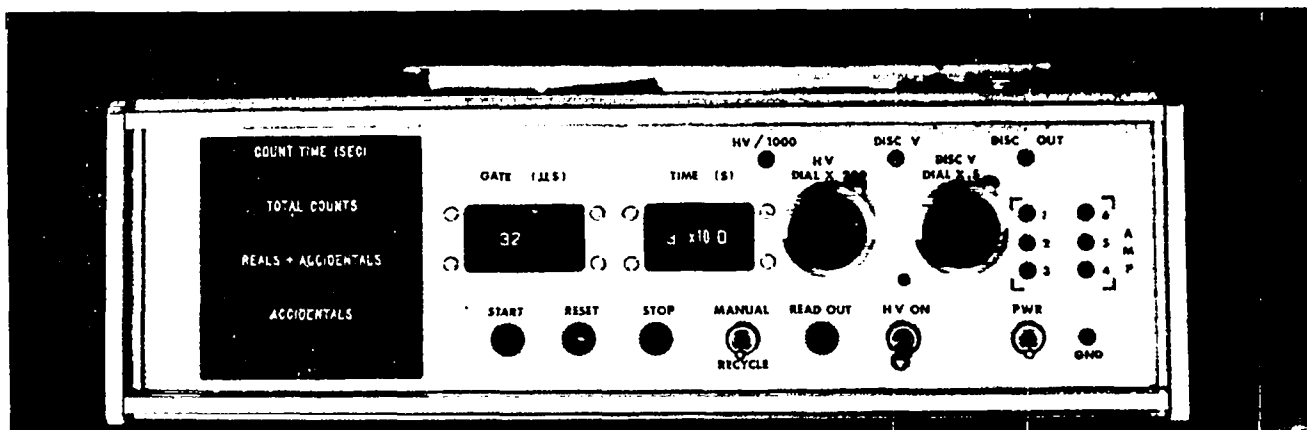


Fig. 2.9.

Front panel of the electronics package.

c. Counting time switch [TIME (s)] .

The counting time can be preset from 1 second to 9×10^9 seconds (real time) by two thumbwheel switches with the format $\text{time(s)} = M \times 10^N$, where M is an integer from 1 through 9 and N is an integer from 0 through 9. E.g., if $M=3$ and $N=2$, the counting time is $3 \times 10^2 = 300$ s. Once started, the counter will stop when the preset time is reached.

d. START pushbutton.

The START pushbutton is a lighted pushbutton switch with a green lens cap. When the counter is running the green lamp is turned on. The counter can be started by depressing the START pushbutton. Once the counter is started, depressing the START pushbutton has no effect.

e. RESET pushbutton.

The RESET pushbutton is a lighted pushbutton switch with a yellow lens cap. Depressing the pushbutton resets the instrument by clearing all internal counters and registers. In particular, the front panel display is set to zero by the RESET switch. The RESET function operates whether the counter is running or stopped. The RESET function does not also stop the counter.

The yellow pushbutton light is not directly related to the RESET operation, but rather is used as a "fault" light. The up-down counter in the SR circuitry (see Fig. 2.7) should never count below zero. If an underflow occurs in this counter, the yellow fault light is turned on to indicate a counting error. The light remains on until the RESET pushbutton is depressed. (The operation of the fault circuit and the yellow lamp may be tested as follows. Operate the instrument with a neutron source in the detector or with a pulse generator applied to the external input. Throw the gate width selector switch up and down while the counter is running. This induces meaningless counts into the up-down counter and will cause frequent fault indications.)

f. STOP pushbutton

The STOP pushbutton is a lighted pushbutton switch with a red lens cap. When the counter is stopped the red light is turned on. The counter can be stopped by depressing the STOP pushbutton. Once the counter is stopped, depressing the STOP pushbutton has no effect.

g. READOUT pushbutton

The READOUT pushbutton is a lighted pushbutton switch with a clear lens cap and is operative only when the counter is stopped. Pressing the READOUT button causes the data to be transferred to the HP-97 and RS-232-C interfaces in that order. The READOUT lamp is turned on whenever a readout operation is in progress.

HP-97 data transfer

The reader is referred to the Hewlett-Packard publication "The HP-97 Programmable Printing Calculator Owner's Handbook and Programming Guide"¹⁶ for details concerning the HP-97 calculator. During a readout operation the time, totals, R+A, and A data are deposited in storage registers R1, R2, R3, and R4, respectively. A "label A" command is then given to start the user's program, which must be written to begin at label A. Six digits are transferred to the time register (R1), and ten digits are transferred to each of the registers R2, R3, and R4. The transfer time is approximately 5 seconds.

RS-232-C data transfer

The time, totals, R+A, and A data are transmitted at 300 baud in serial ASCII code through a standard EIA RS-232-C interface⁹ to drive a communications terminal or data link. The character transmission format is 7 bits/character, with 1 stop bit and even parity.

The microcomputer in the coincidence counter electronics package performs a subtraction of the accidental count from the real-plus-accidental count to form the real coincidence count (R), which is also transmitted. The data transmission format was chosen for viewing convenience when a printing terminal is used as the output device. A heading is printed once above the data line with the first readout which occurs after the RESET pushbutton is depressed while the counter is stopped. An example of the output is shown in Fig. 2.10.

For applications where a computer is used to accept the data via the RS-232-C interface, a knowledge of the exact format is useful; this format is shown in Table 2.1.

h. Manual/recycle switch

Whenever the SR counter stops, the microcomputer (μ C) examines the position of the manual/recycle toggle switch. If the switch is in the manual position, the μ C takes no action and waits for the START, RESET, or

TIME (SEC)	TOTALS	R+A	A	R
100	5,429,551	9,434,629	9,431,381	3,248
100	5,433,513	9,451,419	9,451,432	13
100	5,435,395	9,455,132	9,453,843	1,289
100	5,435,839	9,455,361	9,454,108	1,253
100	5,435,491	9,450,644	9,456,796	6,152
100	5,428,382	9,424,580	9,431,672	7,092
100	5,435,379	9,453,580	9,456,961	3,381
100	5,435,781	9,457,066	9,452,868	4,198
100	5,433,240	9,442,463	9,449,416	6,953
100	5,434,813	9,449,812	9,449,635	177
100	5,428,752	9,429,836	9,436,235	6,399
100	5,430,499	9,436,131	9,439,372	3,241
100	5,431,687	9,440,230	9,441,765	1,535
100	5,430,330	9,436,963	9,437,042	79
100	5,432,385	9,440,434	9,438,321	2,213
100	5,431,579	9,442,290	9,441,092	1,198
100	5,432,717	9,443,717	9,439,934	3,783
100	5,430,072	9,431,897	9,435,264	3,367
100	5,435,525	9,452,374	9,458,696	6,322
100	5,432,013	9,444,617	9,441,984	2,633
100	5,431,926	9,447,186	9,446,618	568
100	5,436,518	9,458,436	9,457,521	915
100	5,429,265	9,428,332	9,431,116	2,784
100	5,437,762	9,458,153	9,463,529	5,376
100	5,433,760	9,447,853	9,452,030	4,177
100	5,434,378	9,445,836	9,454,648	8,812
100	5,434,214	9,449,930	9,452,990	3,060
100	5,432,585	9,448,504	9,440,864	7,640
100	5,433,277	9,441,988	9,444,851	2,863
100	5,430,789	9,434,120	9,435,891	1,771
100	5,432,720	9,442,932	9,438,444	4,488
100	5,435,965	9,456,908	9,457,268	360
100	5,430,559	9,437,011	9,437,312	301
100	5,430,259	9,436,280	9,439,229	2,949
100	5,434,201	9,450,602	9,447,933	2,669
100	5,430,506	9,438,181	9,433,033	5,143
100	5,431,959	9,442,913	9,440,165	2,748
100	5,429,776	9,441,885	9,438,852	3,033
100	5,434,080	9,447,483	9,452,740	5,257

Fig. 2.10.

Example of RS-232-C output to a Texas Instruments model 743 printing terminal.

READOUT pushbutton to be depressed. If the switch is in the recycle position, the μ C tests whether the SR was stopped manually or timed out. If the SR timed out, a readout occurs to the HP-97 and RS-232-C interfaces. If a readout is the first following a depression of the RESET pushbutton when the SR is stopped, then the title line is transmitted to the RS-232-C interface before the data. In the recycle mode the SR is reset and started by the μ C after the readout is completed.

i. High voltage dial (HV DIALx200)

The high voltage for the ^3He proportional counters is set by a 10-turn helipot and is equal (in volts) to the dial setting times 200. The normal operating voltage is 1500 V, which corresponds to a dial setting of 7.50 ($7\frac{1}{2}$ turns). A locking arm on the upper right of the dial prevents accidental changes in the high voltage setting. In its lower position the arm locks the dial and in its upper position releases the dial.

TABLE 2.1

FORMAT FOR RS-232-C DATA TRANSMISSION

Heading Format

1. Carriage return
2. Line feed
3. 1 space
4. TIME(SEC)
5. 10 spaces
6. TOTALS
7. 13 spaces
8. R+A
9. 15 spaces
10. A
11. 16 spaces
12. R
13. 1 space

Data Format*

1. Carriage return
2. Line feed
3. 3 spaces
4. Time: 3 digits, comma, 3 digits
5. 3 spaces
6. Totals: 1 digit, comma, 3 digits, comma, 3 digits, comma, 3 digits
7. 3 spaces
8. R+A : same as for totals
9. 3 spaces
10. A : same as for totals
11. 3 spaces
12. + or - sign
13. R : same as for totals

* Leading zeros and commas are replaced by spaces.

j. High voltage switch (HV ON)

The high voltage (HV) switch is a locking toggle switch which provides separate control of the high voltage supply for the proportional counters. The HV is derived from the low-voltage power supplies and, therefore, the position of the switch has no significance when the main power is turned off. During normal operation the HV switch may be left in the ON (upward) position. When the SR logic is used with an external input or when internal operations are performed on the instrument (such as calibration or diagnostics), it may be desirable to operate the instrument

without the HV. The locking toggle switch prevents the HV from being turned on or off accidentally; the handle is pulled to release the lock. The LED lamp above the switch is lit whenever the HV is turned on.

k. High voltage test point (HV/1000)

A buffered dc level equal to one thousandth of the HV output is connected to the HV test point. This level is normally +1.500 V and is supplied from a low impedance source; it can be measured with a digital voltmeter or a standard 20 000 Ω/V volt-ohm-meter. Because the signal is derived from the HV power supply, it is a direct measure of the HV output and not simply the HV dial setting.

l. Discriminator dial (DISC V DIAL x .5)

The discrimination level for all six discriminators (see Fig. 2.8) is set by a 10-turn helipot and is equal (in volts) to one-half the dial setting. The nominal discrimination level is +1.5 V, which corresponds to a dial setting of 3.0 (3 turns). A locking arm on the upper right of the dial prevents accidental changes in the discrimination level. In its lower position the arm locks the dial and in its upper position releases the dial.

m. Discrimination test point (DISC V)

The output of the discrimination voltage test point is equal to the discrimination level and is used to verify the correct discrimination level. The +1.5 V nominal signal can be monitored with a digital voltmeter or a standard 20 000 Ω/V volt-ohm-meter.

n. Discriminator output test point (DISC OUT)

The ORed output of the six discriminators (see Fig. 2.8) is connected to the discriminator output test point. The same signal is also available on the coaxial connector on the rear panel labeled DISC OUT. The rectangular pulses should be +3 V in amplitude and 150 ns wide. See section 3.6.3 for information on the use of this test point.

o. Amplifier test points (AMP 1,2,3,4,5,6)

The outputs of the six bipolar pulse shaping amplifiers (see Fig. 2.8) are connected to the amplifier test points for inspection. These pulses have the same amplitude as those presented to the discriminators. See section 3.6.2 for details on the use of these test points.

p. Ground test point (GND)

The ground test point provides a convenient ground connection for use with the other test points.

q. Power switch (PWR)

The power toggle switch controls all power to the instrument. Power is on when the switch is in the upward position. No power-on indicator lamp is provided because the LED display serves that purpose. When the power is switched on, the microprocessor is automatically started and test messages are transmitted to the output devices.

2.2.3.3.2 Rear Panel (refer to Fig. 2.11)

a. High voltage output (HV OUT)

The high voltage (+1500 V nominal) for the ^3He proportional counters is provided through this SHV connector. The voltage is switched by the front panel toggle switch labeled "HV ON".

WARNING: When the HV is switched off, the HV decreases with a ~ 5 minute time constant. If high-voltage cables are disconnected when the HV is turned on or before the HV power supply has discharged, high voltages will remain on the HV electrodes. High-voltage electrodes should be purposely grounded before touching any HV conductor in the instrument or the center pin of the SHV connectors.

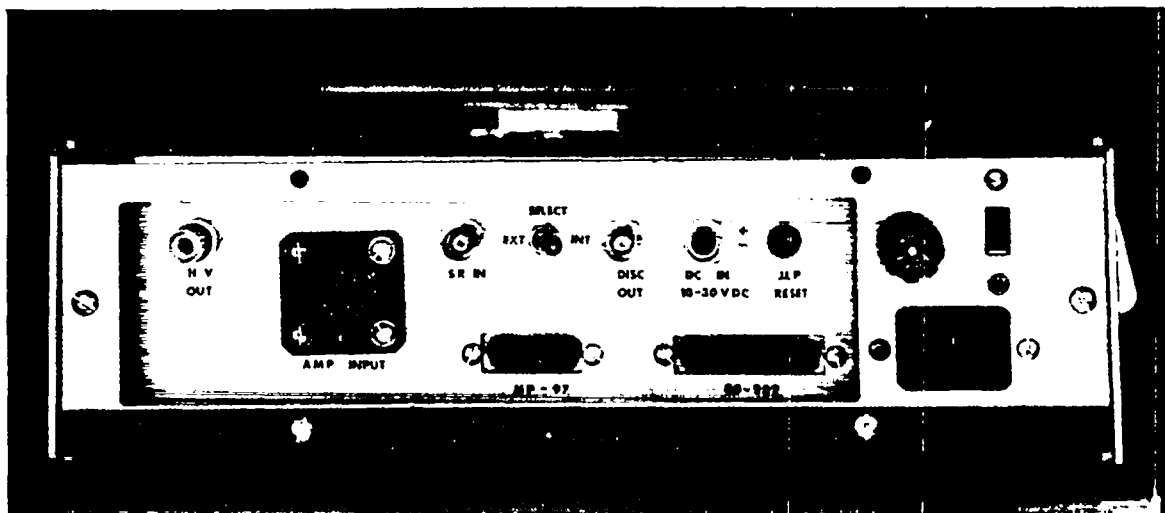


Fig. 2.11.

Rear panel of the electronics package.

b. Amplifier input and preamp power (AMP INPUT)

The circular, multi-conductor connector labeled AMP INPUT connects the six preamplifiers located in the preamplifier box (see Fig. 2.4) to the six pulse-shaping amplifiers in the main chassis. The preamplifier signals are carried on six twisted pairs of wire. Two other twisted pairs carry the power supply voltages to the preamplifier box. Table 2.2 shows the pin assignments for the connector. To fasten the cable to the preamplifier box or main chassis, align the connectors as required by the polarizing keyway, push the connectors together, and twist the outer front shell of the plug clockwise to its locked position. The cable is symmetrical and thus may be connected in either direction.

c. External/internal select switch SELECT(EXT/INT)

The input to the SR coincidence logic circuits may be either the Ored output of the six discriminators or a logic signal from an external source (see Fig. 2.8). The SELECT toggle switch is set to the one desired. When the internal source is selected, any external signal cable should be detached from the connector labeled SR IN (see item d below).

TABLE 2.2

PIN ASSIGNMENTS FOR PREAMPLIFIER CABLE CONNECTORS

<u>Pin Designation</u>	<u>Function</u>
A	channel 1 preamplifier signal
B	channel 1 signal ground
C	no connection
D	no connection
E	-15 V
F	power supply return
G	power supply return
H	+15 V
J	channel 6 signal ground
K	channel 6 preamplifier signal
L	channel 4 preamplifier signal
M	channel 3 preamplifier signal
N	channel 3 signal ground
P	channel 2 preamplifier signal
R	channel 2 signal ground
S	channel 5 signal ground
T	no connection
U	channel 4 signal ground
V	channel 5 preamplifier signal

d. Shift-register input (SR IN)

If an external source is desired as the input to the SR logic circuitry, the signal is supplied through the BNC connector labeled SR IN. The SELECT toggle switch must be set to EXT and the signal source must be compatible with standard transistor-transistor logic (TTL).

e. Discriminator output (DISC OUT)

The ORed output of the six discriminators (see Fig. 2.8) is connected to the BNC connector labeled DISC OUT. The same signal is also available on the test jack on the front panel labeled DISC OUT. The rectangular pulses should be +3 V in amplitude and 150 ns wide. This output may be used as the external input to another SR coincidence electronics package to compare operating characteristics. Note, however, that two SR circuits will not produce identical results, since the SR clocks are not synchronized. (Also see Sec. 3.6.3.)

f. DC input (DC IN 10-30 VDC + -)

The electronics package will operate from either a 100/115/230 Vac, 50/60 Hz power source or a dc source with output voltage between 10 and 30 Vdc and a power rating of at least 24 W. Power is supplied through a BNC twinax connector. The positive lead is connected to the female pin and the negative lead is connected to the male pin of the socket as indicated by the + and - symbols on the panel. (The BNC twinax connector is not properly installed in Fig. 2.11.) If shielded, twisted-pair wire is used to supply the dc power, the shield normally is connected to the ground conductor of the BNC connector.

g. Microprocessor reset (μ P RESET)

The microprocessor (μ P) reset button is a pushbutton switch with a yellow lens cap. Normally the μ P RESET button is not used, because the μ P has an automatic power-up reset function. A temporary (soft) μ P failure may be overcome either by pressing the μ P RESET button or by turning the power off and then on again. Either of these operations should restart the system and transmit test messages to the output devices. (See section 3.4 for details.) The μ P reset button is provided primarily for diagnostic purposes.

h. HP-97 interface connector (HP-97)

A custom interface is used to transmit data from the SR electronics to the HP-97 calculator. Those HP-97 calculators which have been modified for this purpose have a 16-wire ribbon cable connected into them. The other end of the ribbon cable is terminated with a connector which mates with the rear-panel connector labeled HP-97.

i. RS-232-C connector (RS-232)

The connector labeled RS-232 is compatible with standard EIA RS-232-C⁹ communications terminals and data links. The small, light-weight Texas Instruments model 743 printing terminal is well-suited for use with the system. Data may also be transmitted directly to a computer through this interface. The data format is given in Table 2.1 and section 3.4. Connector pin assignments are shown in Table 2.3.

j. Fuse holder (FUSE)

The instrument is equipped with a $\frac{1}{2}$ A, slo-blo fuse.

k. Power line voltage

select switch (115/230)

The instrument will operate from 100/115/230 Vac, 50/60 Hz power sources. It is only necessary to throw the voltage select switch to the desired position before turning the power on. If the line voltage is 100 Vac, the 115 Vac position is satisfactory.

1. Power line connector

The instrument is supplied with a detachable, three-wire, power-line cord.

WARNING: The grounding connector on the cord is connected to the instrument chassis. If an adapter is used with the cord to obtain power from a different type of power receptacle,

TABLE 2.3

PIN ASSIGNMENTS FOR RS-232-C CONNECTOR^a

<u>Pin Number^b</u>	<u>Function</u>
2	data in ^c
3	data out
4	internally connected to pin 8
7	signal ground
8	internally connected to pin 4

a Refs. 1 and 9.

b Pin numbers not listed have no connection.

c The microcomputer read-only-memory could be programmed to accept commands, but presently is programmed for output only.

it is essential that precautions are taken to ensure that the instrument case is firmly connected to earth ground. In some instances this may require the connection of a separate grounding wire from the instrument case to a conductor known to be at earth ground.

2.3 ^{252}Cf Source

A ^{252}Cf source is shipped with the detector to allow calibration of the detector at the measurement site without the shipment of plutonium standards (see section 4.9). The neutron energy spectrum from the spontaneous fission of ^{252}Cf is a close approximation to that from the spontaneous fission of the plutonium isotopes. The 2.64 year half-life of ^{252}Cf is long enough to make the source practical for long-term use and short enough so the source size is small. In addition to the calibration function, the ^{252}Cf source is useful for verifying the correct operation of the instrument and for studying its stability.

The source is attached to a small brass rod and is screwed into a threaded hole in the top or bottom end plug of the detector. This provides a secure storage location for the ^{252}Cf and also provides some neutron shielding. When the ^{252}Cf is used as a calibration source, it is removed from the end plug (with the brass rod) and is screwed into a small bracket attached to the interior of the detector well. This bracket holds the source in a stable and repeatable position near the center of the well. The source strength and calibration date are stamped on the brass rod.

The ^{252}Cf sources are fabricated with an initial source strength of 4×10^4 neutrons/s ($\sim 9 \mu\text{Ci}$ or $\sim 0.02 \mu\text{g}$). This strength provides adequate counting rates for rapid detector calibration for several years, but presents a low radiological hazard and few transportation problems. The active source deposit is ^{252}Cf oxide in a ceramic matrix; it is doubly encapsulated in a stainless steel capsule (9.4 mm diam x 38.6 mm long including a 5 mm long 10-32 stud).

2.4 Measurement Characteristics

2.4.1 Absolute Detector Efficiency. The absolute detector efficiency ϵ is defined as the fraction of source neutrons which produce detectable pulses in the ^3He proportional counters. This fraction is measured with a calibrated neutron source; a deadtime correction may be required (see sections 2.4.5 and 4.4). The efficiency depends on the energy of the source neutrons, the

position of the source in the detector, and the position of the detector relative to the floors, walls, shielding materials, etc. The efficiency of the detector as measured with a calibrated ^{252}Cf source at the center of the sample well was measured to be 12.1% with the end plugs in place and 11.8% without the end plugs; in both cases the detector was resting in its vertical position on a concrete floor with no scattering materials near its sides. Raising the detector 40 cm above the floor decreases its efficiency to 11.9% with end plugs and 11.4% without end plugs. Placing a 10-cm-thick slab of polyethylene against one side of the detector increases the efficiency to 12.5% with end plugs on a concrete floor. The accuracy of the neutron source strength for the ^{252}Cf source used for these measurements is 10% (1 σ).

2.4.2 Coincidence Counting Efficiency. The coincidence counting efficiency ϵ_c of the shift register (SR) circuit is the average number of real coincidence counts measured per event after deadtime correction and is given by the equation^{4,17}

$$\epsilon_c = \epsilon^2 e^{-t_d/\tau} (1 - e^{-t_g/\tau}) \sum_{v=2}^{\infty} \binom{v}{2} P(v), \quad (2-1)$$

where

ϵ = absolute detector efficiency,

t_d = predelay,

τ = detector die-away time (see section 2.4.4),

t_g = gate width,

v = number of neutrons emitted per event,

$$\binom{v}{2} = \frac{v(v-1)}{2}, \text{ and}$$

$P(v)$ = probability for v neutrons to be emitted per event.

$P(v)$ values for ^{252}Cf and the even-mass plutonium isotopes are tabulated in Table 2.4. The two terms involving τ account for the finite length of the coincidence-counting gate, as shown in Fig. 2.12.

Note that ϵ_c is very sensitive to ϵ , since ϵ_c varies as ϵ^2 , and also that ϵ_c is very sensitive to the fission multiplicity, since $\binom{v}{2}$ varies approximately as v^2 for large values of v . Figure 2.13 shows the coincidence counting efficiency as a function of multiplicity for the HLNCC; the predelay is chosen as 4.5 μs and the gate length as 32 μs .

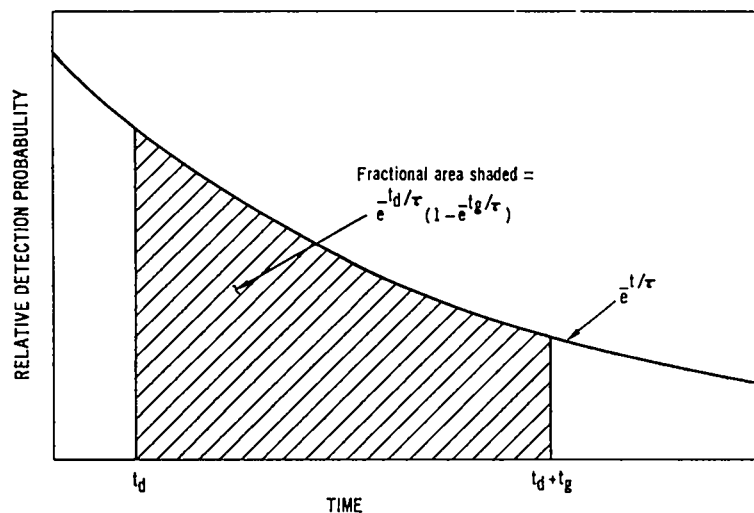


Fig. 2.12.

Diagram showing effect of finite gate width on coincidence counting efficiency.

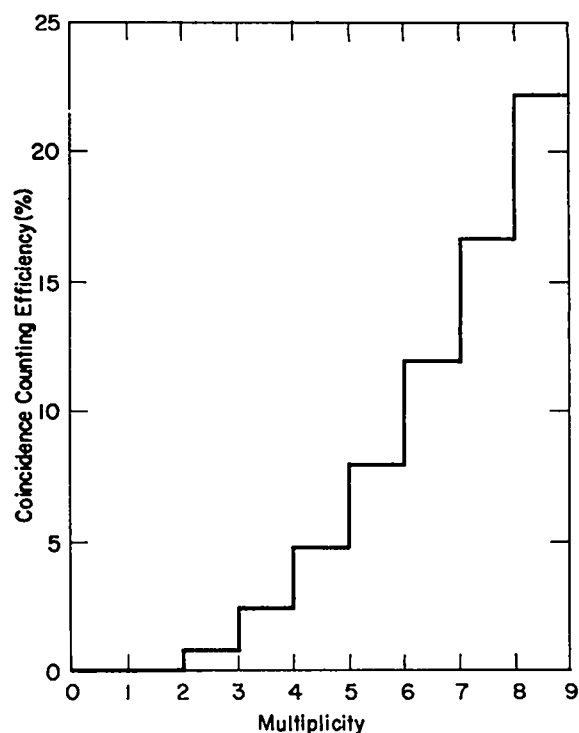


Fig. 2.13.

Coincidence counting efficiency vs integral multiplicity for the HLNCC; the predelay is 4.5 μ s and the gate width is 32 μ s.

2.4.3 Counting Rates and Sensitivity for Plutonium Measurements. The totals and coincidence counting rates for ^{240}Pu were measured in the HLNCC on a concrete floor with end plugs installed and with a 10 g plutonium metal sample having a ^{240}Pu -effective content of 0.529 g. The results are presented in Table 2.5. A gate width of 32 μ s and a predelay of 4.5 μ s were used.

The sensitivity of the HLNCC is arbitrarily defined for this publication as the mass of ^{240}Pu -effective which is determined with a 25% standard deviation in a 1000 s measurement. The sensitivity is plotted vs the background totals counting rate in Fig. 2.14. The background rate includes room background and sample background (primarily due to (α, n) reactions in the sample).

TABLE 2.4

NEUTRON EMISSION PROBABILITIES FOR THE SPONTANEOUS FISSION
OF ^{252}Cf , ^{238}Pu , ^{240}Pu , AND ^{242}Pu

Number of Neutrons	Emission Probability (%)			
	^{252}Cf ^a	^{238}Pu ^b	^{240}Pu ^a	^{242}Pu ^b
0	0.5	4.4	4.9	6.3
1	0.4	17.5	21.4	19.2
2	13.8	38.4	32.1	35.1
3	22.3	23.7	28.2	32.4
4	35.6	12.4	11.2	3.3
5	17.5	3.6	2.1	3.6
6	7.1	-	0.1	-
7	2.2	-	-	-
8	0.6	-	-	-

^a Reference 7.

^b Reference 15.

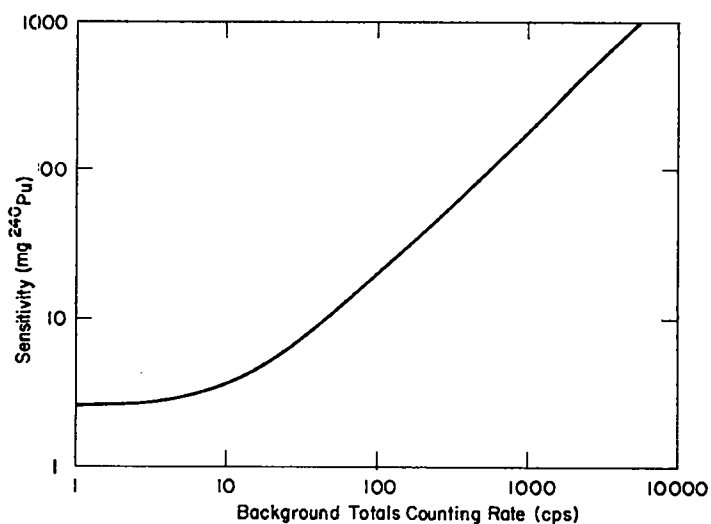


Fig. 2.14.
Sensitivity of the HLNCC for the
assay of ^{240}Pu -effective vs the
background totals counting rate;
sensitivity is defined as the mass
of ^{240}Pu which is determined with
a standard deviation of 25% in a
1000 s measurement.

2.4.4 Detector Die-Away Time. The detector die-away time τ is the average lifetime of a neutron produced in the detector well. As shown in Eq. (2-1), the coincidence-counting efficiency ϵ_c contains τ in the factor $[1 - \exp(-t_g/\tau)]$ where t_g is the gate width. Therefore, the die-away time can be determined experimentally by counting a ^{252}Cf (or other spontaneously fissioning) source with various gate lengths, while holding the source position, predelay, and counting time constant. A normalized plot of the real coincidence rate versus t_g for the HLNCC with end plugs is shown in Fig. 2.15. The points are measured values; the solid curve is a least-squares fit to the data. The die-away time which gives the best fit is $\tau = 33\mu\text{s}$.

TABLE 2.5

HLNCC COUNTING RATES FOR ^{240}Pu

Conditions

1. gate width = $t_g = 32\mu\text{s}$
2. predelay = $t_d = 4.5\mu\text{s}$
3. end plugs installed
4. detector vertical on concrete floor
5. sample at center of detector

Sample data

1. Pu mass = 10.01 g (metal)
2. $^{238}\text{Pu} = 0.01\%$
3. $^{239}\text{Pu} = 94.48\%$
4. $^{240}\text{Pu} = 5.24\%$
5. $^{241}\text{Pu} = 0.20\%$
6. $^{242}\text{Pu} = 0.01\%$
7. ^{240}Pu effective = 0.529 g

Measured counting rates

$$\frac{\text{total counts}}{s \cdot g \text{ } ^{240}\text{Pu}} = 115$$

$$\frac{\text{real coincidence counts}}{s \cdot g \text{ } ^{240}\text{Pu}} = 6.3$$

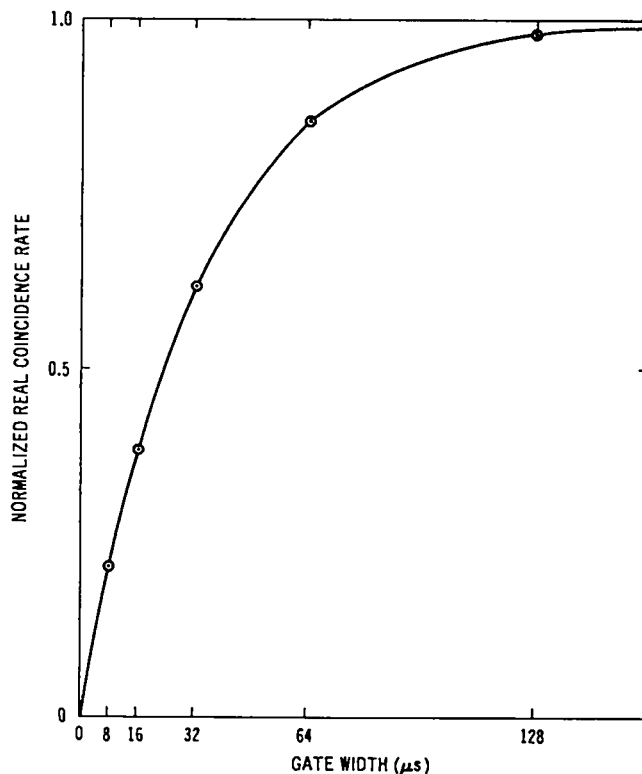


Fig. 2.15.
Normalized real coincidence rate vs the gate width t_g for the HLNCC with end plugs. The points are measured values; the curve is a least-squares fit with $\tau = 33\mu\text{s}$.

As shown in Eq. (2-1), the die-away time also appears in the factor $\exp(-t_d/\tau)$, where t_d is the pre-delay. The die-away time can therefore be determined by measuring the real coincidence response from a ^{252}Cf source for various predelay times while holding other parameters constant. A normalized semilog plot of such a measurement is shown in Fig. 2.16, where the absolute value of the slope of the straight line is the reciprocal of the die-away time τ (33 μs).

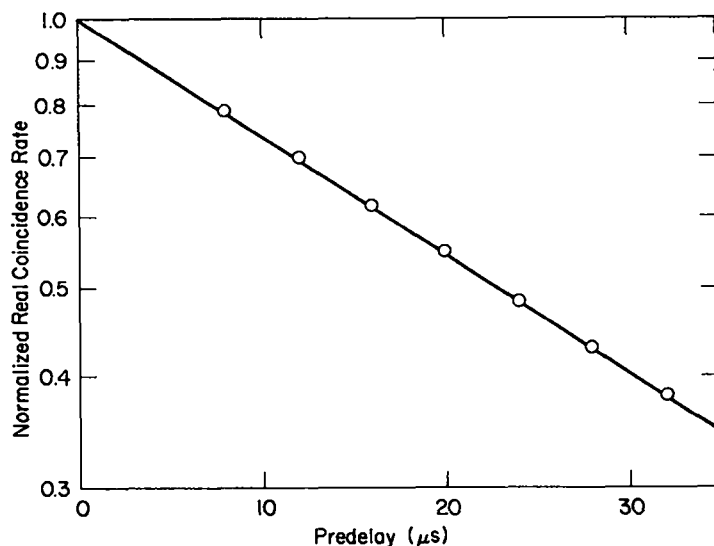


Fig. 2.16. Normalized logarithm of real coincidence rate vs the predelay t_d for the HLNCC with end plugs. The points are measured values; the line is a least-squares fit with $\tau = 33 \mu\text{s}$.

2.4.5 Deadtime. If an amplifier test point on the front panel of the instrument is used to monitor the output pulse shape on an oscilloscope (see Fig. 3.4), it is observed that approximately 4 μs are required for the pulses to recover to the baseline. A second pulse generated by the same group of ^3He tubes within 2 μs of the first pulse has only a small probability of retriggering the discriminator. The effective time for which the discriminator is unresponsive to the second pulse is the detector-amplifier (or totals) deadtime. The total detector-amplifier deadtime for the HLNCC is approximately 0.6 μs and is much less than that for a single channel because six independent channels are operating in parallel.

When the ORed output of the six discriminators is synchronized with the 2 MHz clock for injection into the shift registers, some pulses are lost because not more than one pulse per 0.5 μs can be accepted by the shift registers. The synchronizer is thus another source of deadtime.

The coincidence deadtime, which is of greater interest for measurements than the totals deadtime, can be determined experimentally by measuring the real coincidence rate from a ^{252}Cf source in the presence of varying amounts of a random neutron background. A high-count-rate experiment was performed in which a ^{252}Cf source was measured with zero, one, two, three, and four $^{241}\text{Am-Li}$ sources. The results are shown in Fig. 2.17.

The observed real coincidence counts per fission R^f is described very well by the expression

$$R^f = R_O^f e^{-\delta \dot{T}},$$

where

\dot{T} = observed totals counting rate

δ = effective coincidence deadtime

R_O^f = real coincidence counts per fission at zero counting rate.

The effective coincidence deadtime δ determined in this manner is 2.4 μ s.

Note that the HLNOC was driven to a counting rate of about a quarter MHz. The presence of deadtime effectively reduces the coincidence counting efficiency ϵ_c by the factor $e^{-\delta \dot{T}}$.

2.4.6 Radial and Axial Detector Response. The totals and real coincidence rates were measured with a ^{252}Cf source to determine the axial and radial detector response curves.³⁴ The axial responses are shown in Fig. 2.18, with and without the detector end plugs. The coincidence rate falls off more rapidly than the totals rate at the ends of the detector, because the coincidence-counting efficiency is proportional to the square of the absolute detector efficiency. With the end plugs installed the totals efficiency falls off $\sim 7\%$ from the center of the detector to the end of the active region; the coincidence efficiency falls off $\sim 14\%$. Without the end plugs, the coincidence efficiency falls off $\sim 47\%$.

The radial coincidence-counting efficiency is shown in Fig. 2.19. At the axial center of the detector the efficiency ϵ_c is $\sim 20\%$ higher at the interior counter wall than on the axis.

2.4.7 Accidental Counting Rates. If the totals counting rate \dot{T} is constant and the accidental gate width is t_g , then the average number of pulses in the accidental gate is $\dot{T}t_g$. Because every incoming pulse generates a gate, the accidental rate \dot{A} is $\dot{T}(\dot{T}t_g)$ or $\dot{A} = \dot{T}^2 t_g$. Thus, if the background does not change during a measurement, the accidental rate can be calculated from the totals rate.

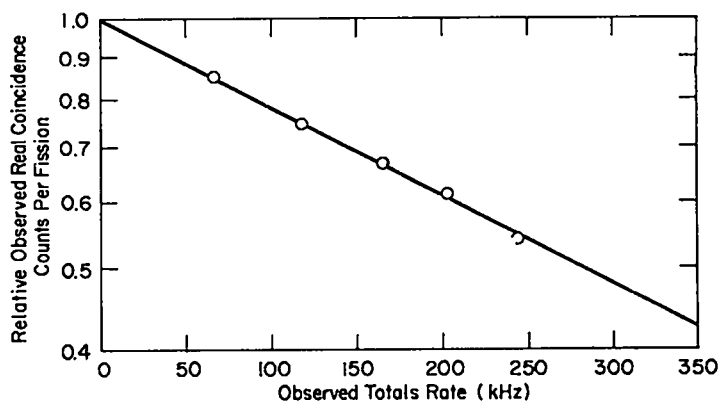


Fig. 2.17.

Normalized logarithm of observed real coincidence counts per fission vs the totals rate \dot{T} . The points are measured values; the line is a least-squares fit to the form $\exp(-\delta \dot{T})$ with $\delta = 2.4 \mu$ s.

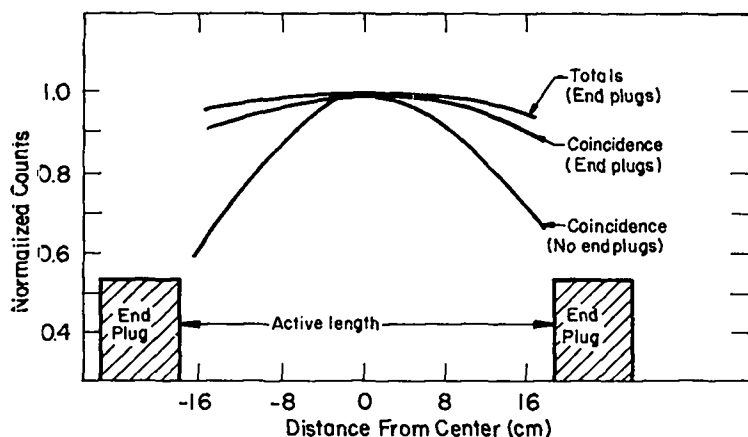


Fig. 2.18.
Axial totals and coincidence rates for the HLNCC with and without end plugs normalized to unity at the center of the detector. (From ref. 34.)

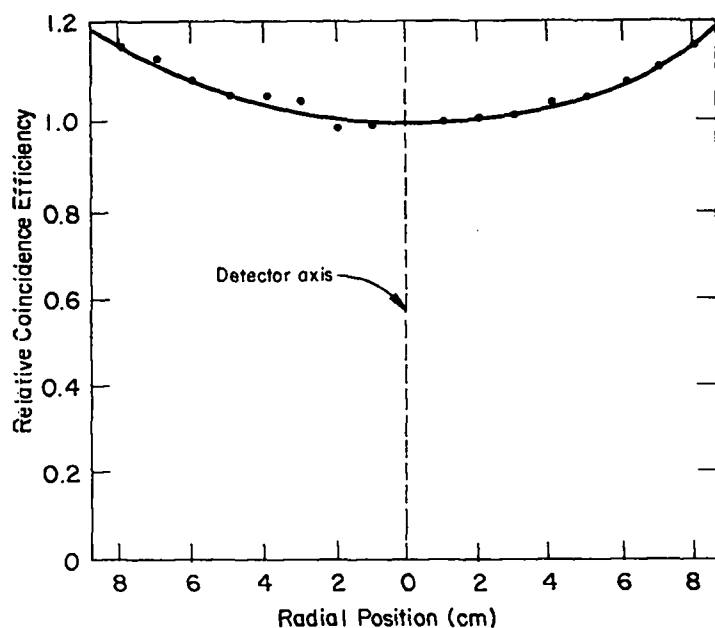


Fig. 2.19.
Radial coincidence rates with end plugs at the axial center of the HLNCC normalized to unity on the axis. (From ref. 24.)

The totals and accidentals counts are measured and displayed separately by the HLNCC, however, because the measured accidental counts are correct whether the background is constant or not. It is a recommended practice to compute the accidental rate from the totals rate and to compare the result with the measured value. This provides a check on the constancy of the background and the correct operation of the coincidence logic circuitry. Agreement between the calculated and measured accidental counting rates should be better than 0.01%, unless the background is changing or the error introduced by counting statistics is larger.

2.4.8 Bias. As explained in section 1.2, a predelay is required in the shift-register, coincidence-counting electronics to avoid a bias in the R+A gate relative to the A gate due to the recovery time of the detectors and amplifiers. Because detector pulses return to their baseline exponentially and because detector pulses can pile up, a true zero-bias condition cannot be achieved theoretically. In practice, however, several microseconds of predelay are adequate to reduce the bias to $< 0.01\%$ at a totals counting rate of 50 kHz.

Bias is determined by counting a random neutron source, such as the (α, n) source $^{241}\text{Am-Li}$. The (α, n) -induced fissions and the spontaneous fissions of the plutonium impurities in the sources used are insignificant for this purpose relative to the (α, n) reaction rate. Table 2.6 shows data accumulated in a series of 100 s measurements with a 5×10^5 neutrons/s source of $^{241}\text{Am-Li}$ and a 6 μs predelay. Because the neutron source is random, the R+A and A coincidence counts should be the same within errors due to counting statistics. The average difference between the R+A and A counts for the data shown is 0.01%.

Similar measurements were performed with various predelays and long measurement times at two high counting rates. A plot of bias vs predelay for a 50 kHz totals counting rate is shown in Fig. 2.20; the plot for a 150 kHz rate is almost identical. Too small a predelay introduces a noticeable negative bias, whereas too large a predelay reduces the coincidence-counting efficiency unnecessarily. A predelay of 4.5 μs is a suitable compromise for most counting situations with the HLNCC. The predelay is set by internal switches and for routine operations need not be changed from the normal 4.5 μs setting.

Bias is not readily determined without a random neutron source, because random pulse generators are not sufficiently random to provide a useful test. It is recommended that an initial bias check be performed with a random neutron source before field use of the HLNCC. After the check and a normalization measurement with the ^{252}Cf calibration source, a bias change sufficiently large to influence assay results may be detectable from changes in the R+A and A counting rates measured with the ^{252}Cf calibration source. Care must always be exercised for measurements where the R+A and A counts differ by a few percent or less.

TABLE 2.6

DATA FROM A SERIES OF MEASUREMENTS WITH AN $^{241}\text{Am-Li}$ SOURCE

<u>Time (s)</u>	<u>Totals</u>	<u>R+A</u>	<u>A</u>		<u>R</u>
100	5,429,551	9,434,629	9,431,381	+	3,248
100	5,433,513	9,451,419	9,451,432	-	13
100	5,435,395	9,455,132	9,453,843	+	1,289
100	5,435,839	9,455,361	9,454,108	+	1,253
100	5,435,491	9,450,644	9,456,796	-	6,152
100	5,428,382	9,424,580	9,431,672	-	7,092
100	5,435,379	9,453,580	9,456,961	-	3,381
100	5,435,781	9,457,066	9,452,868	+	4,198
100	5,433,240	9,442,463	9,449,416	-	6,953
100	5,434,813	9,449,812	9,449,635	+	177
100	5,428,752	9,429,836	9,436,235	-	6,399
100	5,430,499	9,436,131	9,439,372	-	3,241
100	5,431,687	9,440,230	9,441,765	-	1,535
100	5,430,330	9,436,963	9,437,042	-	79
100	5,432,385	9,440,434	9,438,221	+	2,213
100	5,431,579	9,442,290	9,441,092	+	1,198
100	5,432,717	9,443,717	9,439,934	+	3,783
100	5,430,072	9,431,897	9,435,264	-	3,367
100	5,435,525	9,452,374	9,458,696	-	6,322
100	5,432,013	9,444,617	9,441,984	+	2,633
100	5,431,926	9,447,186	9,446,618	+	568
100	5,436,518	9,458,436	9,457,521	+	915
100	5,429,265	9,428,332	9,431,116	-	2,784
100	5,437,762	9,458,153	9,463,529	-	5,376
100	5,433,760	9,447,853	9,452,030	-	4,177
100	5,434,378	9,445,836	9,454,648	-	8,812
100	5,434,214	9,449,930	9,452,990	-	3,060
100	5,432,585	9,448,504	9,440,864	+	7,640
100	5,433,277	9,441,988	9,444,851	-	2,863
100	5,430,789	9,434,120	9,435,891	-	1,771
100	5,432,720	9,442,932	9,438,444	+	4,488
100	5,435,965	9,456,908	9,457,268	-	360
100	5,430,559	9,437,011	9,437,312	-	301
100	5,430,259	9,436,280	9,439,229	-	2,949
100	5,434,201	9,450,602	9,447,933	+	2,669
100	5,430,506	9,438,181	9,433,033	+	5,148
100	5,431,959	9,442,913	9,440,165	+	2,748
100	5,429,776	9,441,885	9,438,852	+	3,033
100	5,434,080	9,447,483	9,452,740	-	5,257

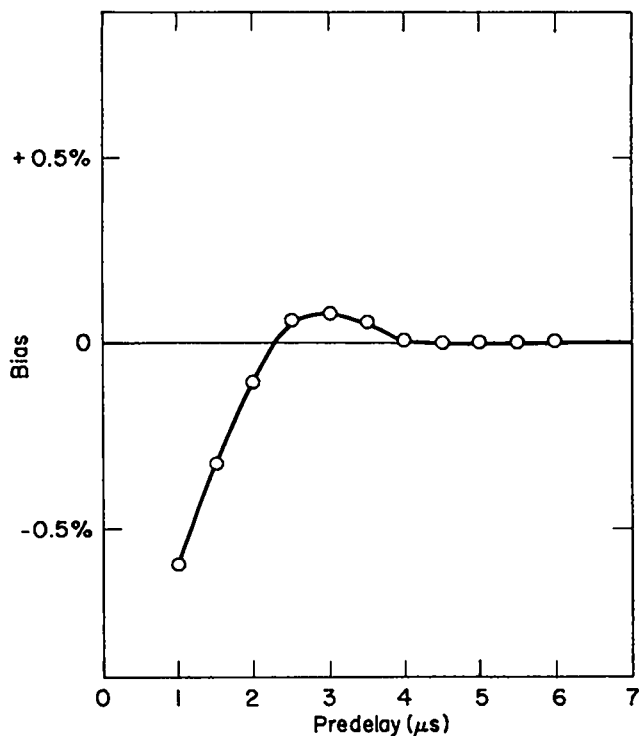


Fig. 2.20.
Measured bias vs predelay for a
totals rate of 50 kHz.

2.5 HLNCC Specification Summary

2.5.1 Detector.

- | | |
|---|--|
| a. Size | ~ 35 cm wide x 65 cm high |
| b. Weight | ~ 35 kg |
| c. Neutron detectors | 18 4-atm ^3He proportional counters |
| d. Absolute neutron
detection efficiency | ~ 12% |
| e. Die-away time | ~ 33 μs |
| f. Coincidence counting
rate | ~ 6 counts/(s \cdot g ^{240}Pu) |
| g. Coincidence deadtime | ~ 2.4 μs |

2.5.2 Electronics Package

- | | |
|-----------------------|-------------------------------|
| a. Size | ~ 30 cm w x 10 cm h x 45 cm d |
| b. Weight | ~ 8 kg |
| c. Power sources | 100/115/230 Vac or 10-30 Vdc |
| d. Power requirements | 24 W |

- | | | |
|----|------------------|---|
| e. | Subsystems | HV power supply, amplifiers, discriminators, shift-register coincidence electronics, readout and display circuitry. |
| f. | Primary controls | Gate length, counting time, predelay, HV, discrimination level. |
| g. | Display | Counting time, total counts, real-plus-accidental coincidence counts, accidental coincidence counts. |
| h. | Interfaces | HP-97 programmable calculator and RS-232-C data communications devices. |

3. OPERATING PROCEDURES

3.1 Warnings

The HLNCC should not be operated until the following warnings are heeded.

1. The HLNCC produces high voltage. Read the Sec. 2.2.3.3.2a titled High voltage output (page 20) before applying power to the instrument.
2. It is essential that the HLNCC be properly grounded. Read the Sec. 2.2.3.3.21 titled Power line connector (page 23) before applying power to the instrument.
3. The assay of plutonium samples involves a nuclear criticality hazard. Read section 4.8 titled Criticality (page 74) before assaying nuclear material.
4. The assay of plutonium involves a radiological health hazard. It is assumed that the reader is familiar with or will obtain the necessary guidance concerning radiation safety.

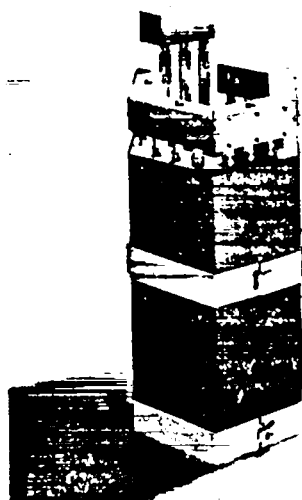
3.2 Assembly

3.2.1 Introduction. The HLNCC is transported in two instrumentation suitcases. One contains the electronics package, the HP-97 calculator, and supplies; the other contains the detector, end plugs, preamplifier package, ²⁵²Cf calibration source, connecting cables and sometimes a sample rotator, lab jack, or support stand for fast critical assembly fuel drawers. Table 3.1 lists the contents of each package, Fig. 3.1 shows separate items,* and Fig. 3.2 shows an assembled system.

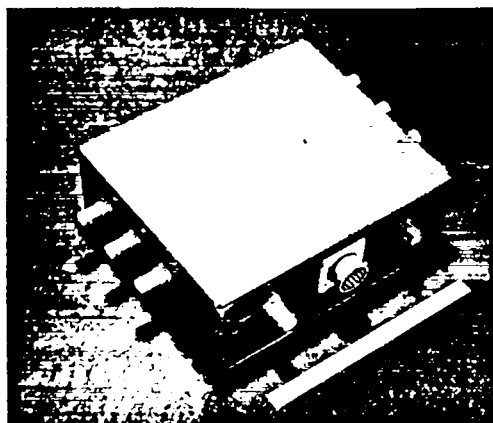
The detector can be operated in a vertical or horizontal position, depending on the application. In the horizontal position, the end plugs are not normally used. In the vertical position, the detector can be operated with or

* A fuel drawer support stand is shown in Fig. 4.7 (page 85).

Fig. 3.1.



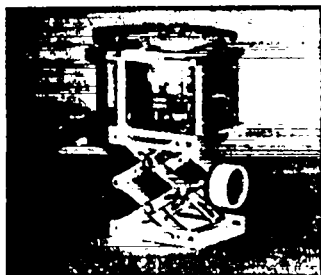
a) HLNCC detector body



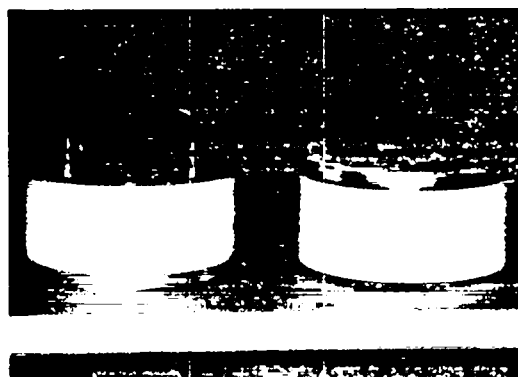
c) preamplifier package,



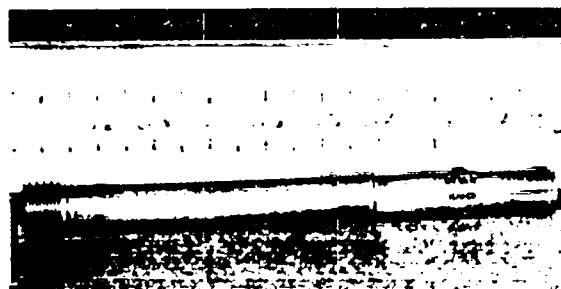
e) HV cables,



g) sample rotator,



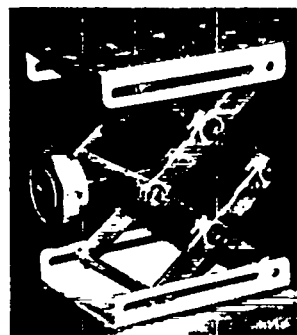
b) top and bottom end plugs,



d) ^{252}Cf calibration source and positioning rod,



f) preamplifier cable,



h) lab jack.

TABLE 3.1

PARTS LIST FOR HLNCC OPERATING SYSTEM

Detector case

1. Detector body
2. Top and bottom end plugs
3. ^{252}Cf calibration source in end plug
4. Sample rotator*
5. Lab jack*
6. Fast critical assembly support stand*
7. Preamplifier box
8. 6 short high-voltage cables
9. 6 "T" connectors and end caps
10. 1 long high-voltage cable
11. 1 preamplifier cable

Electronics case

1. HLNCC electronics package
2. Power cord
3. Power plug adapter
4. HP-97 calculator
5. 2 power supplies for HP-97 (115 and 230 Vac)
6. HP-97 instruction manual
7. HP-97 programming cards and head-cleaning card
8. Spare HP-97 thermal paper

* not included in all systems

without the end plugs. The bottom end plug does not have a handle and simply slides from the bottom into the lower portion of the detector well. The top end plug has a handle and cap; it is lowered to rest at the top of the well. The ^{252}Cf calibration source is stored at the center of the top or bottom plug on the end of a threaded rod.

3.2.2 Procedure.

1. Unpack both HLNCC packages.
2. Remove the ^{252}Cf source from the end plug and put it aside temporarily.
3. Set up the detector in the desired location. Note that the nature of the floors, walls, shielding materials, etc. in the vicinity of the detector will influence its performance. If possible, the setups for calibration and assay should be the same; if not, the ^{252}Cf calibration source can be used to correct for efficiency variations. (If the detector is to be used for assaying samples larger than the

detector well can accommodate, remove the three brackets which hold the segments of the detector together and reconfigure the segments as desired.)

4. Slide the preamplifier package into the bracket on the side of the detector. It may be necessary to readjust the segment brackets to obtain a proper fit. (If the detector is operated as six separated segments, place the preamplifier package at any convenient location close to the segments.)
5. Connect the six short high-voltage cables from the preamplifier package to the six detector segments. Use the "T" adapters and end caps at the detector end of the cables to keep the cables out of the way (see Fig. 3.2).
6. Connect the multiconductor cable from the preamplifier box to the rear panel of the electronics package. This cable is symmetrical and can be installed either way.
7. Connect the long high-voltage cable from the preamplifier box to the rear panel of the electronics package.
8. Connect the HP-97 calculator interface cable to the rear panel of the electronics package.
9. If an (RS-232-C)-compatible device (such as a computer or data terminal) is to be used, connect the interface cable to the rear panel of the electronics package.

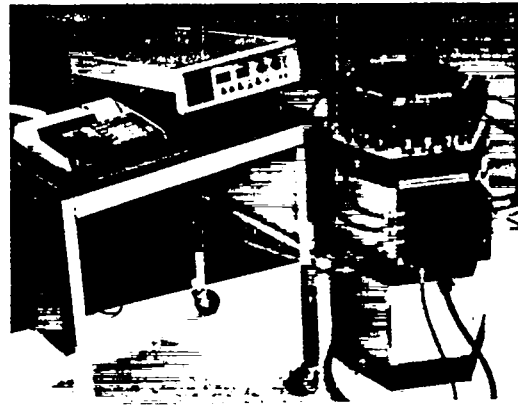


Fig. 3.2.
Assembled operating system.

3.3 Power

1. Connect the power cord to the electronics package, but do not plug it into the power source.
2. Be certain that the power (PWR) and high-voltage (HV ON) switches on the lower-right front panel are turned to their off (i.e., downward) positions. The high-voltage switch has a locking lever as a safety feature; to move the lever up or down, pull on the lever to release the catch.

3. If the HLNCC is operated from a 100/115/230 Vac, 50/60 Hz power source, set the slide switch on the right-hand side of the rear panel to the desired voltage setting and insert the line cord plug into the power source socket.
4. If the HLNCC is operated from a dc supply, be certain that the polarity is correct (see section 2.2.3.3.2f), that the dc voltage is in the range of 10-30 Vdc, and that the dc supply can deliver 24 W for the duration of the measurements before connecting the supply.
5. If the HLNCC is operated from an ac supply with dc backup, both power sources may be connected to the instrument simultaneously. The dc supply must have an output voltage between 10 and 15 volts, so it will deliver power only if the ac supply fails.
6. Connect the HP-97 to an ac power source. Two power supplies are included for 100/115 or 230 Vac operation. Operation from the calculator's battery pack should be restricted to short-term use, because damage to the calculator's circuitry can occur if the printing mechanism operates with low battery voltage.
7. Turn the calculator on.

3.4 Instrument Setup and Testing: Primary Procedures

1. Verify that the power source is connected correctly as described in the previous section, that the instrument cables are connected as described in section 3.2, and that the power and high-voltage switches are turned to their off (downward) positions.
2. The internal predelay setting should be set to its normal value of 4.5 μ s. If the setting is not known or must be changed, refer to section 3.6.1 for details on inspecting and resetting the predelay switches.
3. If the HP-97 calculator is connected to the instrument, a test output is transmitted to the HP-97 immediately after the HLNCC power is turned on. If the HP-97 is turned on, the registers R1, R2, R3, and R4 are filled with the following numbers:

R1 = 444 444

R2 = 3 333 333 333

R3 = 2 222 222 222

R4 = 1 111 111 111

A "label A" instruction is then sent to the calculator. (Refer to Ref. 16 for details on the HP-97.)

To prepare the calculator for the test, some program which starts at label A and which uses the data in R1-R4 is desirable. A simple program which prints the contents of R1-R4 is listed in Table 3.2. Insert this or another suitable program into the calculator. Set the MAN-TRACE-NORM switch to MAN and the PRGM-RUN switch to RUN.

If the HP-97 is not programmed to perform some appropriate operation beginning at label A, an error message will be displayed after the "label A" instruction is given by the HLNCC. However, the contents of registers R1-R4 can still be recalled manually for examination.

4. If a data terminal or computer is connected to the HLNCC via the RS-232-C interface, the following or similar test message is also transmitted to these devices when the HLNCC power is turned on:

IAEA HLNCC

V 1.2

6 JUN 78

The serial ASCII output is at 300 baud with 7 bits per character (1 stop bit, even parity). If a computer is used as the output device, it must be programmed in accordance with the format of the output as detailed in Table 2.1.

5. Turn the power switch (PWR) on (upward). The STOP and READOUT lights and the display will be turned on. The four scaler readouts will each display 00. The READOUT light will remain on until the test outputs are transmitted to the HP-97 and RS-232-C interfaces. If the program listed in Table 3.2 is in the HP-97, then the printed output will be

444 444.

3 333 333 333.

2 222 222 222.

1 111 111 111.

This tests the microprocessor and interface circuitry.

6. Set the high-voltage helipot dial (HV DIAL x200) on the front panel to 7.50 (7½ turns). This sets the high voltage to 1500 V.
7. Set the discriminator helipot dial (DISC V DIAL x .5) to 3.00 (3 turns). This sets the discrimination level at 1.50 V.

TABLE 3.2

HP-97 PROGRAM TO PRINT HLNCC DATA

<u>Program Step</u>	<u>Function</u>	<u>Comment</u>
001	*LBLA	start
002	DSP0	display integers
003	FIX	choose fixed display
004	RCL1	recall time
005	PRTX	print time
006	RCL2	recall totals
007	PRTX	print totals
008	RCL3	recall R+A
009	PRTX	print R+A
010	RCL4	recall A
011	PRTX	print A
012	SPC	print a space
013	R/S	stop

8. Set the internal/external switch (INT/EXT) on the rear panel to INT. This selects the internal discriminator as the input to the shift-register circuitry.
9. Turn the high voltage on by pulling on the HV switch lever and moving it to its upward position. The red lamp above the switch will come on to indicate that high voltage is present in the instrument.
10. Set the gate length to 32 μ s.
11. Set the time to 100 s (1×10^2)
12. Screw the ^{252}Cf source into its holder at the center-side of the detector well.
13. Set the manual/recycle switch to manual.
14. Press the START pushbutton. The green start light will come on, the red stop light will go out, and the display will continuously monitor the data collection process. After 100 s (real time) the counter will stop and the lights will indicate accordingly. The contents of the time, totals, R+A, and A data registers will be displayed.
15. Press the READOUT pushbutton if the HP-97 or an RS-232-C device is connected to the HLNCC.

- (1) If the HP-97 program listed in item 3 above has not been disturbed, the calculator will print the time, totals, R+A, and A data approximately as follows:

100.
415 396.
93 027.
55 086.

- (2) If a data terminal is connected to the system, the output will appear similar to the following:

TIME(SEC)	TOTALS	R+A	A	R
100	415,396	93,027	55,086 +	37,941

R is the real coincidence count [(R+A) - A].

16. Compare the transmitted data carefully with the displayed data to verify that the readout circuitry is working correctly.
17. Compare the accidental counting rate with that calculated from the

relation $\dot{A} = \dot{T}^2 t_g$, where
 \dot{A} = accidental rate,
 \dot{T} = totals rate, and
 t_g = gate width.

E.g., for the data shown in item 15 above, the rates are

$$\dot{T} = 4154$$

and

$$\dot{A} = 550.9.$$

The calculated value for A is

$$\begin{aligned} \dot{A} &= \dot{T}^2 t_g \\ &= (4154)^2 (32 \times 10^{-6}) \\ &= 552.2, \end{aligned}$$

which agrees with the measured value within statistical errors (see Sec. 4.2 for details on counting errors).

18. Subtract A from R+A and divide by the time to obtain the real coincidence rate \dot{R} . The data of section 15 give $\dot{R} = 379$ cps.
19. Remove the ^{252}Cf source to some distance from the detector.

20. Press the RESET pushbutton. The display will show 00 for each of the four data rows. The yellow fault lamp in the RESET pushbutton should not light.
21. Press the START pushbutton to measure the background for 100 seconds. The background can be as low as 5 totals counts per second. If the background totals rate is later found to exceed $\sim 10\%$ of the sample totals rate, it may be worthwhile to seek a lower background by moving or shielding the detector. Remember, however, that close shielding of the detector will change its operating characteristics.
22. Subtract A from R+A to obtain the real coincidence count R. R may be positive or negative, but $|R|$ generally should not be much larger than $\sim 3\sqrt{A}$ where A is the accidental count. (If the background rate is very low, a statistically significant real coincidence count due to cosmic ray events can be observed with long counting times.)
23. Divide the totals count by the time to obtain the background totals counting rate \dot{B} . Subtract \dot{B} from the \dot{T} of item 17 to obtain the background-corrected totals counting rate from the ^{252}Cf source.
24. The ^{252}Cf source holder is stamped with the ^{252}Cf source strength and calibration date. Calculate the present ^{252}Cf strength with the equation

$$S = S_0 e^{-\lambda t},$$

where

S_0 = source strength on calibration date,

S = present source strength

t = time between calibration date and the present in days,

and $\lambda = 7.19 \times 10^{-4} \text{ d}^{-1}$.

25. Divide the background-corrected totals counting rate from the ^{252}Cf source by the ^{252}Cf source strength to obtain the absolute detector efficiency ϵ . Calculate the fission rate for the ^{252}Cf source:

$$\text{fission rate (s}^{-1}\text{)} = \frac{\text{source strength (n/s)}}{\bar{\nu}}$$

where $\bar{v} = 3.76$ for ^{252}Cf . Then divide the real coincidence rate by the fission rate to obtain the coincidence-counting efficiency ϵ_c . With a 32 μs gate and a 4.5 μs predelay, these values should be approximately

$$\epsilon = 12.1\%$$

and

$$\epsilon_c = 4.2\%$$

These values can vary by about ten percent due to uncertainties in the calibration source strength. The totals-to-coincidence ratio $(T-B)/R$ or $\bar{v}\epsilon/\epsilon_c$ is independent of the ^{252}Cf source strength and should be approximately

$$\frac{\dot{T} - \dot{B}}{\dot{R}} = 10.9$$

(Deadtime corrections are very small for the ^{252}Cf calibration source and are ignored here.)

26. If the HP-97 calculator is being used, study the stability of the HLNOC by using the program listed in Table 3.3. Place the ^{252}Cf source in its holder in the detector well, insert the program into the calculator, press label B to initialize the program, set the manual/recycle switch to recycle, set the measurement time to 100 s, press RESET, and then press START. The program calculates the mean value \bar{R} for the real coincidence count and the estimate s_R for the standard deviation

$$s_R = \sqrt{\frac{\sum_{i=1}^N (R_i - \bar{R})^2}{N - 1}}$$

where

N = number of measurements,

i = i -th measurement, and

R_i = measured real coincidence counts for i -th measurement.

For the first four cycles, the program prints the number of the cycle and the real coincidence count for that cycle. After the fifth cycle and for each cycle thereafter, the program prints the number of the cycle, the real coincidence count for that cycle, the average real coincidence count R , the estimated standard deviation s_R , and the standard deviation due to counting statistics σ_R . The standard deviation σ_R is approximately

$$\sigma_R \approx \sqrt{(R+A) + (A)} ,$$

where

$R+A$ = real-plus-accidental counts in counting interval,

A = accidental counts in the same counting interval, and

$R = (R+A) - A$.

A sample output is listed in Table 3.4. The standard deviation depends on the ^{252}Cf neutron source strength at the time of the measurement; for a source strength of 4×10^4 neutrons/s, σ_R due to counting statistics only should be approximately 1% for a 100 s measurement. For overnight stability tests, 2000 s measurement times are recommended.

27. If a random neutron source (such as $^{241}\text{Am-Li}$) is available, measure the source and verify that there is negligible bias on the real coincidence count R . The value for R can be positive or negative, but $|R|$ should be less than $\sim 3\sqrt{A}$, where A is the accidental count.

3.5 Short-Form Setup Procedures

For an operator familiar with the HLNCC, the following sequence is the recommended procedure for setting up the instrument in preparation for a measurement. It is assumed that the operator has read section 3.1 titled Warnings (page 35).

1. Assemble the system.
2. Select 115 or 230 Vac or dc operation.
3. Set high voltage to 1500 V.
4. Set discrimination level to 1.5 V.
5. Set predelay to 4.5 μs . (This is set by internal switches and is not changed in routine applications.)
6. Set gate width to 32 μs .
7. Set measurement time to 100 s.
8. Set external/internal switch to internal.

TABLE 3.3

HP-97 PROGRAM TO STUDY THE STABILITY OF THE HLNCC

<u>Program Step</u>	<u>Function</u>	<u>Comment</u>
001	*LBLB	initialize
002	FIX	fix display
003	DSP0	display integers
004	CLRG	clear registers
005	P/S	clear protected registers
006	R/S	stop
007	*LBLA	start
008	ISZI	increment I
009	RCLI	recall I
010	PRTX	print I
011	RCL3	recall R+A
012	RCL4	recall A
013	-	calculate R
014	PRTX	print R
015	$\Sigma+$	perform statistical calculation
016	RCLI	recall I
017	5	enter 5
018	X>Y?	I < 5?
019	GTOC	yes, go to C
020	\bar{x}	no, calculate \bar{R}
021	PRTX	print \bar{R}
022	s	calculate s
023	PRTX	print s
024	RCL3	recall R+A
025	RCL4	recall A
026	+	add
027	\sqrt{x}	calculate $\sqrt{(R+A) + A}$
028	PRTX	print σ_R
029	*LBLC	
030	SPC	print a space
031	R/S	stop

TABLE 3.4

SAMPLE OUTPUT FROM HP-97 STABILITY TEST PROGRAM

1.	***	8.	***
38669.	***	38095.	***
		38648.	***
2.	***	298.	***
38668.	***	388.	***
3.	***	9.	***
38546.	***	38615.	***
		38644.	***
4.	***	279.	***
38943.	***	389.	***
5.	***	10.	***
38698.	***	38643.	***
38705.	***	38644.	***
145.	***	263.	***
389.	***	388.	***
6.	***	11.	***
38484.	***	37892.	***
38668.	***	38576.	***
158.	***	337.	***
389.	***	387.	***
7.	***	12.	***
39081.	***	38253.	***
38727.	***	38549.	***
213.	***	335.	***
389.	***	389.	***
13.	***		
38119.	***		
38516.	***		
342.	***		
389.	***		

cycle 13
 real coincidence counts from cycle 13
 average real coincidence counts per cycle
 estimated standard deviation s
 standard deviation expected from counting statistics

-
9. Set manual/recycle switch to manual.
 10. Turn on the HP-97, set the MAN-TRACE-NORM switch to MAN, set the PRGM-RUN switch to RUN, and load an operating program.
 11. Turn the HLNCC power on and verify a correct test response from the HP-97 (and RS-232-C interface, if used).

12. Remove the ^{252}Cf calibration source to some distance from the detector, measure background for 100 s, and verify reasonable values for R+A and A.
13. If a random neutron source (such as $^{241}\text{Am-Li}$) is available, measure the source and verify that there is no observable bias on the net real coincidence count.
14. Mount the ^{252}Cf source in its holder in the detector well and measure for 100 s.
15. Press the READOUT button and compare the output with the displayed data.
16. Compare the accidental and total rates with the $\dot{A} = \dot{T}^2 t_g$ formula.
17. Verify that the totals (background corrected) and coincidence rates agree with those predicted from the present ^{252}Cf source strength.
18. Verify a reasonable totals/coincidence ratio (background corrected).
19. If time permits, use the recycle mode to test the system stability.

If the instrument passes the above tests satisfactorily, it is probably working correctly. If the instrument fails any of these tests, refer to section 3.7 on field diagnostics.

3.6 Instrument Setup and Testing: Secondary Procedures

3.6.1 Predelay Setting. The predelay is set by internal switches to a value from 1.0 to 32.5 μs in steps of 0.5 μs . The usual setting is 4.5 μs and in normal operations need not be changed. However, the flexibility of a variable predelay is essential for general experimental purposes. In particular, if the instrument is used with an external amplifier and discriminator, a longer predelay may be required to avoid a bias.

To inspect or change the predelay setting, proceed as follows:

1. Turn off the instrument power and unplug the power cord.
2. Remove the top cover by
 - a) removing the two screws holding the cover at the top rear of the package, and
 - b) sliding the cover back and out of the package.
3. Refer to Fig. 3.3a, which shows the top view of the instrument with the top cover removed. The predelay switches are mounted on the shift-register circuit board, which is immediately under the top (amplifier) board. The position of the predelay switches is shown by the arrow labelled PREDELAY in Fig. 3.3a.

4. Gain access to the switches as follows:
 - a) Release the black plastic circuit-board clamp (shown by the arrow labelled CLAMP in Fig. 3.3a) by pushing the top of the clamp toward the rear of the instrument. (In some instruments the clamp is fastened to the circuit boards with a screw which must first be removed.) The clamp will swivel backwards to free the rear portion of the circuit boards.
 - b) Pull the white nylon pin (shown by the arrow labelled PIN in Fig. 3.3a) to the right (as seen from the top-front of the instrument. This will release the pivoting mechanism for the circuit boards.
 - c) Rotate the circuit board assembly to its upward position as shown in Fig. 3.3b. Lift the assembly by the rear corners of the top circuit board. Do not lift by pulling on the coaxial cables.
 - d) Reinsert the nylon pin to lock the pivoting mechanism.
5. The predelay switches, located on the shift-register circuit board at row E, are shown in Fig. 3.3c. The six switches are numbered 1 through 6 and have predelay values of 0.5, 1, 2, 4, 8, and 16 μ s, respectively, as shown on the circuit board. A switch in the upward position (i.e., with the lever away from the circuit board) adds its value to the predelay. A switch in the downward position has no effect. Any combination of switches may be used. The predelay is 1 μ s plus the sum of the values of all switches thrown to their upward positions. E.g., the usual 4.5 μ s predelay has switch 1(0.5 μ s), switch 2(1 μ s) and switch 3(2 μ s) thrown upwards; this configuration is shown in Fig. 3.3c. Set the predelay to the desired value.
6. Place the instrument back into operation as follows:
 - a) Release the white locking pin.
 - b) Rotate the circuit board assembly down to its original position.
 - c) Insert the white locking pin.
 - d) Rotate the black circuit board clamp back into position (and insert the screw, if applicable).
 - e) Slide the top cover into place.

- f) Insert the two screws to hold the cover plate.
- g) Plug in the power cord.
- h) Turn on the power.

3.6.2 Amplifier Test Outputs (AMP 1 2 3 4 5 6). The six amplifier test jacks on the instrument front panel allow the user to observe the analog signal from each of the six channels at the input to the discriminator circuits. The pulse-shaping amplifiers produce positive-leading, bipolar pulses with 0.5 μ s integrating and differentiating time constants. A photograph of an oscilloscope display taken under normal operating conditions with a ^{252}Cf calibration source is shown in Fig. 3.4. The peak positive amplitude of pulses due to thermal-neutron capture in the ^3He counters is set for 6.0 volts. The smaller peaks are normal and are due to partial charge collection events in the counter. Note that approximately 4 μ s is required for the pulses to return to the baseline. The ground test jack is connected to signal ground and is intended for use with the signal test jacks. The six amplification channels can be observed independently to verify the correct operation of the analog circuitry. Proceed as follows.

1. Connect a high impedance oscilloscope probe to test jack #1; connect the probe ground to the ground test jack. (It may be found convenient to insert short pieces of bare wire into each of the test jacks to facilitate making the probe connections; probe tips and ground clips can be attached to the protruding wires.)
2. Observe the test pulses with the ^{252}Cf calibration source in its holder near the center of the detector. Verify that the shape of the pulses is as shown in Fig. 3.4, that the positive pulse amplitude for the full-charge-collection events is 6.0 V, and that the pulses recover in $\sim 4\mu$ s.
3. Repeat step 2 for each of the other channels.
4. Remove the ^{252}Cf source and place it some distance from the detectors.
5. Observe each of the signal test points under background conditions. Problems are indicated by an unusually large number of pulses from one test point relative to the others, pulses of unusually large amplitude, or noise bursts.

3.6.3 Discriminator Output (DISC OUT). Connect the oscilloscope (as described in section 3.6.2) to the discriminator output on the front panel; use the ground test point as the signal ground connection. Place the ²⁵²Cf calibration source in its holder in the detector and observe the output pulses. The discriminator pulses should be 3 V high and 150 ns wide. Figure 3.5 shows a normal display from the test point.

3.6.4 High-Voltage Test Point (HV/1000). Verify that the high-voltage power supply is operating as indicated by the front-panel control settings. The instrument power and high-voltage switches must both be in their "ON" positions. Set the high-voltage dial to 7.50 (7½ turns); this should produce an output of 1500 V. A dc signal of 1.50 V should be present at the HV/1000 test point. Verify this with a dc voltmeter; the ground test point may be used as the ground connection for the measurement.

3.6.5 Discriminator Test Point (DISC V). The six discriminators on the six analog channels are all controlled from the same discrimination level, which is normally 1.50 V. Set the discriminator dial (DISC V, DIAL x .5) to 3.00 (three turns) to produce a discrimination level of 1.50 V. Verify that the discrimination level is set correctly by measuring the output of the discriminator test point with a dc voltmeter; the output should be 1.50 V. The ground test point may be used as the ground connection for this measurement.

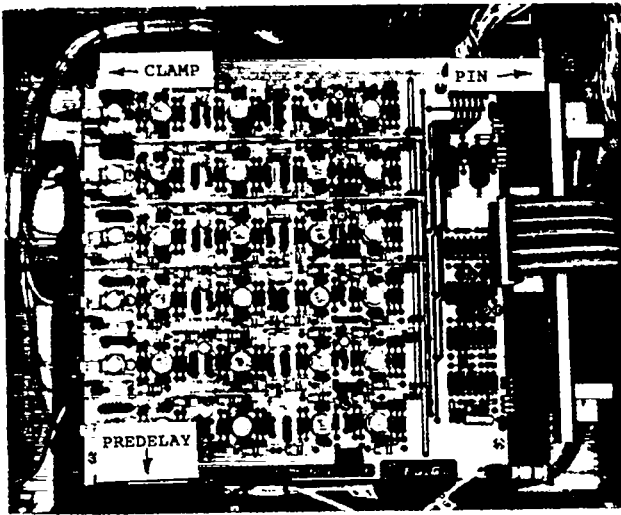
3.7 Field Diagnostics

If the HLNCC fails the checkout tests of sections 3.4-3.6, it probably requires the aid of an electronics specialist. The technical manual¹ should be consulted for details on the HLNCC circuitry. A few field diagnostics discussed below might aid in detecting an operator error or allow a defective instrument to be used until proper repairs can be made.

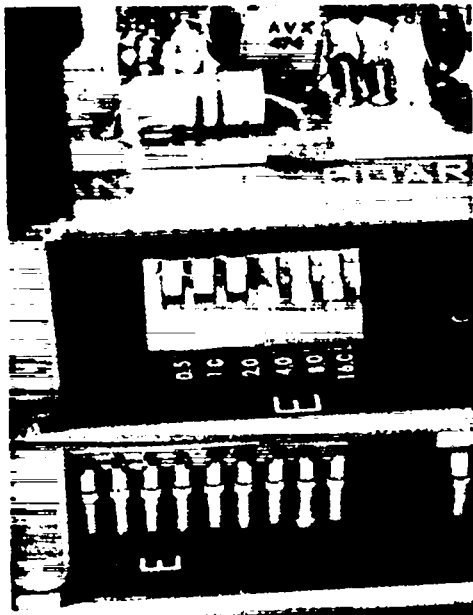
3.7.1 Symptom: No Power. If the display and STOP indicator lamp do not light when the power switch is thrown to the PWR position, be certain that (a) the instrument is connected to a proper power source, (b) the 115/230 switch is in the correct position if an ac supply is being used, (c) the polarity is correct if a dc supply is being used, and (d) the fuse is not blown.

3.7.2 Symptom: No Test Output to HP-97 or RS-232-C Devices. If the HP-97 or RS-232-C devices do not appear to receive the test output from the instrument when power is turned on or when the microprocessor RESET pushbutton on the rear of the instrument is depressed, perform the following checks:

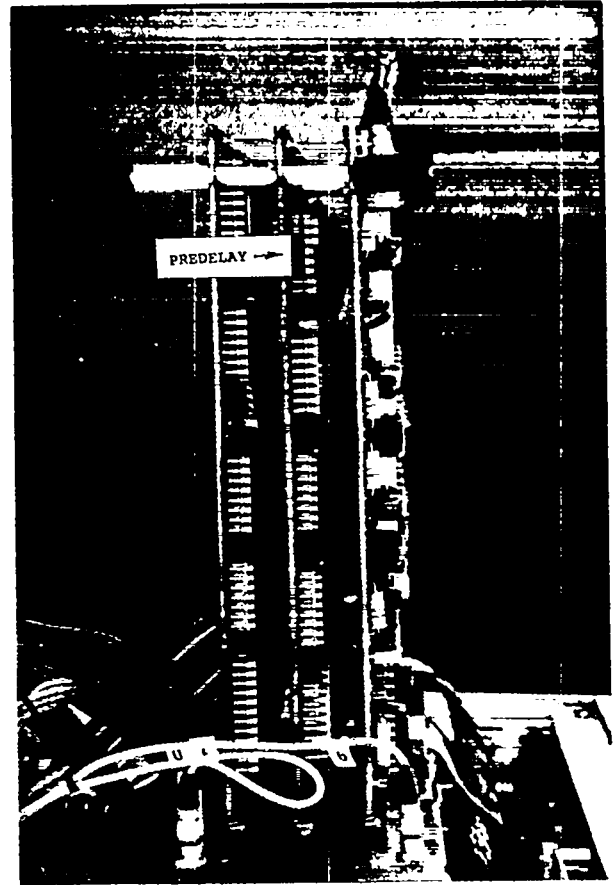
Fig. 3.3



- a) Top view of electronics package with the top cover removed showing the location of the predelay switches, the circuit board clamp and the nylon pin.



- c) Predelay switches on shift register circuit board.



- b) Electronics package with circuit boards rotated to their upright position.

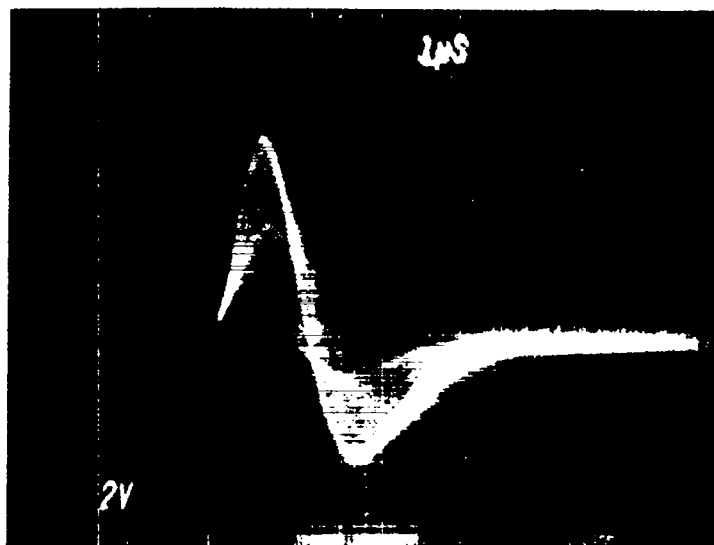


Fig. 3.4.
Oscilloscope display of an amplifier
test point signal with the ^{252}Cf
calibration source in the detector.
Vertical scale = 2 V/div; horizontal
scale = 1 μs /div.

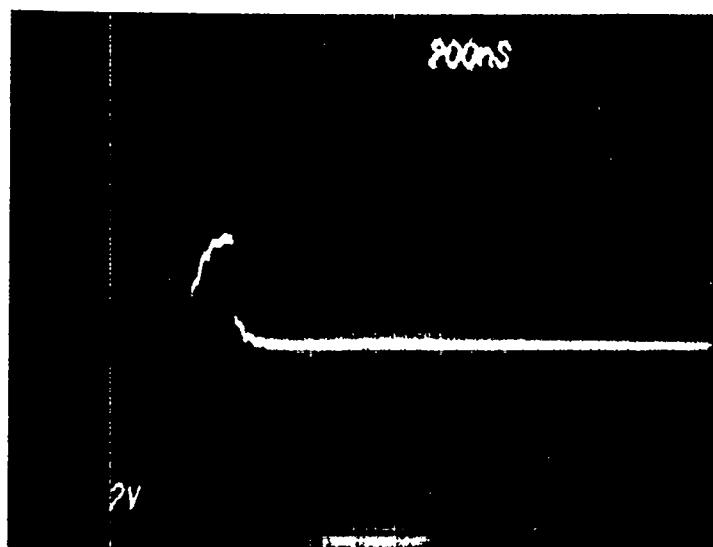


Fig. 3.5.
Oscilloscope display of the discrim-
inator output test point signal with
the ^{252}Cf source in the detector.
Vertical scale = 2 V/div; horizontal
scale = 0.2 μs /div.

- a) Be sure that the devices are turned on.
- b) Be sure that the connectors are making firm contact.
- c) For the HP-97, do the following:
 - i) Be sure that the PRGM/RUN switch is in the RUN position and that the MAN-TRACE-NORM switch is in the MAN position.
 - ii) Observe the HP-97 display to see if data appear to be entering; the transfer rate is slow and the characters are displayed as they are transmitted.
 - iii) After the attempted transfer recall registers R1, R2, R3, and R4; perhaps the transfer was successful, but the HP-97 was programmed incorrectly to process the numbers.
 - iv) Try another HP-97 if one is available.
- d) For the RS-232-C device, do the following:
 - i) Be sure that the device is set to accept 7 bit (even parity, one stop bit) serial ASCII code at 300 baud and that the device control lines are connected properly.
 - ii) Check the device in local mode to verify that it is functional.
 - iii) Try another device if one is available.

If the readout devices fail to operate, the instrument may still be usable because the readout circuitry is largely independent of the shift-register and display circuitry. However, it will be necessary to copy the data by hand directly from the front-panel display.

3.7.3 Symptom: No Totals Counts. If the instrument is started, the timer is running, and no counts are observed in the totals scaler, check the following:

- a) Be certain that the external/internal switch is set to internal (for normal operation).
- b) Be certain that the high-voltage is turned on and that the HV/1000 test point measures 1.5 Vdc.
- c) Be certain that the discrimination level as measured at the test point is 1.5 Vdc.
- d) Be certain that the high-voltage and signal cables from the junction box to the instrument and from the junction box to the detector are connected properly.
- e) Place the ²⁵²Cf calibration source in its holder in the detector and observe the discriminator output test signal with an oscilloscope (see Fig. 3.5).

- i) If no discriminator pulses are observed, the instrument is faulty. However, it is possible that the instrument can still be used with an external discriminator input. Use an external preamplifier-amplifier-discriminator system and feed the discriminator output to the external input of the unit. See section 3.7.8.
- ii) If discriminator pulses are observed, the instrument is faulty and cannot be used.

3.7.4 Symptom: No High Voltage. If the measurement at the HV/1000 test point shows that the high voltage cannot be set correctly, use an external high voltage supply (+1500 Vdc), if available, to supply HV directly to the preamplifier box.

3.7.5 Symptom: Inconsistent Totals and Accidentals Rates. If the accidental rate \dot{A} is not equal to $\dot{T}^2 t_g$ to within 0.01% (or statistical error), where t_g is the gate width and \dot{T} is the totals rate, perform the following checks:

- a) Repeat the calculation; ensure that the correct value for t_g is used and that the units for \dot{A} , \dot{T} , and t_g are consistent.
- b) Repeat the measurement; beware of changing backgrounds.
- c) Try other values for t_g ; perhaps the gate width switch is defective.
- d) Compare the displayed data to the transmitted data to verify that the data are being transferred correctly.
- e) Check the stability of the counting rates. If unstable, refer to Sec. 3.7.8.

If the instrument cannot pass the $\dot{T}^2 t_g$ test, it is defective and should not be used.

3.7.6 Symptom: Incorrect Counting Rates from the ^{252}Cf Calibration Source. If the totals rate (\dot{T}) or reals rate (\dot{R}) from the ^{252}Cf calibration source appear to be incorrect, do the following:

- a) Verify that all six detector sections are connected properly.
- b) Verify that the correct source is being measured and is positioned properly in the source holder.
- c) Verify that the background rate was subtracted and that the decay correction was calculated correctly.
- d) Verify that the values for predelay and gate width are set as desired.

e) Verify that the high-voltage and discrimination levels are set correctly; measure the test points with a voltmeter.

f) Refer to sections 3.7.7 and 3.7.8 for other possible problems.

If \dot{T} and \dot{R} are in apparent error by the same percentage, some kind of calibration error is likely at fault. If the percentage error for \dot{R} is about twice that for \dot{T} , an efficiency change is likely at fault. If the percentage errors for \dot{R} and \dot{T} seem to be unrelated, a noise problem may be at fault.

3.7.7 Symptom: Abnormal Amplifier Output. If any of the six amplifier test outputs appear abnormal on an oscilloscope display (poor shape, wrong size, noisy, etc.; see Fig. 3.4) disconnect the offending section by removing the high-voltage cable which connects this section of ^3He counters to the junction box. (The channel numbers marked on the preamplifier box correspond to the same numbers on the front panel at the amplifier test points.) Place a protective cap on the junction-box, high-voltage connector. The instrument is completely useful with one bank of tubes disconnected, although the absolute detector efficiency is reduced to $5/6$ of the initial value and the coincidence counting efficiency is reduced to $(5/6)^2$ of the initial value. The coincidence deadtime will also increase to about $2.6 \mu\text{s}$.

3.7.8 Symptom: Unstable Counting Rates. Unstable counting rates can be caused by a faulty bank of tubes or amplification channel, by a noisy environment, by temperature changes, by faulty high-voltage or discrimination circuits, or by faulty coincidence circuitry. Test for noise-induced counts by observing the totals rate with the high voltage turned off. The rate should be nearly zero; if it is not, check each of the six channels by observing the amplifier output test signals with an oscilloscope (see section 3.7.7).

With the high voltage on and the ^{252}Cf calibration source in the detector, study the stability of each bank individually by disconnecting the high-voltage cables from the preamplifier box five at a time. If a bad channel is found, refer to section 3.7.7.

If all channels are bad, a single external preamplifier- amplifier- discriminator can be used with all tubes connected in parallel. A general purpose charge-sensitive preamplifier and a shaping amplifier with $\sim 0.5 \mu\text{s}$ time constants will be satisfactory for emergency use. The largest pulses should have $\sim 6 \text{ V}$ peak amplitude and the discrimination level should be set to $\sim 1.5 \text{ V}$. The discriminator output should be a $\sim 0-5 \text{ V}$, positive-leading-edge pulse (TTL compatible) about 150 ns wide; this output should be connected to

the external input on the rear of the instrument and the external/internal switch should be set to the external position. The coincidence deadtime of the system will depend on the electronics used, but will be approximately 10 μ s.

Noise and temperature problems might be improved by relocating the HLNCC. Extreme noise problems might also be improved by the use of line conditioners and ground straps. The stability of the digital electronics can be studied by using a random pulse generator as an external digital pulse source. However, "random" pulse generators will not produce equal R+A and A counts within statistical errors. A bias observed in this test should be considered normal.

4. APPLICATIONS

4.1 Introduction

The HLNCC is a versatile coincidence counter that can be applied to a large variety of plutonium sample types including PuO_2 , mixed oxide ($\text{PuO}_2\text{-UO}_2$), metal, carbides, fuel rods, fast critical assembly (FCA) plates, solutions, scrap, and waste. Sections 4.2-4.11 describe general problems and procedures associated with practical coincidence counting applications. Section 4.12 describes some specific applications.

In addition to the assay of plutonium samples, the HLNCC can be used for the passive and active assay of uranium samples. Large samples of low enriched uranium can be assayed passively by the coincidence counting of the spontaneous-fission neutrons from ^{238}U . Also, large samples of highly enriched uranium can be assayed by operating the HLNCC in an active mode; small $^{241}\text{Am-Li}$ sources are placed in the end plugs to induce fissions in the ^{235}U . However, the use of the HLNCC for uranium assay will not be discussed further in this publication.

Ideally the real coincidence counting rate would be directly proportional to the plutonium mass (for a fixed isotopic composition) and would be independent of the random neutron background. In practice this is not true for several reasons.

1. The efficiency of the counter is dependent on the position of the source neutrons. Therefore, two samples with the same isotopic composition and plutonium mass, but with different geometry, may not produce the same real coincidence counting rate.

2. The efficiency of the counter is dependent on the energy of the source neutrons. Therefore, two samples with the same isotopic composition and plutonium mass, but with a different content of moderating material, may not produce the same real coincidence rate.
3. The efficiency of the counter is dependent on the absorption of source neutrons in the sample. This effect is similar to and related to item 2 above.
4. The effect of the random neutron background, mostly from (α, n) reactions in the sample, is largely eliminated by the use of the coincidence circuitry. However, some of the (α, n) neutrons may induce fissions in the sample. The prompt fission neutrons from these fissions produce true coincidences which cannot be directly distinguished from the spontaneous-fission coincidences.
5. Spontaneous-fission neutrons may also induce fissions in the sample. When this occurs, spontaneous fissions are converted to combined (spontaneous fission)-(induced fission) events which have a higher average multiplicity than the spontaneous fissions alone and hence a higher coincidence-counting efficiency (see section 2.4.2).

Methods for dealing with these complications are described in this chapter.

4.2 Counting Statistics Calculations

Because some of the neutrons produced by a fissioning source and detected in a coincidence counter are correlated, the exact treatment of errors due to counting statistics is complex. The reader is referred to the work by Böhnelt⁴ for a discussion of this problem. However, the efficiency of the HINCC is sufficiently low that the correlations are weak and approximate expressions for the errors due to counting statistics are more than adequate for most applications.

The standard deviation σ_T of the totals count T (due to counting statistics only) may be approximated by

$$\sigma_T \approx \sqrt{T} \quad (4-1)$$

and the standard deviation σ_R of the real coincidence counts may be approximated by

$$\sigma_R \cong \sqrt{(R+A) + (A)} , \quad (4-2)$$

where $R+A$ is the real-plus-accidental count and A is the accidental count.

As an illustration, Table 4.1 shows HLNCC data accumulated in 100s measurement intervals with combined ^{252}Cf and $^{241}\text{Am-Li}$ sources. The standard deviation of the real coincidence counts per 100 s due to counting statistics is

$$\sigma_R \cong \sqrt{(R+A) + A} \cong \sqrt{768\,000 + 727\,000} \cong 1220.$$

The actual standard deviation can be estimated from the equation

$$s_R = \sqrt{\frac{\sum_{i=1}^N (\bar{R} - R_i)^2}{N - 1}} ,$$

where

\bar{R} = average real coincidence counts per 100 s,

R_i = real coincidence counts for i -th measurement, and

N = number of measurements.

The value for s_R obtained from the data of Table 4.1 is 1280 and agrees within statistical errors with the standard deviation calculated above. Because correlations between neutron events and miscellaneous uncertainties both contribute to increasing the standard deviations of the totals and real coincidence counts relative to Eqs. (4-1) and (4-2), the good agreement between the expected and estimated standard deviations indicates that these effects are small for the measurement conditions studied.

Let R , A , and t be the real coincidence count, the accidental coincidence count, and the measurement time, respectively. Then the percent standard deviation of the real coincidence count is approximately

$$\sigma_R (\%) = \frac{\sqrt{(R+A) + (A)}}{R} 100 = \frac{\sqrt{R + 2A}}{R} 100$$

If a short measurement is performed to estimate the real and accidental coincidence rates (\dot{R} and \dot{A} , respectively), then the time t required to obtain a percent standard deviation $\sigma_R(\%)$ due to counting statistics is

$$t \approx (\dot{R} + 2\dot{A}) \left[\frac{100}{\dot{R}\sigma_R(\%)} \right]^2 .$$

For example, if a short measurement on a plutonium oxide sample gives the data

$$\begin{aligned} t &= 100 \text{ s} \\ T &= 1\,040\,216 \\ R+A &= 387\,957 \\ A &= 346\,241, \\ R &= 41\,716, \end{aligned}$$

then the measurement time required to obtain a standard deviation of 0.25% on the real coincidence rate due to counting statistics is

$$t \approx \left[417.16 + 2(3462.41) \right] \left[\frac{100}{(417.16)(0.25)} \right]^2 \approx 6750 \text{ s} .$$

4.3 Coincidence-Gate-Length Selection

For most coincidence-counting applications the gate length is chosen to be about the same duration as the detector die-away time, which is 32 μs for the HLNCC. This gate is sufficiently wide to accept the majority of true coincidence events and yet is not so wide as to produce an unreasonably low real/accidental ratio. If a sample has a low totals counting rate, a gate width greater than 32 μs may produce a smaller statistical error in a fixed counting time than the 32 μs gate in the HLNCC.

Figure 4.1 shows the relative standard deviation on the real coincidence counts as a function of gate width calculated from data obtained by measuring a ~ 600 g PuO_2 sample. The standard deviation is normalized to 1.0 at the 42 μs minimum. The circles indicate the relative errors at 8, 16, 32, 64, and 128 μs gate lengths. The switch-selectable gate length which produces the smallest error is 32 μs , as is usually the case for the HLNCC.

TABLE 4.1

HLNCC DATA ACQUIRED WITH COMBINED ^{252}Cf AND $^{241}\text{Am-Li}$ SOURCES

Totals	R+A	A		R
1,507,643	768,830	726,617	+	42,213
1,507,750	770,105	728,091	+	42,014
1,508,898	769,410	729,701	+	39,709
1,508,554	769,912	727,495	+	42,417
1,506,800	766,376	726,551	+	39,825
1,508,758	768,960	728,524	+	40,436
1,507,460	766,739	728,135	+	38,604
1,507,481	768,078	726,939	+	41,139
1,508,348	769,748	726,838	+	42,910
1,508,350	769,075	728,509	+	40,566
1,508,193	767,065	727,867	+	39,198
1,507,564	767,074	726,896	+	40,178
1,508,519	768,276	727,730	+	40,546
1,509,163	770,536	728,768	+	41,768
1,506,842	767,156	728,523	+	38,633
1,507,564	768,109	729,078	+	39,031
1,508,050	768,552	727,786	+	40,766
1,507,118	767,459	728,002	+	39,457
1,507,645	768,543	726,532	+	42,011
1,509,193	769,779	727,897	+	41,882
1,509,776	770,001	728,134	+	41,867
1,508,836	770,138	729,422	+	40,716
1,505,704	765,964	726,306	+	39,658
1,506,859	768,461	727,578	+	40,883
1,507,997	767,863	727,992	+	39,871
1,507,845	767,967	726,978	+	40,989
1,511,157	771,719	730,206	+	41,513
1,509,784	768,410	728,275	+	40,135
1,509,316	770,497	729,113	+	41,384
1,507,692	767,585	725,071	+	42,514
1,507,030	768,134	727,658	+	40,476
1,509,971	769,642	728,992	+	40,650
1,510,301	770,559	729,857	+	40,702
1,508,167	768,120	727,882	+	40,238
1,508,422	770,130	727,163	+	42,967
1,507,745	769,765	725,748	+	44,017
1,507,142	768,247	727,061	+	41,186
1,507,894	769,339	727,901	+	41,438
1,508,368	767,333	727,878	+	39,455
1,508,038	768,215	729,526	+	38,689

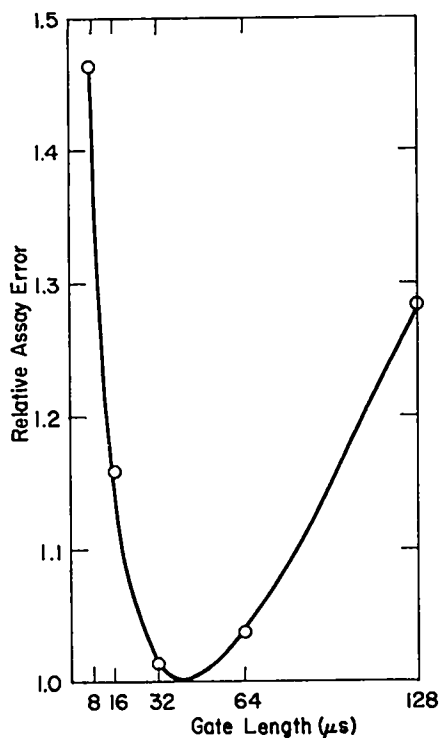


Fig. 4.1.

Relative assay error vs coincidence gate length for a 600 g PuO₂ sample in the HLNCC. The error is normalized to 1.000 at the 32 μs minimum. The circles indicate the errors at 8, 16, 32, 64, and 128 μs.

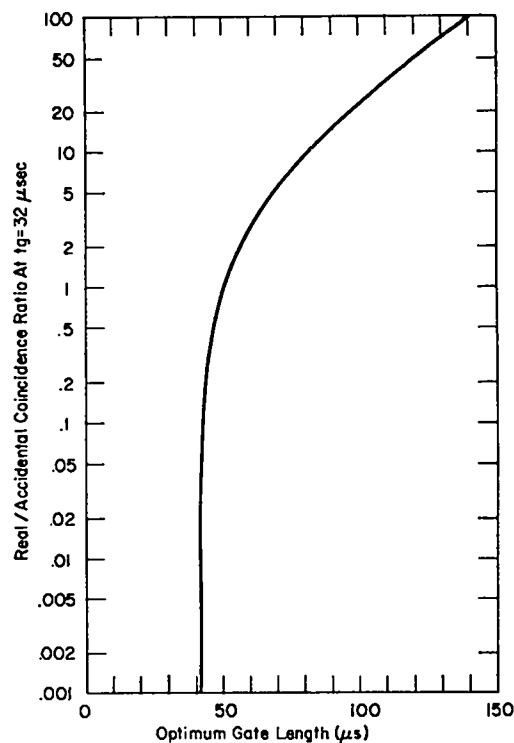


Fig. 4.2.

Optimum gate length vs real/accidental coincidence ratio for the HLNCC.

Figure 4.2 shows the gate length which produces the smallest error in a fixed counting time as a function of the real/accidental coincidence ratio in the HLNCC measured with a 32 μs gate. For most applications the real/accidental coincidence ratio is $\ll 1$, and therefore the 32 μs gate is generally used. However, the 64 μs gate may provide a lower statistical error for samples which produce low counting rates and which have small $(\alpha, n)/\text{fission neutron ratios}$.

The HLNCC electronics package is provided with selectable gate lengths of 8, 16, 32, 64, and 128 μs for general experimental purposes and for use with thermal-neutron coincidence counters other than the HLNCC detector.

4.4 Deadtime Correction

The deadtime of the HLNCC depends on the manner in which it is used. For the normal mode of operation, in which the electronics package is connected to

the hexagonal counter and all six channels are operating, the real coincidence deadtime has been measured as 2.4 μ s. The measured real coincidence counts are corrected with the equation

$$\dot{R}_O = \dot{R} e^{\delta \dot{T}},$$

where

$$\begin{aligned}\dot{R}_O &= \text{real coincidence rate after deadtime correction,} \\ \dot{R} &= \text{real coincidence rate before deadtime correction,} \\ \delta &= \text{coincidence deadtime, and} \\ \dot{T} &= \text{measured totals rate.}\end{aligned}$$

The totals rate is corrected by a similar equation:

$$\dot{T}_O = \dot{T} e^{\Delta \dot{T}},$$

where \dot{T}_O is the totals rate after deadtime correction and where $\Delta = 0.6 \mu$ s.

If one of the six detector banks is disconnected because of some operational problem, the deadtime correction is performed the same way, except that $\delta = 2.6 \mu$ s. If other detector-amplifier-discriminator combinations are used with the external input to the shift-register circuitry, the deadtime must be determined by a method similar to that described in section 2.4.5. (See also sections 3.7.7 and 3.7.8.)

4.5 ^{240}Pu Effective

The quantity of the even-mass plutonium isotopes in a sample is often referred to by its ^{240}Pu -effective content, which is usually defined as the mass of ^{240}Pu which would emit the same number of spontaneous fission neutrons per second as the combined ^{238}Pu , ^{240}Pu , and ^{242}Pu in the sample.

Relative neutron emission rates of the plutonium isotopes are tabulated in Table 4.2, where $\bar{\nu}_p$ is the average number of prompt neutrons emitted per spontaneous fission and where SF/g.s is the number of spontaneous fissions per gram per second. From the ratios shown in the last column of Table 4.2, the following equation can be written for the effective mass of ^{240}Pu (m_{eff}^{240}) as defined above:

$$m_{\text{eff}}^{240} = 2.43m^{238} + m^{240} + 1.69m^{242}, \quad (4-3)$$

where m^A is the mass of the isotope with mass number A.

However, the coincidence-counting efficiency of a shift register (SR) counter is not linearly dependent on \bar{v}_p ; therefore, Eq. (4-3) does not apply exactly for the coincidence counting of plutonium. A formula for ^{240}Pu -effective values for use with SR coincidence counters can be derived by evaluating the coincidence-counting efficiency for the individual plutonium isotopes. This efficiency ϵ_c (average number of real coincidence counts per spontaneous fission) is given by Eq. (2-1):

$$\epsilon_c = \epsilon^2 e^{-t_d/\tau} (1 - e^{-t_g/\tau}) \sum_{v=2}^{\infty} \binom{v}{2} P(v) ,$$

where the symbols are defined in section 2.4.2.

A preliminary and semiempirical evaluation of the neutron emission probabilities $P(v)$ was performed to estimate relative ϵ_c values for the even-mass plutonium isotope¹⁸. The results are shown in Table 4.3. The estimate for the ^{240}Pu -effective formula for use with real coincidence counts is then

$$m_{\text{eff}}^{240} = 2.49m^{238} + m^{240} + 1.57m^{242} .$$

This formula will be revised when the coefficients for the plutonium isotopes can be measured directly.

TABLE 4.2

NEUTRON EMISSION RATES OF EVEN-MASS PLUTONIUM ISOTOPES RELATIVE TO ^{240}Pu a

Isotope	\bar{v}_p	SF/g·s	n/s·g	n/s·g (Relative to ^{240}Pu)
^{238}Pu	2.26	1100	2486	2.43
^{240}Pu	2.17	471	1022	1.00
^{242}Pu	2.16	800	1728	1.69

^a Data from Ref. 2.

TABLE 4.3

RELATIVE RESPONSES OF A SHIFT-REGISTER COINCIDENCE
COUNTER TO THE EVEN-MASS PLUTONIUM ISOTOPES

Isotope	SF/g·s ^a	Coincidence	
		Counts ^b per SF (Relative to ²⁴⁰ Pu)	Counts per g·s (Relative to ²⁴⁰ Pu)
²³⁸ Pu	1100	1.067	2.49
²⁴⁰ Pu	471	1.000	1.00
²⁴² Pu	800	0.926	1.57

^a Data from Ref. 2.

^b Data from Ref. 18.

4.6 Matrix Effects

When neutron coincidence counters are used to measure bulk plutonium samples that are combined with large amounts of nonfissionable matrix materials, it is important to understand the influence of the matrix materials on the assay results so one can minimize the sensitivity of coincident-neutron assay techniques to the physical form and spatial configuration of such matrix materials.

A series of measurements was made^{23,24} with 12-cm-diam by 16-cm-high cans filled with materials typical of plutonium scrap output. The materials investigated are listed in the first column of Table 4.4. A small ²⁵²Cf source of spontaneous-fission neutrons was placed in the center of each can for counting both total and coincident-neutron events. The resulting count rates were normalized to unity for the case of the empty can - thus the deviation from unity represents the net effect of the added matrix material. The matrix effects are small except for the last two materials, which contain large amounts of hydrogen.

The last column of Table 4.4 gives the ratio of the square of the total counts to the coincidence counts. Because the total counts vary as the detector efficiency and the coincidence counts vary as the square of the efficiency, this ratio is independent of efficiency to a first-order approximation. Thus

TABLE 4.4

MATRIX MATERIAL EFFECTS ON HLNCC ASSAYS^b

<u>Matrix Material</u>	<u>Density (g/cm³)</u>	<u>Grams Matrix</u>	<u>Normalized Totals</u>	<u>Normalized Coincidences</u>	<u>Totals²/ Coincidences</u>
Empty can			1.000	1.000	1.000
MgO	0.702	703.5	1.014	1.008	1.019
Sand	1.753	1549.0	1.033	1.056	1.011
Ash	1.081	1437.0	1.030	1.044	1.016
Poly (chips)	0.052	92.5	1.017	1.033	1.002
Poly ^a (0.5 cm)	0.92	44.3	1.045	1.102	0.992
Poly ^a (1.2 cm)	0.92	139.9	1.073	1.166	0.988
Poly ^a (1.8 cm)	0.92	288.05	1.063	1.148	0.985
Poly ^a (4.3 cm)	0.92	1120.9	0.907	0.830	0.990

^a The 0.5 cm, etc., correspond to CH₂ wall thickness inside the can.

^b Data from Ref. 24.

the ratio shown in column 5 is relatively independent of detector-efficiency changes due to sample matrix materials. This consistency check can be used as a diagnostic tool in neutron coincidence counting to verify that observed rate changes are not caused by efficiency changes or electronics problems.

It is concluded that most carbides and oxides have little effect on the observed coincident-neutron response and that the observed perturbation is approximately the same for all cases except those where large quantities of hydrogenous matrix materials are involved.

In general, when a standard which closely matches the characteristics of the assay sample is available as a calibration standard for the assay, the influence of the matrix material is taken into account by the calibration. However, when little is known about the sample, some additional measurement is required to determine the influence of the matrix material.

A source-addition technique has been developed²⁰ for the correction of matrix effects in the coincidence counting of plutonium scrap. A similar technique can be used with the HLNCC as follows. A small spontaneous-fission source, such as the ²⁵²Cf calibration source, is placed in the sample holder

in the detector well and the totals count rate observed. Then the unknown sample is positioned in the detector well directly on top of the fission source. The observed change in the known source counting rate provides a measure of the perturbation due to the matrix material in the unknown sample.

This technique was applied²⁰ to the materials listed in Table 4.5; the corrected efficiencies are given in the last column of the table. It was necessary to increase the measured source perturbation by ~5% to account for the difference in geometric coupling between the actual source location as compared to a (more exact) central source location in the interior of the can. It can be seen that the corrected coincidence-counting efficiencies are all within a few percent of the empty can case. Although these measurements were not performed with the HLNCC, the same procedure should apply.

A study of matrix effects in the counting of fast critical assembly drawers is described in section 4.12.1.2.

4.7 Multiplication Effects

4.7.1 Introduction. Neutron coincidence counting of large plutonium metal and plutonium oxide samples is strongly influenced by neutron multiplication, which is due to spontaneous-fission neutrons or (α, n) neutrons inducing fissions in the plutonium samples. This increases the total neutron production rate and the average multiplicity of the neutron-producing events. Because the coincidence counting rate is much more sensitive to multiplication than is the total neutron counting rate, the ratio of coincidence to totals counting rates can be used to correct for the multiplication effects in some sample categories.

4.7.2 Multiplication in Metal Plutonium Samples. For plutonium metal samples, where (α, n) reactions are negligible, a simple multiplication correction¹⁰ can be performed. Let M represent the neutron multiplication, $\bar{\nu}$ the average neutron multiplicity for spontaneous fission in the sample, ρ the ratio of the coincidence to totals counting rates for a small nonmultiplying sample (corrected for background), and ρ_M the same ratio for a sample with multiplication M . Then the multiplication is

$$M \approx \frac{1}{\bar{\nu}} \left[1 + (\bar{\nu} - 1) \frac{\rho_M}{\rho} \right]$$

TABLE 4.5

CORRECTION OF MATRIX MATERIAL EFFECTS ON THE PASSIVE NEUTRON ASSAY OF
Pu IN ONE-GALLON SCRAP RECOVERY CANS^C

<u>Matrix Material</u>	<u>Material Mass (kg)</u>	<u>Relative Singles Counting Efficiency^a</u>	<u>Relative Coincidence Counting Efficiency^a</u>	<u>Corrected Coincidence Efficiency^b</u>
Empty 1-Gal. Can	—	1.00	1.00	1.00
Carbon Pellets	1.89	1.03	1.05	0.97
Metal Parts	3.60	1.04	1.09	1.02
Slag-Crucible	1.80	1.03	1.08	1.01
Concrete	3.24	1.05	1.10	1.02
String Filters	0.60	1.07	1.17	1.05
CH ₂ (ρ=0.065 g/cc)	0.27	1.06	1.11	1.00
CH ₂ (ρ=0.12 g/cc)	0.43	1.09	1.19	0.98
CH ₂ (ρ=0.27 g/cc)	0.97	1.19	1.36	1.04
H ₂ O (ρ=1.00 g/cc)	3.62	0.98	0.98	0.96

^a Efficiencies normalized to case of an empty can.

^b The counting rate was corrected using the source addition technique described in text.

^c Data from Ref. 20.

and the corrected real coincidence counting rate \dot{R}_C is

$$\dot{R}_C = \frac{\dot{R}_m}{M} \frac{\rho}{\rho_M} \quad (4-4)$$

where \dot{R}_m is the measured real coincidence counting rate. For example, the measurement of a small (10 g) metal plutonium sample in the HLNCC gives a background-corrected coincidence-to-totals ratio $\rho = 0.053$. If the measurement of a large plutonium metal sample gives a background-corrected and dead-time-corrected ratio $\rho_M = 0.061$, then the multiplication is

$$M \approx \frac{1}{2.17} \left[1 + (2.17-1) \frac{0.061}{0.053} \right] = 1.081 .$$

If the deadtime-corrected real coincidence rate from the large sample is 683 s^{-1} , then the real coincidence rate corrected for multiplication is

$$\dot{R}_c = \frac{683}{1.081} \frac{0.053}{0.061} = 549 \text{ s}^{-1}.$$

This multiplication-correction procedure was applied to a series of measurements designed to emphasize multiplication in a coincidence-counting experiment. Two groups of fast-critical-assembly fuel plates (see section 4.12.1) with total plutonium mass of $\sim 900 \text{ g}$ were counted 10 times. Each successive measurement had a closer geometric coupling than the previous one, as illustrated in Fig. 4.3. Since each measurement had the same plutonium mass and nearly the same absolute counting efficiency, the difference in response was due to multiplication. The real coincidence counting rate is shown in Fig. 4.4 as a function of position (upper curve). Also shown is the response as corrected with the procedure outlined above. One small fuel plate was used to determine ρ . The real coincidence rate per gram of ^{240}Pu -effective increased as much as 47% over a nonmultiplying plate; however, after correction all real coincidence rates are constant within the statistical errors. The largest multiplication calculated for this series of measurements was $M = 1.15$. The multiplication correction procedure thus appears to correct the real coincidence response of plutonium metal in any geometry for multiplication enhancement if $M \leq 1.15$. If $M \gg 1.15$, a more elaborate correction procedure will probably be required. The upper limit to M for which the correction procedure is useful is not yet known.

4.7.3 Multiplication in Samples with (α, n) background. Plutonium samples which contain certain elements of low atomic number (such as C, O, and F) produce random neutron backgrounds from the (α, n) reactions between the plutonium and americium alpha particles and the light elements. E.g., a PuO_2 sample generates random neutrons from (α, n) reactions on ^{17}O and ^{18}O ; the neutron production from these (α, n) reactions is comparable to that from spontaneous fission. The relative (α, n) neutron production rates for various light elements may be estimated from Table 4.6, which shows the thick-target neutron yield per 10^6 polonium alpha particles. The neutron yields from oxides and fluorides of plutonium are shown in Table 4.7; the yield from $^{241}\text{AmO}_2$ is 3754 neutrons/(s·g Am).²

Two types of multiplication occur in plutonium samples

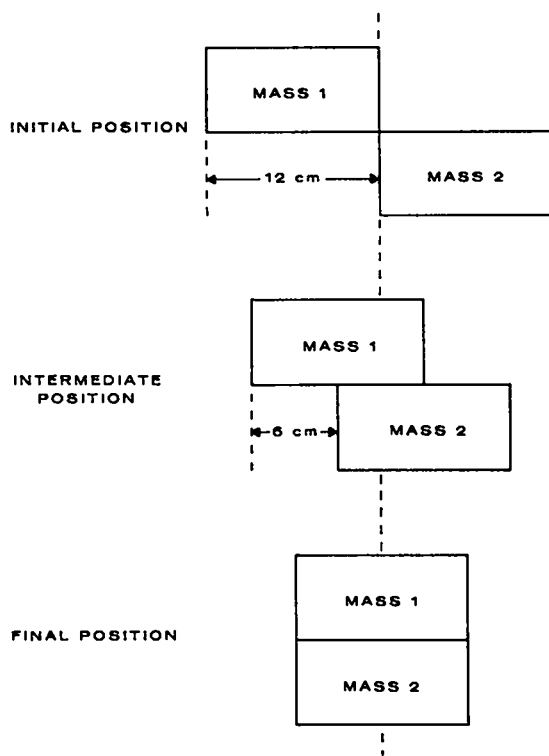


Fig. 4.3.

Diagram of neutron multiplication experiment with two groups of fast critical assembly fuel plates.

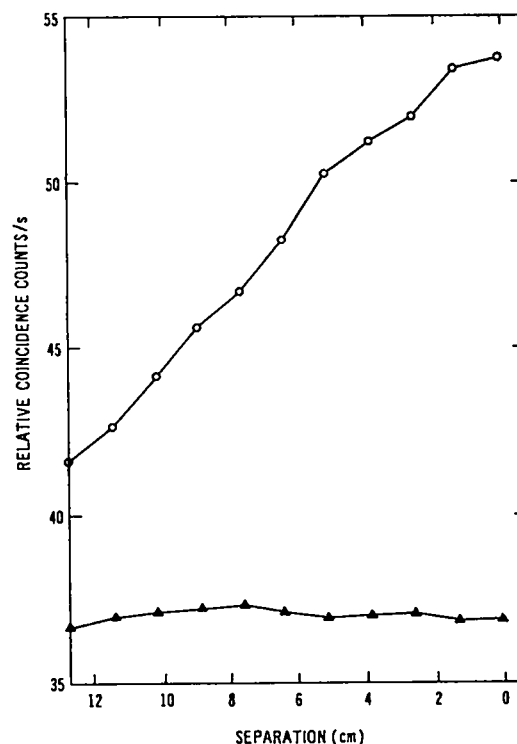


Fig. 4.4.

Relative coincidence counts per second vs the separation between two groups of ZPPR fuel plates. The upper and lower curves show the data before and after correction for multiplication, respectively. (From ref. 35.)

which have (α, n) neutron production. The first is the same as for the plutonium metal samples discussed in the previous section, where a spontaneous-fission neutron induces an additional fission (or fissions) in the plutonium. The second is where an (α, n) neutron induces a fission (or, indirectly, fissions) in the plutonium.

In general it is not presently possible to separate these effects and correct the measured real coincidence rate for multiplication in samples with (α, n) neutron production. However, if the samples to be assayed are all of the same material type and if the fractional (α, n) production can be measured or calculated, then a multiplication correction¹⁰ can be performed in a

manner similar to that described in the previous section. The multiplication M is

$$M = \frac{1}{\bar{v}} \left[1 + \frac{(\bar{v}-1)}{1+\beta} \frac{\rho_M}{\rho} \right] , \quad (4-5)$$

where

$$\beta = \alpha \left(\frac{M-1}{M} \right) \left(\frac{\bar{v}_I}{\bar{v}_I-1} \right) \frac{M\bar{v}_I-1}{M\bar{v}_I-1} , \quad (4-6)$$

α = ratio of (α, n) to spontaneous-fission neutrons,

\bar{v}_I = average multiplicity for induced fission,

and where the other parameters have the same meaning as in the previous section.

TABLE 4.6

(α, n) NEUTRON PRODUCTION RATES FROM VARIOUS LIGHT ELEMENTS^a

<u>Element</u>	<u>Neutron Yield per 10⁶ α's^b</u>	<u>Yield Relative to Beryllium</u>
Be	80	1.00
B	24	3.0×10^{-1}
F	12	1.5×10^{-1}
Li	2.6	3.6×10^{-2}
Na	1.5	1.9×10^{-2}
Mg	1.4	1.8×10^{-2}
Al	0.74	9.3×10^{-3}
As	0.38	4.8×10^{-3}
Si	0.16	2.0×10^{-3}
Cl	0.11	1.4×10^{-3}
C	0.11	1.4×10^{-3}
O	0.07	8.8×10^{-4}
N	0.01	1.25×10^{-4}

^a Data from reference 2.

^b Polonium alpha particles.

The multiplication M can be obtained by eliminating β from Eqs. (4-5) and (4-6) and solving the resulting quadratic equation for M . The corrected real coincidence counting rate is then obtained from Eq. (4-4), as in the case of metal samples.

The procedures outlined above were applied to data from an experiment designed to study multiplication effects in PuO_2 samples. An on-line, thermal-neutron coincidence counter attached to a glovebox in a plutonium facility was used to count high density PuO_2 . A glass jar was filled with oxide in carefully measured increments ranging from 10 to 50 g.

Measurements covered the mass range of 10 to 500 g; backgrounds were carefully measured and subtracted from the totals and real coincidence counts. The observed coincidence-to-totals ratios were extrapolated to zero mass to obtain the nonmultiplying coincidence-to-totals ratio $\rho = 0.0337$. The (α, n) to spontaneous-fission neutron ratio α was determined in two ways.

- (1) The background-corrected totals counting rate, the detector efficiency, and the known ^{240}Pu -effective content of the smallest sample were used to calculate α .
- (2) The ratio was calculated from the data in Table 4.7.

The former calculation depends on the detector efficiency; the latter depends on assumptions about the impurity composition of the samples. The two methods agreed within 15%.

Figure 4.5 shows the corrected and uncorrected real coincidence rates per gram of ^{240}Pu versus the PuO_2 mass, with $\rho = 0.0337$ and $\alpha = 1.8$. The uncorrected response increases by 85% between 10 and 500 g, whereas the corrected response is constant within 1%. Fluctuations in the uncorrected response due to slight variations in powder geometry have also been smoothed out.

TABLE 4.7

(α, n) YIELDS FROM OXIDES AND FLUORIDES OF PLUTONIUM^a

Compound	Yield (neutrons/s·(g Pu))
$^{238}\text{PuO}_2$	14000
$^{239}\text{PuO}_2$	45
$^{240}\text{PuO}_2$	170
$^{241}\text{PuO}_2$	~ 10
$^{242}\text{PuO}_2$	~ 10
$^{238}\text{PuF}_4$	2.1×10^6
$^{239}\text{PuF}_4$	4.3×10^3
$^{240}\text{PuF}_4$	1.6×10^4

^a Data from reference 2.

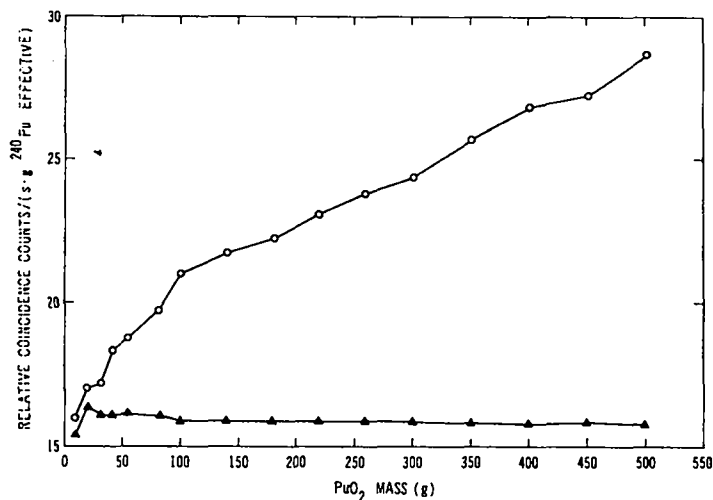


Fig. 4.5.
Relative coincidence counts per gram of effective ²⁴⁰Pu vs the PuO₂ sample mass. The upper and lower curves show the data before and after correction for multiplication, respectively. (From ref. 35).

The correction procedure for PuO₂ in the HLNOC is as follows:³⁵

1. If the (α,n) to spontaneous-fission neutron ratio α is not known and if a small, nonmultiplying sample of the material is available with known plutonium mass and isotopic composition, then α can be determined from the equation

$$\alpha = \frac{\dot{T} - \dot{T}_S}{\dot{T}_S},$$

where

$\dot{T}_S = \epsilon(1022) m_{\text{eff}}^{240}$ = totals counting rate due to spontaneous-fission neutrons,

\dot{T} = measured totals counting rate,

ϵ = absolute detector efficiency measured with the ²⁵²Cf calibration source, and

m_{eff}^{240} = ²⁴⁰Pu-effective mass calculated from $m_{\text{eff}}^{240} = 2.43m^{238} + m^{240} + 1.69m^{242}$, where m^A is the mass of plutonium isotope A in grams.

If no small sample is available for the measurement of α, it can be calculated [on the assumption that the (α,n) yields from chemical impurities in the oxide are small] from the equation

$$\alpha = \frac{140f_{238} + 0.45f_{239} + 1.7f_{240} + 0.1f_{241} + 0.1f_{242} + 3.75f_{241}(\text{Am})}{10.22 [2.43f_{238} + f_{240} + 1.69f_{242}]},$$

where f_A is the relative mass of the plutonium isotope with mass number A and where $f_{241(\text{Am})}$ is the relative mass of ^{241}Am .

2. Calculate the coincidence-to-totals ratio ρ for a nonmultiplying sample from the relation

$$\rho = \frac{0.053}{1+\alpha}.$$

3. Measure the unknown sample and determine the deadtime-corrected and background-corrected coincidence-to-totals ratio ρ_M . The multiplication M for the unknown sample is

$$M = \frac{-B + \sqrt{B^2 - 4AC}}{2A},$$

where

$$A = 2.17 + 4.5,$$

$$B = -\left(\frac{1.17 \rho_M}{\rho} + 6\alpha + 1\right), \text{ and}$$

$$C = 1.5\alpha.$$

4. Calculate the corrected real coincidence rate \dot{R}_C from the equation

$$\dot{R}_C = \frac{\dot{R}_m \rho}{M \rho_M},$$

where

\dot{R}_m = measured real coincidence rate corrected for deadtime and background,

M = multiplication,

ρ = coincidence-to-totals ratio (corrected for deadtime and background) for a nonmultiplying sample, and

ρ_M = same as above for the multiplying sample.

4.8 Criticality

Because the HLNCC was designed primarily for the assay of high-mass plutonium samples and because the polyethylene in the HLNCC is a good

reflector and moderator, particular emphasis must be placed on criticality safety. The user must make arrangements with the facility in which the measurements are to be made to ensure that the proposed measurement procedures will not produce a criticality hazard.

Plutonium metal and oxide samples with total sample masses below 2.5 kg do not present a criticality hazard in the HLNCC, provided that not more than one sample is present in the detector at a time. Nevertheless, it will generally be necessary to obtain approval from the facility for specific procedures for the measurement of any material in the HLNCC.

4.9 Total Plutonium

Two general methods are used to obtain the total plutonium content of a sample from the data provided by the HLNCC. The first involves the use of calibration curves which relate the measured real coincidence rates to the total plutonium masses. Calibration curves have the advantage that matrix, geometric, multiplication, and other effects (including deadtime, if desired) are corrected automatically. For each sample type, several plutonium standards which closely match the characteristics of the unknowns are used to construct a calibration curve. Once the fitting parameters and associated errors are determined, the measured real coincidence rate determines the plutonium mass and its standard deviation. (See Sec. 4.10, Calibration Procedures.) However, two corrections may be required.

1. The calibration procedure will frequently be performed at a different location than the assays. To account for possible changes in detector efficiency, the measured real coincidence rate can be multiplied by a normalization factor η determined from the ^{252}Cf calibration source:

$$\eta = \frac{\dot{R}_O^{\text{Cf}} e^{-\lambda t}}{\dot{R}^{\text{Cf}}} ,$$

where

\dot{R}_O^{Cf}	=	measured real coincidence rate from the ^{252}Cf calibration source at the calibration location,
\dot{R}^{Cf}	=	same rate at the assay location,
λ	=	^{252}Cf decay constant = $7.19 \times 10^{-4} \text{ d}^{-1}$, and
t	=	time between calibration and assay in days.

The normalization factor η should not be applied unless the correction is larger than the error on the correction. For 1000 s measurements on the ^{252}Cf calibration source, correction factors between 0.995 and 1.005 are not statistically significant.

2. Calibration standards rarely have characteristics identical to the assay samples. If the differences in characteristics are great, sophisticated modeling may be required to extrapolate the calibration curve into a form usable with the assay samples. However, if the differences are slight, a simple renormalization may provide an adequate correction. A common situation occurs when the material types are the same (for example, cans of PuO_2 powder), but the isotopic composition is different. In such a case the plutonium mass of the assay sample determined from the calibration curve can be multiplied by the normalization factor

$$\xi = \frac{(^{240}\text{Pu-effective per g Pu})_{\text{standard}}}{(^{240}\text{Pu-effective per g Pu})_{\text{unknown}}}$$

to obtain an approximate isotopic correction for the determination of total plutonium.

The second method is used when it is difficult or impossible to construct a calibration curve of the measured real coincidence rate vs the plutonium mass. For example, the coincidence rate measured for Zero Power Plutonium Reactor (ZPPR) fuel plate storage canisters depends not only on the plutonium mass of the fuel plates, but also (due to multiplication) on the relative positions of the plates in the canister. In the second method corrections to the real coincidence rate are made for deadtime, multiplication, geometric and other effects; then the total plutonium is calculated from the isotopic composition and the known response of the HLNCC to a small sample of ^{240}Pu (see Sec. 2.4.3). Normalization to the ^{252}Cf calibration source may also be required.

A combination of the two methods is sometimes useful. For example, a calibration curve for cans of PuO_2 powder can be constructed to relate the ^{240}Pu -effective mass to the real coincidence rate after correction for deadtime and multiplication effects. Such a curve removes the effects of varying multiplication due to differing powder geometry and density.

Any method requires a knowledge of the isotopic composition of the assay sample to obtain the total plutonium content. If the isotopic composition is not known, supplementary high-resolution, gamma-ray measurements can be used to estimate the composition by analyzing gamma-ray line ratios.⁶ For example, a combined neutron-coincidence, gamma-ray measurement is shown in Fig. 4.7, where the HLNOC is used for coincidence counting and an intrinsic germanium detector is used for gamma-ray spectrometry on a ZPPR fuel drawer mockup.²⁸

4.10 Calibration Procedures

A detailed guide to calibration procedures is given in the "American National Standard Guide to Calibrating Nondestructive Assay Systems".³⁰ A simple discussion of two-parameter analysis and a procedural example is presented in the Appendix as an illustration. A more general procedure, which allows three calibration constants to be used and which allows uncertainties in the standard masses to be considered, is presented in ref. 30.

For two-parameter analysis the object is to determine a calibration curve or response function $R = R(a,b,m)$ which relates the detector response R to the sample mass m with calibration parameters a and b . If N standards are available which closely match the characteristics of the unknown sample, then the measured responses R_i to standard masses m_i ($i=1,N$) can be used to determine a and b by least-squares analysis. Typical response functions are chosen of the form $am+bm^2$, $am/(1+bm)$, am^b , or $a(1-e^{-bm})$. Once the calibration parameters have been determined, the assay mass of an unknown is calculated from its measured detector response R and the inverse calibration function $m = m(a,b,R)$. The estimated standard deviation s_m of m is⁵

$$s_m = \left(\frac{\partial R}{\partial m} \right)^{-1} \left[s_R^2 + \left(\frac{\partial R}{\partial a} \right)^2 s_a^2 + \left(\frac{\partial R}{\partial b} \right)^2 s_b^2 + 2 \operatorname{cov}(a,b) \left(\frac{\partial R}{\partial a} \right) \left(\frac{\partial R}{\partial b} \right) \right]^{1/2}, \quad (4-7)$$

where s_R , s_a , s_b are the estimated standard deviations of the detector response and the calibration parameters, and where $\operatorname{cov}(a,b)$ is the estimated covariance of the calibration parameters. The value for s_R is determined by the measurement; the values for s_a , s_b , and $\operatorname{cov}(a,b)$ are determined by the least-squares fitting procedure. For detailed examples, see the Appendix and section 4.11.2.

4.11 HP-97 Programming

Detailed information on the programming of the HP-97 calculator can be obtained from the HP-97 Owner's Handbook and Programming Guide.¹⁶ This section provides two programs to illustrate the use of the HP-97 with the HLNCC. Other programs can be readily created to satisfy the user's specific requirements. When a readout occurs in the HLNCC, the time, totals, R+A, and A data are transferred to registers R1, R2, R3, and R4, respectively, in the HP-97. The HLNCC then sends a "label A" instruction to the HP-97 which starts the calculator program at label A.

4.11.1 Example 1 - Basic Utility Routine. The basic information normally desired from the HLNCC is the real coincidence counting rate and the associated standard deviation. Frequently the totals rate is also useful. The program listed in Table 4.8 is a utility routine which provides the following output:

1. The time, totals, R+A, and A data to provide a permanent record.
2. The totals rate \dot{T} .
3. The real coincidence rate \dot{R} .
4. The standard deviation $\sigma_{\dot{R}}$ on the real coincidence rate due to counting statistics only.
5. $\sigma_{\dot{R}}$ expressed in percent.

A sample output is shown in Table 4.9.

4.11.2 Example 2 - Calculation of ^{240}Pu -Effective Mass From HLNCC Data and Calibration Curves. The program listed in Table 4.10 uses the data transferred by the HLNCC to calculate the ^{240}Pu -effective mass of the sample from a calibration curve of the form

$$\dot{R} = \frac{am}{1+bm} ,$$

where \dot{R} is the measured real coincidence rate, m is the ^{240}Pu -effective mass in grams and a and b are calibration constants. (See section 4.10, Calibration Procedures.) The program also calculates the estimated standard deviation s_m of m from Eq. (4-7):

$$s_m = \left(\frac{\partial \dot{R}}{\partial m} \right)^{-1} \left[s_{\dot{R}}^2 + \left(\frac{\partial \dot{R}}{\partial a} \right)^2 s_a^2 + \left(\frac{\partial \dot{R}}{\partial b} \right)^2 s_b^2 + 2 \text{cov}(a,b) \left(\frac{\partial \dot{R}}{\partial a} \right) \left(\frac{\partial \dot{R}}{\partial b} \right) \right]^{1/2} ,$$

TABLE 4.8

HP-97 BASIC UTILITY ROUTINE FOR THE HLNCC

<u>Program Step</u>	<u>Function</u>	<u>Comment</u>
001	*LBLA	start
002	FIX	
003	DSP0	display integers
004	RCL1	recall time
005	PRTX	print time
006	RCL2	recall totals
007	PRTX	print totals
008	$X \leftrightarrow Y$	exchange time and totals
009	\div	calculate T
010	STO5	store T in register 5
011	RCL3	recall R+A
012	PRTX	print R+A
013	RCL4	recall A
014	PRTX	print A
015	SPC	print space
016	-	calculate R
017	RCL1	recall time
018	\div	calculate R
019	STO6	store R in register 6
020	RCL5	recall T
021	DSP4	display 4 decimal places
022	PRTX	print T
023	SPC	print a space
024	RCL3	recall R+A
025	RCL4	recall A
026	+	calculate (R+A) + (A)
027	\sqrt{X}	calculate σ_R
028	RCL1	recall time
029	\div	calculate σ_R
030	RCL6	recall R
031	PRTX	print R
032	$X \leftrightarrow Y$	exchange R and σ_R
033	PRTX	print σ_R
034	$X \leftrightarrow Y$	exchange R and σ_R
035	\div	calculate σ_R/R
036	1	
037	0	
038	0	enter 100
039	x	calculate σ_R in %
040	DSP2	display 2 decimal places
041	PRTX	print % error (10)
042	SPC	
043	SPC	print 2 spaces
044	R/S	stop

TABLE 4.9

SAMPLE HP-97 OUTPUT FROM BASIC UTILITY ROUTINE

<u>Output</u>		<u>Comment</u>
1000.	***	time
35896261.	***	totals
41758772.	***	R+A
41233334.	***	A
35896.2610	***	totals rate \dot{T}
525.4380	***	real coincidence rate \dot{R}
9.1100	***	estimated standard deviation of \dot{R} ($s_{\dot{R}}$)
1.73	***	$s_{\dot{R}}$ in %

where the terms have been defined in section 4.10 (the response is chosen as the real coincidence rate \dot{R}).

The program operates as follows.

1. The HLNCC data are printed to produce a permanent record.
2. The real coincidence rate \dot{R} and estimated standard deviation $s_{\dot{R}}$ are calculated and printed.
3. The ^{240}Pu -effective mass m is calculated from the inverse calibration equation

$$m = \frac{\dot{R}}{a - b\dot{R}}$$

and is printed.

4. The standard deviation s_m is calculated from the equation for s_m above and is printed.

It is assumed for this illustration that deadtime corrections have been incorporated into the calibration curve.

The calculation requires the values for a , b , s_a , s_b , and $\text{cov}(a,b)$, which must be obtained from the calibration procedure and stored in registers A, B, C, D, and E, respectively. Once the calibration parameters are entered and the HLNCC started, the measurement and calculations are performed automatically. The use of the storage registers is detailed in Table 4.11. An example of the program's output is presented in Table 4.12.

TABLE 4.10

HP-97 PROGRAM TO CALCULATE ^{240}Pu -EFFECTIVE MASS
FROM HLNCC DATA AND A CALIBRATION CURVE

Program Step	Function	Comment
001	*LBLA	start
002	FIX	
003	DSP0	display integers
004	RCL1	
005	PRTX	print time
006	RCL2	
007	PRTX	print totals
008	RCL3	
009	PRTX	print R+A
010	RCL4	
011	PRTX	print A
012	-	calculate R
013	RCL1	
014	\div	calculate \dot{R}
015	STO5	
016	SPC	print space
017	DSP2	display 2 decimal places
018	PRTX	print \dot{R}
019	RCL3	
020	RCL4	
021	+	
022	\sqrt{X}	calculate $\sqrt{(R+A) + (A)}$
023	RCL1	
024	\div	calculate $s_R^{\dot{}}$
025	STO6	
026	PRTX	print $s_R^{\dot{}}$
027	SPC	
028	RCL5	
029	RCLA	
030	RCLB	
031	RCL5	
032	x	
033	-	
034	\div	calculate $m = \dot{R}/(\dot{a}-\dot{b}\dot{R})$
035	PRTX	print m
036	STO7	
037	RCLB	
038	x	
039	1	
040	+	calculate $(1+bm)$
041	STO8	
042	RCL7	
043	X \neq Y	

TABLE 4.10 (cont)

Program Step	Function	Comment
044	\div	calculate $\left(\frac{\partial \dot{R}}{\partial a}\right)$
045	STO9	
046	RCL7	
047	RCL8	
048	\div	
049	x ²	
050	RCLA	
051	x	
052	CHS	calculate $\left(\frac{\partial \dot{R}}{\partial b}\right)$
053	STO0	
054	RCL6	
055	x ²	calculate $s_{\dot{R}}^2$
056	RCL9	
057	RCLC	
058	x	
059	x ²	calculate $\left[\left(\frac{\partial \dot{R}}{\partial a}\right) s_a\right]^2$
060	+	
061	RCL0	
062	RCLD	
063	x	
064	x ²	calculate $\left[\left(\frac{\partial \dot{R}}{\partial b}\right) s_b\right]^2$
065	+	
066	2	
067	RCLE	
068	x	
069	RCL9	
070	x	
071	RCL0	
072	x	calculate $2 \text{ cov}(a,b) \left(\frac{\partial \dot{R}}{\partial a}\right) \left(\frac{\partial \dot{R}}{\partial b}\right)$
073	+	
074	\sqrt{x}	
075	RCL8	
076	x ²	
077	x	
078	RCLA	
079	\div	calculate s_m
080	PRTX	print s_m
081	SPC	
082	SPC	print 2 spaces
083	R/S	stop

4.12 Examples

4.12.1 Plutonium in Fast Critical Assembly Drawers

4.12.1.1 General Considerations. Critical assembly mockups of fast breeder reactors require large inventories of plutonium fuel. The plutonium is usually in the form of thin plates, 1.6 to 6.4 mm thick, 5 cm wide, and up to 22.9 cm long. These plates are interspersed with appropriate nonfissile mockups of fertile, structural, and coolant materials and placed in "trays" or "drawers" approximately 5 cm square and up to 91 cm long (see Fig. 4.6). A typical drawer may contain 0.5 to 1.0 kg of fissile plutonium. The drawers are then stacked into two halves of the critical assembly machine, which are brought together remotely to perform the measurements.

TABLE 4.11

HP-97 REGISTER USAGE FOR ^{240}Pu -EFFECTIVE-MASS PROGRAM

<u>Register</u>	<u>Use</u>
1	time
2	totals
3	R+A
4	A
5	\dot{R}
6	s_R
7	m
8	$1 + bm$
9	$\partial \dot{R} / \partial a$
0	$\partial \dot{R} / \partial b$
A	a
B	b
C	s_a
D	s_b
E	cov(a,b)

TABLE 4.12

SAMPLE HP-97 OUTPUT FROM ^{240}Pu -EFFECTIVE-MASS PROGRAMCalibration Parameters

$a = 6.515$
 $b = -3.048 \times 10^{-3}$
 $s_a = 0.1558$
 $s_b = 3.049 \times 10^{-4}$
 $\text{cov}(a,b) = 4.339 \times 10^{-5}$

<u>Output</u>		<u>Comment</u>
1000.	***	time
35896261.	***	totals
41758772.	***	R+A
41233334.	***	A
525.44	***	\dot{R}
9.11	***	s_R^*
64.74	***	$m(\text{g } ^{240}\text{Pu-effective})$
1.04	***	$s_m(\text{g } ^{240}\text{Pu-effective})$

Because of the large number of fuel plates involved and their disposition inside the drawers, verification of the plutonium content of each plate individually is difficult and time-consuming. A good measurement technique is needed to verify the fissile content of an entire drawer without removal of the individual plates.

Experiments were performed²⁸ to investigate the feasibility of nondestructive assay measurements on integral drawers. Fuel plates containing 28 w/o plutonium with 11.5 a/o ^{240}Pu or 20 w/o plutonium with 8.6 a/o ^{240}Pu were combined with plates of aluminum, sodium, carbon, iron, and depleted uranium to form assemblies as shown in Fig. 4.6.

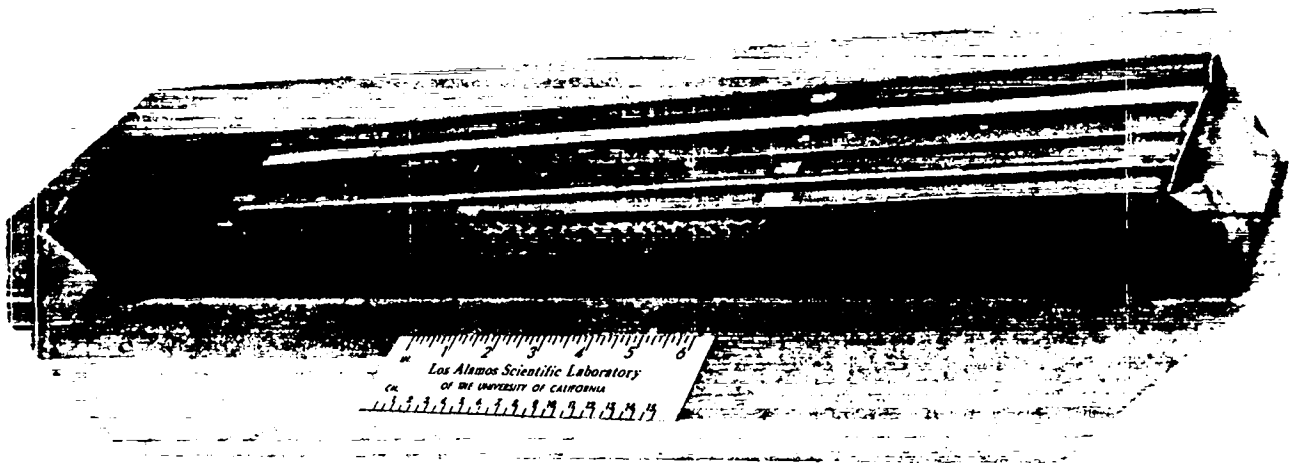


Fig. 4.6.

ZPPR drawer containing two rows of plutonium plates interspersed with plates of depleted uranium, sodium, aluminum, carbon, and iron to mock up structure and coolant materials in a fast critical assembly. (From ref. 28.)

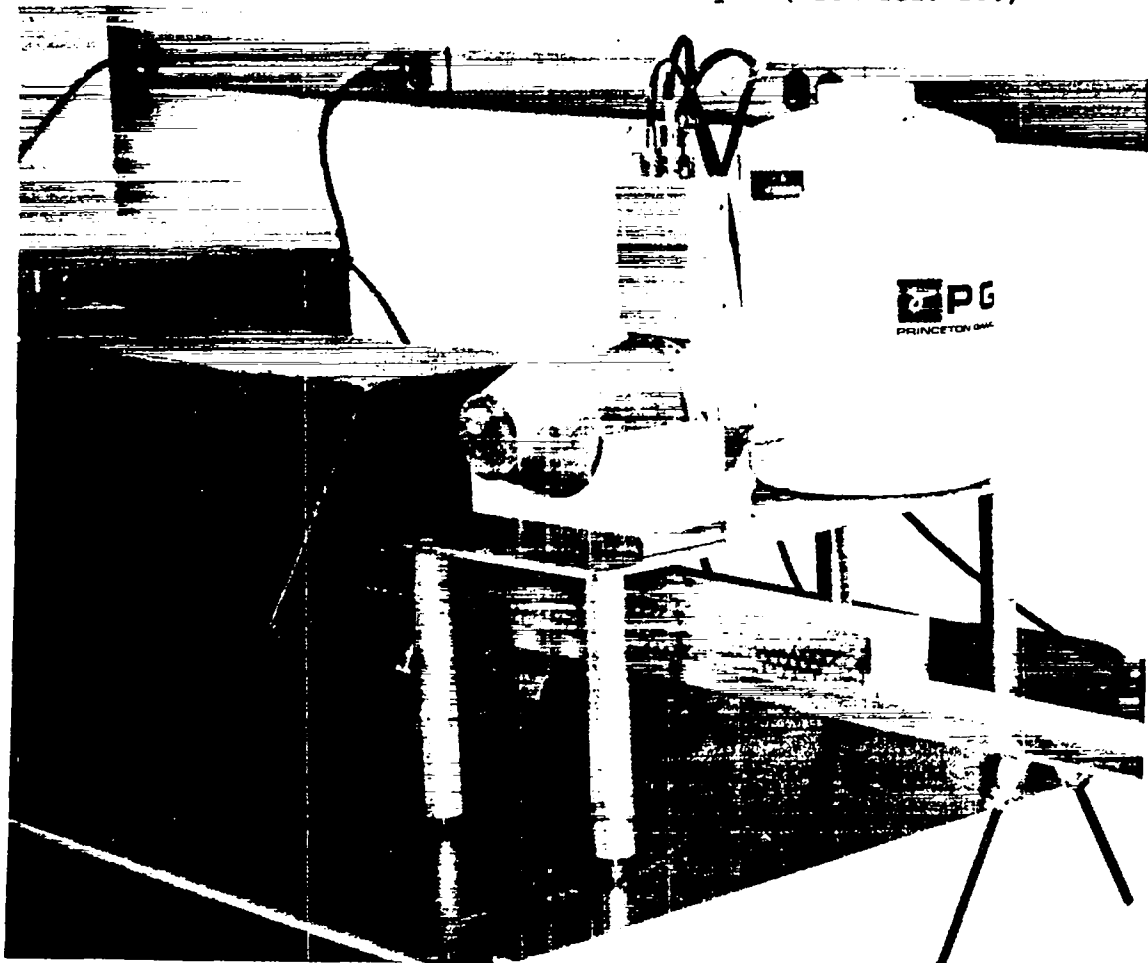


Fig. 4.7.

Measurement setup for a ZPPR drawer, showing the HINCC for neutron coincidence counting and the IAEA intrinsic germanium detector with its collimator for measurement of plutonium gamma-ray line ratios. (From ref. 28.)

For this application, the detector was placed on its side for the horizontal handling of the FCA drawers as shown in Fig. 4.7. Also shown in Fig. 4.7 is the International Atomic Energy Agency (IAEA) intrinsic germanium detector which is being evaluated for plutonium isotopic measurements by using gamma-ray line ratios.⁶ The combination of the neutron and gamma-ray detectors gives an independent verification of the total plutonium content in the sample.

The initial goal was to develop a measurement technique for assaying the plutonium in drawers from fast critical assemblies. A two-position measurement technique for FCA drawers was developed to give a uniform assay weight to the plutonium regardless of its axial position in the drawer. The full width at half maximum (FWHM) of the efficiency curve without end plugs is 40 cm. If a sample container is positioned so its center is located ± 20 cm from the center of the detector, the resulting sum from the two-position count gives a uniform counting efficiency over a sample length of approximately 40 cm. Figure 4.8 shows the sum of two sets of data taken with a small ^{252}Cf neutron source that was moved along the axis of the detector.²⁴ The data centroids are separated by 40 cm resulting in the extended region of uniformity for the sum. Because the FCA drawers typically contain the plutonium in a 5 x 5 x 40-cm section, the two-position count gives uniform weight to the plutonium regardless of its position in the 40-cm-long section. A special support tray can be included in the HLNCC detector shipping container for the assay of FCA drawers.

4.12.1.2 FCA Matrix Effects. For the quantitative nondestructive assay of FCA drawers, it is necessary to have standards that approximate the actual FCA drawers. If the plutonium content is varied in the standard drawers, a calibration curve is generated. However, the question must be answered as to whether the coincidence rate is also a function of the nonfissile matrix materials in the drawers. These materials are typically Na, Al, Fe, and depleted uranium plates positioned in parallel to the plutonium plates.

To evaluate this problem,²² several matrix samples were fabricated that matched the general shape of the FCA drawer but had the full density of the metal in question. Thus the matrix effect of the metal would be larger than for the actual FCA drawer. A ^{252}Cf neutron source was placed in the center of the 5x5x30-cm matrix sample to simulate a plutonium spontaneous-fission source. Table 4.13 lists the materials that were studied along with an actual ZPPR drawer with the plutonium plates removed. The totals rates and coincidence rates have been normalized to the rate of the ^{252}Cf source in an empty

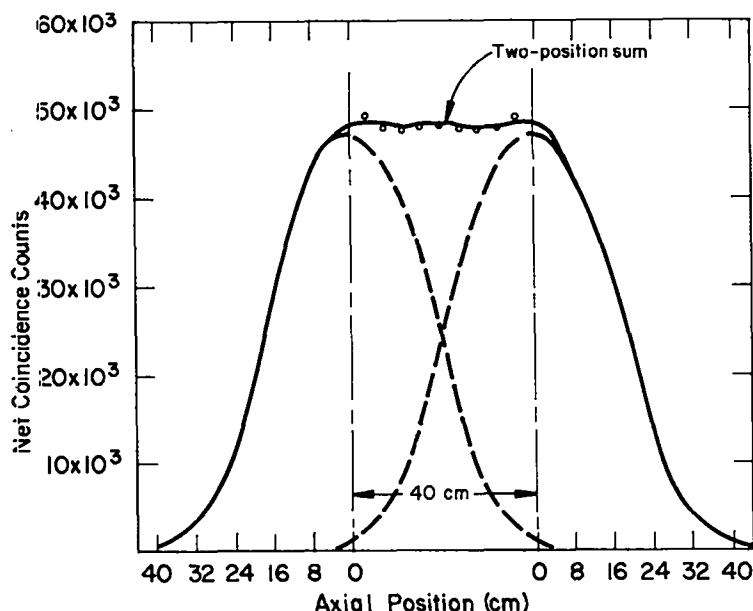


Fig. 4.8.
Axial coincidence efficiency for the two-position count to obtain a uniform sum over an extended region (40 cm). (From ref. 24.)

drawer. It can be seen that all of the matrix materials increase the totals and coincidence rates. In general, this increased counting efficiency is a result of the scattering back into the detector of neutrons that would otherwise leak out the open ends. If the efficiency changes only from neutron scattering and moderation effects, the normalized ratio of (coincidence counts)/(totals squared) will remain unity because the coincidence rate depends on the efficiency squared. This is true for all the samples except the depleted uranium where fast-neutron multiplication is taking place. This multiplication effect increases the effective multiplicity and thus increases the coincidence rate as seen in Table 4.13. Also, the normalized ratio of the (coincidence rate)/(totals rate squared) increases to 1.10.

Excluding the solid depleted-uranium case, the matrix effect of the actual ZPPR drawer was quite similar to the other matrix materials investigated. The rate from the iron core was relatively high because of iron's high macroscopic neutron scattering cross section. The loading of an unknown drawer with depleted uranium is not a practical problem because of the excessive weight that would be involved.

It is concluded from this study that FCA standards should have the same geometry as the assay samples, but that the matrix materials need not exactly match the materials in the unknown drawers. However, when the appropriate matrix filler materials are available, they should be used in the standard drawers to improve the accuracy of the assay.

TABLE 4.13

MATRIX MATERIAL EFFECTS ON THE ASSAY OF FAST CRITICAL ASSEMBLY
DRAWERS WITH THE HLNCC^b

<u>Matrix Material</u>	<u>Normalized Totals</u>	<u>Normalized Coincidence Counts</u>	<u>Coincidence/Totals²</u>
None	1.000	1.000	1.00
Na (5 x 5 x 30 cm)	1.042	1.114	1.03
Al (5 x 5 x 30 cm)	1.068	1.142	1.00
CH ₂ (5 x 5 x 30 cm)	1.078	1.163	1.00
Fe (5 x 5 x 30 cm)	1.120	1.291	1.03
ZPPR Drawer ^a	1.107	1.224	1.00
0.2% Dep U (5 x 5 x 20 cm)	1.233	1.668	1.10

^a The ZPPR drawer (5 x 5 x 60 cm) was filled with the normal matrix of Na, Al, Fe, and depleted uranium (0.2% ²³⁵U), but without any plutonium plates.

^b Data from Ref. 22.

4.12.1.3 Multiplication Effects. A general discussion of multiplication effects in plutonium metal samples is given in section 4.7.2; an example of a correction for multiplication effects was given for fast critical assembly fuel plates. The ability to correct for multiplication is particularly significant for fast critical assembly drawers and canisters because it excludes the possibility of compensating for diverted fuel plates by rearranging the geometrical configuration of the remaining plates to restore the original counting rates by increasing the multiplication.

4.12.2 Plutonium in Cans or Bottles. For the measurement of plutonium in cans or bottles, the counter should be used in a vertical orientation with the end plugs in place. The efficiency profile of the counter will then be similar to the curves shown in Figs. 2.18 and 2.19, and the center of the plutonium-bearing material should be positioned at roughly the center of the detector. The sample rotator, which can be included with the HLNCC, need be used only when the coincidence detector is combined with the intrinsic germanium detector to obtain the plutonium isotopic ratios. In this case the rotation of the sample gives a more uniform measurement with the germanium detector.

For samples having negligible neutron multiplication, there is great flexibility in matching (or mismatching) the standard to the assay samples. Because of the enclosed (4π) counting geometry, the standards need not have exactly the same chemical composition, isotopic mixture, geometric size, density, matrix materials, and containment as the assay samples. For example, a small standard of PuO_2 powder in a doubly encapsulated metal container can be used to assay a fuel-rod pellet, a can of mixed-oxide pellets, small fuel-rod sections, and cans of scrap and waste in polyethylene bags. For the larger assay samples whose geometric configuration extends beyond the central axial 10-15 cm of the detector, the small-calibration standard should be positioned in this larger volume, and the results of the different positions should be averaged to represent the larger sample.

Bottles or other containers filled with liquids can be assayed in the HLNCC; however, the hydrogen content in the liquid will usually be large resulting in a significant change in the detector efficiency (see section 4.6). In this case the standard should be contained in a bottle with a similar amount of liquid.

When a standard closely matching the sample is available for an assay application, the influence of the matrix material or multiplication can be effectively accounted for by the calibration procedure. An example of a calibration curve for PuO_2 powder in cans is presented in Fig. A.1.

When little is known about the assay sample, the matrix and multiplication perturbations can be measured by the source-addition technique, as explained in section 4.6.

4.12.3 Plutonium in Fuel Rods or Assemblies. For fuel rods or assemblies the sample will, in general, extend beyond the ends of the HLNCC. The detector can be placed on its side to accommodate the long sample if there is no special overhead-crane handling setup. The end plugs will be removed and the efficiency profile will be similar to that shown in Fig. 2.18. Thus, the detector measures the ^{240}Pu -effective content per unit length weighted by the axial efficiency profile. The end of the rod or assembly should extend at least 15 cm beyond the geometric end of the detector unit to avoid an end effect in the measurement. In most cases, the sample will be scanned through the detector for its entire length and the results will be integrated to yield the total ^{240}Pu -effective content. The standard should be scanned in the same manner.

For International Atomic Energy Agency (IAEA) inspection and verification purposes, a technique is needed for measuring the plutonium content in mixed-oxide fuel assemblies. In cooperation with the IAEA, a series of measurements was made to evaluate the HLNCC for use with mixed-oxide fuel assemblies typical of those encountered during inspections.²⁵ A 28-rod mockup boiling water reactor (BWR) assembly shown in Fig. 4.9 was fabricated. The fuel rods are easily removed or added to the assembly so that geometric effects and neutron penetration from the interior of the fuel bundle can be investigated. The 11.2-cm-diam assembly contains 3 rings of fuel rods, with 16 rods in the outside ring, 8 in the second ring, and 4 in the center ring. All fuel rods contain 3 w/o PuO_2 .

In making the measurements the fuel assembly was placed in the center of the HLNCC in a vertical orientation. By removing rods from the assembly, the counter's sensitivity to rod substitutions could be observed. The results of the measurements are given in Fig. 4.10. One missing rod can be detected in a 200-s count, and a rod positioned in the center of the assembly has a sensitivity equal to that of a rod in the outer ring. This good penetrability is attributable to the fast neutrons, which are scattered but usually not absorbed by the $\text{PuO}_2\text{-UO}_2$ rods. The slight increase in the coincidence response as a function of rod loading is caused by end-effect backscattering into the counter.



Fig. 4.9.
Mixed-oxide BWR fuel-rod assembly
mockup for measurement with the
HLNCC. (From ref. 25.)

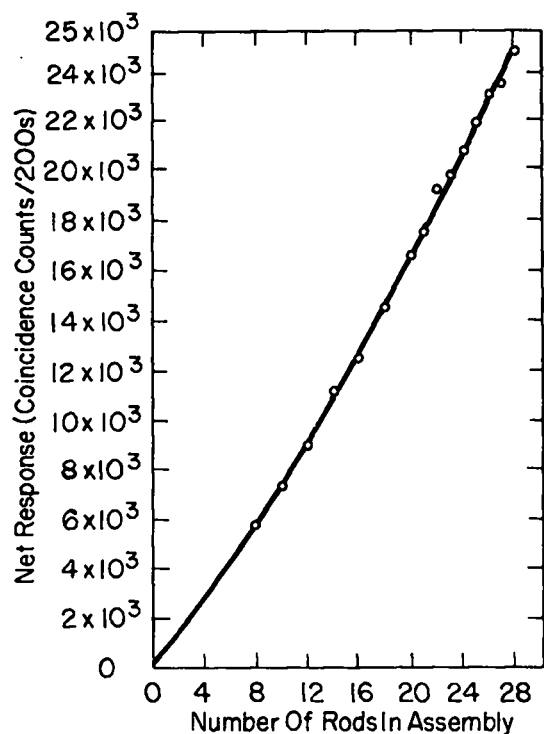


Fig. 4.10.
Coincidence response measured with
the HLNCC vs number of fuel rods in
a $\text{PuO}_2\text{-UO}_2$ fuel assembly
mockup. (From ref. 25.)

These experiments show that the HLNCC can be used to verify the effective ^{240}Pu loading in full fuel assemblies for cases in which the assembly can be lowered into the detector. If the plutonium isotopic composition is not known, a supplementary gamma-ray ratio measurement must be performed to deduce the total plutonium loading.⁶

APPENDIX

TWO-PARAMETER CALIBRATION PROCEDURE

1. GENERAL

The object is to determine parameters a and b for the response function $R = R(a, b, m)$ which relates the sample mass m to the detector response R . Assume that N standards are available with masses m_i ($i=1, N$) which are known with negligibly small error. Let R_i and s_i represent the detector responses and estimated standard deviations of the responses, respectively, to

the standards with masses m_i . Then the parameters a and b can be determined by an iterative, least-squares fitting procedure³ which minimizes the chi-square

$$\chi^2 = \sum_{i=1}^N Q_i^2 ,$$

where N is the number of standards and

$$Q_i = \frac{R_i - R(a,b,m_i)}{s_i} ,$$

where Q_i is the weighted difference between the measured response R_i and that calculated from the response function $R(a,b,m)$ for the standard with mass m_i ; the factor $1/s_i$ provides greater weight to those measurements with smaller estimated standard deviations (s_i).

To perform the iterative, least-squares analysis, initial estimates are made for the parameters a and b . Then the first-order Taylor's expansion for χ^2 ,

$$\chi^2 = \chi_0^2 + \left(\frac{\partial \chi_0}{\partial a} \right)^2 \Delta a + \left(\frac{\partial \chi_0}{\partial b} \right)^2 \Delta b ,$$

is minimized by setting its first order derivatives with respect to a and b equal to zero and solving for Δa and Δb . The procedure is then iterated with new estimates ($a+\Delta a$, $b+\Delta b$) for the fitting parameters until Δa and Δb become arbitrarily small. For each iteration the differences Δa and Δb are

$$\Delta a = \frac{1}{\Delta} \begin{vmatrix} s_4 & s_2 \\ s_5 & s_3 \end{vmatrix} \quad \text{and} \quad \Delta b = \frac{1}{\Delta} \begin{vmatrix} s_1 & s_4 \\ s_2 & s_5 \end{vmatrix} , \quad (\text{A.1})$$

where

$$\Delta = \begin{vmatrix} s_1 & s_2 \\ s_2 & s_3 \end{vmatrix} \quad (\text{A.2})$$

and where

$$s_1 = \sum_{i=1}^N \left(\frac{\partial Q_i}{\partial a} \right)^2, \quad s_2 = \sum_{i=1}^N \left(\frac{\partial Q_i}{\partial a} \right) \left(\frac{\partial Q_i}{\partial b} \right), \quad s_3 = \sum_{i=1}^N \left(\frac{\partial Q_i}{\partial b} \right)^2, \quad (\text{A.3})$$

$$s_4 = - \sum_{i=1}^N Q_i \left(\frac{\partial Q_i}{\partial a} \right), \quad \text{and} \quad s_5 = - \sum_{i=1}^N Q_i \left(\frac{\partial Q_i}{\partial b} \right). \quad (\text{A.4})$$

The error matrix

$$\epsilon = \frac{1}{\Delta} \begin{vmatrix} s_3 & -s_2 \\ -s_2 & s_1 \end{vmatrix} = \begin{vmatrix} s_a^2 & \text{cov}(a,b) \\ \text{cov}(a,b) & s_b^2 \end{vmatrix} \quad (\text{A.5})$$

gives the estimated variances and covariance of the parameters, where Δ , s_1 , s_2 , and s_3 are evaluated at convergence. The quality of the fit of the calibration function to the standards is measured by the reduced chi-square $\chi^2/(N-2)$, which should have a value close to unity (~ 0.3 to ~ 2). A large deviation of the reduced chi-square from unity is likely to be caused by an inadequate calibration function or by an underestimation of the measurement errors for the standards. The error s_m calculated from Eq. (4-7) is not meaningful if the reduced chi-square is not close to unity.

II. EXAMPLE

A calibration curve of the form $R = am/(1+bm)$ was fit to the standard data of Table A.1 with a short computer program. The standard masses m_i were assumed to be known exactly and the errors s_i were assumed to be due to counting statistics only. For the calibration function above,

$$Q_i = \frac{R_i - R(a,b,m_i)}{s_i} = \frac{R_i}{s_i} - \frac{am_i}{s_i(1+bm_i)}$$

and

$$\frac{\partial Q_i}{\partial a} = - \frac{m_i}{s_i(1+bm_i)},$$

$$\frac{\partial Q_i}{\partial b} = \frac{am_i^2}{s_i(1+bm_i)^2} , \text{ and}$$

$$\frac{\partial Q_i}{\partial m} = \frac{-a}{s_i(1+bm_i)^2} .$$

The initial estimates for a and b were chosen as $b = 0$ and $a \approx R/m = 69746/81.3 \approx 800$. Then Δa and Δb were calculated from Eqs. (A.1) to (A.4), with the result that $\Delta a = -167.73$ and $\Delta b = -0.0035442$. The new estimates for the parameters were $a = 800 - 167.73 = 632.27$ and $b = 0 - 0.0035442 = -0.0035442$, and the cycle was repeated. Table A.2 shows a, b, S1-S4, Δa and Δb for each iteration. The procedure was terminated when $|\Delta a| < 10^{-3}$ and $|\Delta b| < 10^{-7}$. The final values for a and b are

$$a = 651.50$$

$$b = -0.0030483.$$

Figure A.1 shows the calibration curve and the data points. Errors on the calibration parameters calculated from Eq. (A.5) are

$$s_a = \sqrt{\frac{S_3}{\Delta}} = \sqrt{\frac{64675100}{266305}} = 15.584 \text{ (2.39\%)} , \text{ and}$$

$$s_b = \sqrt{\frac{S_1}{\Delta}} = \sqrt{\frac{0.0247595}{266305}} = 0.00030492 \text{ (10.0\%)} .$$

The covariance of the parameters calculated from Eq. (A.5) is

$$\text{cov}(a,b) = -\frac{S_2}{\Delta} = -\frac{(-1155.43)}{266305} = 0.0043388 .$$

TABLE A.1

DATA ON PuO_2 STANDARDS FOR CONSTRUCTION OF CALIBRATION CURVE

<u>Standard Mass (m_i)</u> <u>(g ^{240}Pu-effective)</u>	<u>Detector Response (R_i)</u> <u>(real coincidence counts)</u>	<u>Estimated Standard</u> <u>Deviation on R_i (s_i)</u>
0.38	223	20
7.67	5051	175
43.4	32655	625
54.9	43803	795
81.3	69746	1133

TABLE A.2

CONVERGENCE DATA FROM ITERATIVE, LEAST SQUARES FITTING PROCEDURE

Iteration	0	1	2	3	4
Calibration Parameters					
a	800	632.272	651.644	651.510	651.504
b	0	-0.0035442	-0.0030522	-0.0030482	-0.0030483
Summations					
S1	0.0170217	0.0266384	0.0247736	0.024759	0.0247595
S2	-723.65	-1279.15	-1156.86	-1155.41	-1155.43
S3	36865200	73770500	64799300	64673300	64675100
S4	0.290234	0.113268	0.00806753	0.00000227	-0.00000171
S5	9281.95	-11513.2	-420.905	1.23877	0.0166016
S6	83.0327	6.56686	3.18744	3.18461	3.18464
Differences					
Δa	-167.728	19.3713	-0.13424	-0.005925	0.000344
Δb	-0.0035442	0.00049196	0.00000410	-0.00000013	0.000000006

The reduced χ^2 was calculated with $N=5$ from the final values for the a and b parameters as

$$\frac{\sum_{i=1}^N Q_i^2}{N-2} = 1.062 ,$$

which indicates that the assumed calibration curve is consistent with the data and the assigned errors.

Another standard was then measured as an unknown with the result that $R \pm s = 52544 \pm 911$ counts. The effective ^{240}Pu mass of this sample is calculated from the inverse response function

$$m = \frac{R}{a-bR} = \frac{52544}{651.50 + (0.0030483)(52544)} = 64.74 \text{ g}$$

and the estimated standard deviation is calculated from Eq. (4-7):

$$s_m = \left(\frac{\partial R}{\partial m} \right)^{-1} \left[s_R^2 + \left(\frac{\partial R}{\partial a} \right)^2 s_a^2 + \left(\frac{\partial R}{\partial b} \right)^2 s_b^2 + 2 \text{cov}(a,b) \left(\frac{\partial R}{\partial a} \right) \left(\frac{\partial R}{\partial b} \right) \right]^{1/2} .$$

From $R = am/(1+bm)$,

$$\frac{\partial R}{\partial a} = \frac{m}{1+bm} = 80.650 ,$$

$$\frac{\partial R}{\partial b} = \frac{-am^2}{(1+bm)^2} = -4237699 ,$$

and

$$\frac{\partial R}{\partial m} = \frac{a}{(1+bm)^2} = 1011.22 ,$$

so from Eq. (4-7)

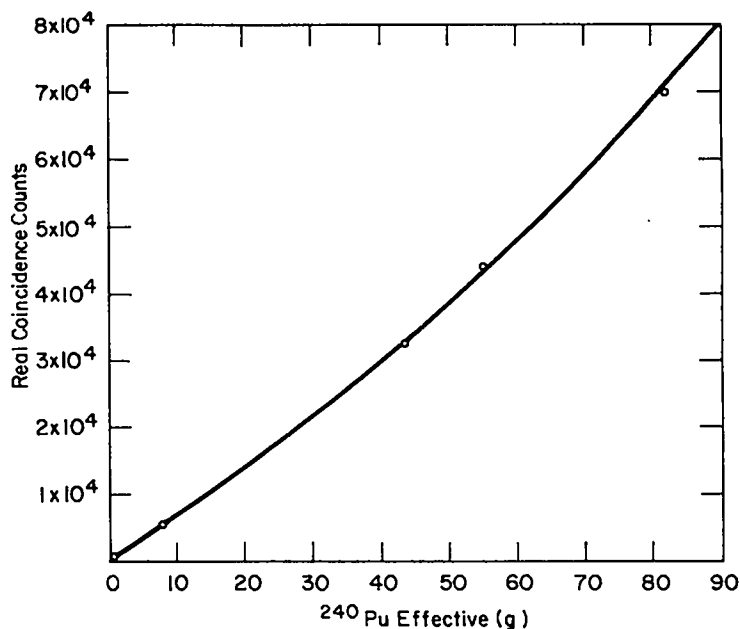


Fig. A.1.
Calibration curve and data points
from PuO_2 standards.

$$\begin{aligned}
s_m &= \frac{1}{1011.22} \left[911^2 + (80.650)^2 (15.584)^2 + (-4237699)^2 (0.00030492)^2 \right. \\
&\quad \left. + 2(0.0043388)(80.650)(-4237699) \right]^{\frac{1}{2}} \\
&= \frac{1}{1011.22} \left[829921 + 1579671 + 1669675 - 2965747 \right]^{\frac{1}{2}} \\
&= 1.04 \text{ g,}
\end{aligned}$$

and the assay result is

$$m \pm s_m = 64.74 \pm 1.04(1\sigma) \text{ g effective } {}^{240}\text{Pu}.$$

The accepted value for the effective ${}^{240}\text{Pu}$ content of this standard is 65.0 g, so the assay result is consistent with the accepted value.

The procedure illustrated above may be used with other forms of the calibration function. It is only necessary to evaluate $\partial R/\partial a$, $\partial R/\partial b$, and $\partial R/\partial m$ for the function chosen.

REFERENCES

1. D. Altman, "High Level Neutron Coincidence Counter (HLNCC): Maintenance Manual," EG&G report EGG-1183, 5091 (1978).
2. R. H. Augustson and T. D. Reilly, "Fundamentals of Passive Nondestructive Assay of Fissionable Material," Los Alamos Scientific Laboratory report LA-5651-M (1974).
3. P. R. Bevington, "Data Reduction and Error Analysis for the Physical Sciences," McGraw-Hill Book Company, New York (1969).
4. K. Böhnel, "Die Plutoniumbestimmung in Kernbrennstoffen mit der Neutronen Koinzidenzmethode," Karlsruhe report KFK2203 (1975); also AWRE translation No. 70 (54/4252) (1978).
5. T. W. Crane, "Alternative Approach for Determining an Assay Value from a Calibration Function," Los Alamos Scientific Laboratory report LA-7439-PR (1978) p. 59.
6. M. de Carolis, W. Alston, N. Beyer, A. Ramalho, and D. E. Rundquist, "Nondestructive Assay of Large Quantities of Plutonium," International Symposium on Nuclear Material Safeguards, Vienna, IAEA-SM-231/107 (1978).

7. B. C. Diven, H. C. Martin, R. F. Taschek, and J. Terrell, "Multiplicities of Fission Neutrons," Phys. Rev. 101, 1012 (1956) .
8. L. V. East, "Improved Coincidence Circuit for Use with Thermal-Neutron Coincidence Counters," Los Alamos Scientific Laboratory report LA-5091-PR (1972) p. 26.
9. "Interface Between Data Terminal Equipment and Data Communication Equipment Employing Serial Binary Data Interchange," EIA Standard RS-232-C, Electronic Industry Association, Washington, DC (1969).
10. N. Ensslin, "Self-Multiplication Correction Factors for Neutron Coincidence Counting," Los Alamos Scientific Laboratory report LA-7439-PR (1978) p. 15.
11. N. Ensslin, M. L. Evans, H. O. Menlove, and J. E. Swansen, "Neutron Coincidence Counters for Plutonium Measurements," INMM Journal 7, 43 (1978).
12. M. L. Evans and H. O. Menlove, "IAEA Portable High-Level Neutron Coincidence Counter," Los Alamos Scientific Laboratory report LA-6530-PR (1976) p. 10.
13. M. L. Evans, H. O. Menlove, and L. G. Speir, "Dual Range Thermal Neutron Coincidence Counter," Los Alamos Scientific Laboratory report LA-6788-PR (1976) p. 8.
14. J. E. Foley, in preparation.
15. D. A. Hicks, J. Ise, Jr., and R. V. Pyle, "Probabilities of Prompt-Neutron Emission from Spontaneous Fission," Phys. Rev. 101, 1016 (1956).
16. "The HP-97 Programmable Printing Calculator Owner's Handbook and Programming Guide," 00097-90001, Rev. D 3/77, Hewlett Packard Company, 1000 N.E. Circle Blvd, Corvallis, Oregon, 97330, USA (1977).
17. M. S. Krick, "Calculations of Coincidence Counting Efficiency for Shift-Register and OSDOS Coincidence Circuits," Los Alamos Scientific Laboratory report LA-7030-PR (1977) p. 14.
18. M. S. Krick, "²⁴⁰Pu-Effective Mass Formula for Coincidence Counting of Plutonium with SR Electronics," Los Alamos Scientific Laboratory report LA-7030-PR (1977) p. 16.
19. M. S. Krick, M. L. Evans, N. Ensslin, C. Hatcher, H. O. Menlove, J. L. Sapir, J. E. Swansen, M. de Carolis, and A. Ramalho, "A Portable Neutron Coincidence Counter for Assaying Large Plutonium Samples," International Symposium on Nuclear Material Safeguards, Vienna, IAEA-SM-231/50 (1978).
20. H. O. Menlove and R. B. Walton, "⁴ π Coincidence Unit for One-Gallon Cans and Smaller Samples," Los Alamos Scientific Laboratory report LA-4457-MS (1970) p. 27.

21. H. O. Menlove, N. Ensslin, M. L. Evans, and J. E. Swansen, "Portable High-Level Neutron Coincidence Counter," Los Alamos Scientific Laboratory report LA-6675-PR (1976) p. 10.
22. H. O. Menlove, M. S. Krick, J. Swansen, C. R. Hatcher, M. L. Evans, and E. Medina, "High-Level Neutron Coincidence Counter (HLNCC) for IAEA Inspection Applications," Los Alamos Scientific Laboratory report LA-7030-PR (1977) p. 18.
23. E. Medina, M. P. Baker, M. L. Evans, and H. O. Menlove, "Matrix Material Effects Study for the Dual Range Thermal-Neutron Coincidence Counter," Los Alamos Scientific Laboratory report LA-6849-PR (1977) p. 6.
24. E. Medina Ortega, private communication.
25. H. O. Menlove, E. Medina, and M. de Carolis, "Evaluation of IAEA HLNCC for Mixed-Oxide Fuel-Rod Assemblies," Los Alamos Scientific Laboratory report LA-6849-PR (1977) p. 5.
26. W. J. Price, Nuclear Radiation Detection, McGraw-Hill Book Company, Inc., New York, 1964.
27. Reuter-Stokes, 18530 South Miles Parkway, Cleveland, OH, 44128, USA.
28. J. L. Sapir, H. O. Menlove, W. L. Talbert, M. de Carolis, and N. Beyer, "Calibration of the IAEA High-Level Neutron coincidence Counter for Plutonium Plates in ZPPR Drawers," Los Alamos Scientific Laboratory report LA-6849-PR (1977) p. 4.
29. R. Sher, "Operating Characteristics of Neutron Well Coincidence Counters," Brookhaven National Laboratory report BNL-50332 (1972).
30. D. B. Smith, et al., "American National Standard Guide to Calibrating Nondestructive Assay Systems," American National Standards Institute, ANSI N15.20-1975.
31. C. V. Strain, "Potential and Limitations of Several Neutron Coincidence Equipments," Naval Research Laboratory memorandum report 2127 (1970).
32. M. M. Stephens, J. E. Swansen, and L. V. East, "Shift Register Neutron Coincidence Module," Los Alamos Scientific Laboratory report LA-6121-MS (1975).
33. J. E. Swansen, N. Ensslin, M. S. Krick, and H. O. Menlove, "New Shift Register for High Count Rate Coincidence Applications," Los Alamos Scientific Laboratory report LA-6788-PR (1976) p. 4.
34. E. Medina and H. O. Menlove, "Evaluation of Neutron Reflectors for the HLNCC," Los Alamos Scientific Laboratory report LA-6849-PR (1977) p. 13.
35. N. Ensslin, private communication.

LASL
CLASSIFIED
REPORT LIBRARY

AUG 29 1979

RECEIVED